Nuclear Science
NEA/NSC/DOC(2005)5

ISBN 92-64-01088-2

NEA NUCLEAR SCIENCE COMMITTEE
NEA COMMITTEE ON SAFETY OF NUCLEAR INSTALLATIONS
US NUCLEAR REGULATORY COMMISSION

NUPEC BWR Full-size Fine-mesh Bundle Test (BFBT) Benchmark

Volume I: Specifications

B. Neykov, F. Aydogan, L. Hochreiter, K. Ivanov
The Pennsylvania State University

H. Utsuno, F. Kasahara
Japan Nuclear Energy Safety Organization

E.Sartori
OECD Nuclear Energy Agency

M. Martin
Commissariat à l'Énergie Atomique

NEA No. 6212

NUCLEAR ENERGY AGENCY
ORGANISATION FOR ECONOMIC CO-OPERATION AND DEVELOPMENT

ORGANISATION FOR ECONOMIC CO-OPERATION AND DEVELOPMENT

The OECD is a unique forum where the governments of 30 democracies work together to address the economic, social and environmental challenges of globalisation. The OECD is also at the forefront of efforts to understand and to help governments respond to new developments and concerns, such as corporate governance, the information economy and the challenges of an ageing population. The Organisation provides a setting where governments can compare policy experiences, seek answers to common problems, identify good practice and work to co-ordinate domestic and international policies.

The OECD member countries are: Australia, Austria, Belgium, Canada, the Czech Republic, Denmark, Finland, France, Germany, Greece, Hungary, Iceland, Ireland, Italy, Japan, Korea, Luxembourg, Mexico, the Netherlands, New Zealand, Norway, Poland, Portugal, the Slovak Republic, Spain, Sweden, Switzerland, Turkey, the United Kingdom and the United States. The Commission of the European Communities takes part in the work of the OECD.

OECD Publishing disseminates widely the results of the Organisation's statistics gathering and research on economic, social and environmental issues, as well as the conventions, guidelines and standards agreed by its members.

* * *

This work is published on the responsibility of the Secretary-General of the OECD. The opinions expressed and arguments employed herein do not necessarily reflect the official views of the Organisation or of the governments of its member countries.

NUCLEAR ENERGY AGENCY

The OECD Nuclear Energy Agency (NEA) was established on 1st February 1958 under the name of the OEEC European Nuclear Energy Agency. It received its present designation on 20th April 1972, when Japan became its first non-European full member. NEA membership today consists of 28 OECD member countries: Australia, Austria, Belgium, Canada, the Czech Republic, Denmark, Finland, France, Germany, Greece, Hungary, Iceland, Ireland, Italy, Japan, Luxembourg, Mexico, the Netherlands, Norway, Portugal, Republic of Korea, the Slovak Republic, Spain, Sweden, Switzerland, Turkey, the United Kingdom and the United States. The Commission of the European Communities also takes part in the work of the Agency.

The mission of the NEA is:

- to assist its member countries in maintaining and further developing, through international co-operation, the scientific, technological and legal bases required for a safe, environmentally friendly and economical use of nuclear energy for peaceful purposes, as well as
- to provide authoritative assessments and to forge common understandings on key issues, as input to government decisions on nuclear energy policy and to broader OECD policy analyses in areas such as energy and sustainable development.

Specific areas of competence of the NEA include safety and regulation of nuclear activities, radioactive waste management, radiological protection, nuclear science, economic and technical analyses of the nuclear fuel cycle, nuclear law and liability, and public information. The NEA Data Bank provides nuclear data and computer program services for participating countries.

In these and related tasks, the NEA works in close collaboration with the International Atomic Energy Agency in Vienna, with which it has a Co-operation Agreement, as well as with other international organisations in the nuclear field.

FOREWORD

The need to refine models for best-estimate calculations, based on good-quality experimental data, has been expressed in many recent meetings concerning nuclear applications. The needs arising in this respect should not be limited to the currently available macroscopic methods but should be extended to next-generation analysis techniques that focus on more microscopic processes. One of the most valuable databases identified for thermal-hydraulics modelling was developed by the Nuclear Power Engineering Corporation (NUPEC) of Japan which includes sub-channel void fraction measurements in a representative BWR fuel assembly. Part of this database has been made available for this international benchmark activity. This project has been officially approved by the Japanese Ministry of Economy, Trade and Industry (METI), the US Nuclear Regulatory Commission (NRC), and endorsed by the OECD/NEA. The benchmark team has been organised based on collaboration between Japan and the United States. A large number of international experts have agreed to participate in this programme.

The fine-mesh high-quality sub-channel void fraction and critical power data help advance understanding and modelling of complex two-phase flow behaviour in real bundles. Considering that the present theoretical approach is relatively immature, the benchmark specification has been designed so that it will systematically assess and compare the participants' analytical models on the prediction of detailed void distributions and critical powers. The development of truly mechanistic models for critical power prediction is currently under way. These innovative models include processes such as void distributions, droplet deposition and liquid film entrainment. The benchmark problem includes both macroscopic and microscopic measurement data. In this context, the sub-channel grade void fraction data are regarded as the macroscopic data and the digitised computer graphic images are the microscopic data, which provide void distribution within a sub-channel.

The NUPEC BWR Full-size Fine-mesh Bundle Test (BFBT) benchmark consists of two phases. Each phase is composed of several exercises:

- *Phase I – Void Distribution Benchmark*
  Exercise 1: Steady-state sub-channel grade benchmark,
  Exercise 2: Steady-state microscopic grade benchmark,
  Exercise 3: Transient macroscopic grade benchmark,
  Exercise 4: Uncertainty analysis of the void distribution benchmark.
- *Phase II – Critical Power Benchmark*
  Exercise 0: Steady-state pressure drop benchmark,
  Exercise 1: Steady-state critical power benchmark,
  Exercise 2: Transient benchmark.

This report provides the specifications for the international NUPEC BFBT benchmark. The specification has been prepared jointly by Pennsylvania State University (PSU), USA and the Japan Nuclear Energy Safety (JNES) Organisation, in co-operation with the OECD/NEA and the *Commissariat à l'énergie atomique* (CEA), France. The work is sponsored by the US NRC, METI-Japan, OECD/NEA and the Nuclear Engineering Program (NEP) at Pennsylvania State University. The specifications cover the four exercises of Phase I and the three exercises of Phase II. In addition, a CD-ROM has been prepared with the complete NUPEC BWR database and distributed along with the specifications to the participants, who have signed the OECD/NEA confidentiality agreement. The agreement as well as other related information concerning the BFBT benchmark can be found at: www.nea.fr/html/science/egrsltb/BFBT/.

Acknowledgments

The authors would like to thank Professor Hideki Nariai, President of the JNES, Japan, whose support and encouragement in establishing and carrying out this benchmark are invaluable.

This report is the sum of many efforts, the participants, the funding agencies and their staff, the METI, Japan, US NRC and the Organisation of Economic Co-operation and Development (OECD). Special appreciation goes to the report reviewers: Maria Avramova and Andrew Ireland from Pennsylvania State University. Their comments, corrections and suggestions were very valuable and significantly improved the quality of this report.

The authors wish to express their sincere appreciation for the outstanding support offered by the JNES personnel in providing the test data and discussing the test characteristics.

The authors would like also to acknowledge the contribution of Daniel Caruge and Eric Royer of CEA, Saclay, France in enriching this benchmark activity with uncertainty analyses.

Particularly noteworthy are the efforts of Farouk Eltawila and Gene Rhee from US NRC. With their help funding is secured, enabling this project to proceed. We also thank them for their excellent technical advice and assistance.

The authors would like to thank Dr. A. Hotta from TEPSYS, Japan, Professor J. Aragones from Universidad Politecnica Madrid (UPM), Spain and member of NSC/NEA, and Professor F. D'Auria of University of Pisa (UP), Italy and member of CSNI/NEA, whose support and encouragement in establishing and carrying out this benchmark are invaluable.

The authors wish to express their appreciation to Paul Clare for his help in improving the information on the grid and ferrule spacers.

Finally, we are grateful to Amanda Costa for having devoted her competence and skills to the final editing of this report.

TABLE OF CONTENTS

List of figures

List of tables

Chapter 1

INTRODUCTION

1.1 Background

In the past decade, a large amount of effort has been made toward the direct simulation of the boiling transition (BT) for boiling water reactor (BWR) fuel bundles. The most advanced sub-channel codes explicitly take into account entrained droplet behaviour along with liquid film and vapour. Their calculations predict the dry-out process as disappearance of the liquid film on the fuel rod surface, taking into consideration the competing mechanisms of entrainment, deposition and evaporation. Through a series of comparisons with full length/scale bundle data, it was shown that the codes can predict the critical power of the conventional BWR fuel type, but with high level of uncertainty. However, these sub-channel codes are not yet utilised in new fuel designs. The adequacy of fuel lattice geometries, spacer configurations, etc., is still confirmed mainly by costly experiments using partial- and full-scale mock-ups. The main reason for this situation is a shortage of high resolution and full-scale experimental data, on a sub-channel basis, under actual operating conditions.

The detailed void distribution inside the fuel bundle has been regarded as one of the important factors in the boiling transition in BWRs. With regard to the sub-channel void distribution, it is clear that the cross-flow through the sub-channel gap can dominate the void distribution in the sub-channel.

Most of the well-known sub-channel codes still employ the classic Lahey's void drift model [1] or modified versions of this model. Although there have been substantial efforts to establish a sound theoretical background of detailed void distributions, models that have been verified over a wide range of geometrical and thermal-hydraulic conditions are not yet available. In this sense, this subject remains a major unsolved problem for two-phase flow in BWR fuel bundles. The main reason for this lack of resolution is the paucity of a reliable full bundle database under prototypical operating conditions. Up to now, only partial bundle (3×3 or 4×4) test data under relatively low pressure (≈ 1 MPa) conditions have been made available [2-3].

During the 4th OECD/NRC BWR TT Benchmark Workshop held on 6 October 2002 in Seoul, Korea, the need to refine models for best-estimate calculations based on a good-quality experimental data was discussed [4]. It was agreed that the need arising in this respect should not be limited to currently available macroscopic approaches but should be extended to next-generation analysis and techniques that focus on a more microscopic process. It was suggested that a new international benchmark be established based on data made available from the Nuclear Power Engineering Corporation (NUPEC) database obtained in Japan. From 1987 to 1995, NUPEC performed a series of void measurement tests using full-size mock-up tests for both BWRs and pressurised water reactors (PWRs) [5]. Based on state-of-the-art computer tomography (CT) technology, the void distribution was visualised at the mesh size smaller than the sub-channel under actual plant conditions. NUPEC also performed a steady-state and transient critical power test series based on the equivalent full-size mock-ups. Considering the reliability not only of the measured data, but also other relevant parameters

such as the system pressure, inlet sub-cooling and rod surface temperature, this test series supplied the first substantial database for the development of truly mechanistic and consistent models for void distribution and boiling transition on a sub-channel basis.

1.2 Objective

The international OECD/NRC BWR Full-size Fine-Mesh Bundle Tests (BFBT) benchmark, based on the NUPEC database, encourages advancement in sub-channel analysis of two-phase flow in rod bundles, which has great relevance with regard to the nuclear reactor safety margin evaluation. This benchmark specification is being designed so that it can systematically assess and compare the participants' numerical models for the prediction of detailed sub-channel void distributions and critical powers to full-scale experimental data on a prototypical BWR rod bundle. Currently the numerical modelling of sub-channel void distribution has no theoretical approach that can be applied to a wide range of geometrical and operating conditions. In the past decade, experimental and computational technologies have tremendously improved the study of the two-phase flow structure. Over the next decade, it can be expected that mechanistic approaches will be more widely applied to the complicated two-phase fluid phenomena inside fuel bundles. The development of truly mechanistic models for critical power prediction is currently underway. These models must include processes such as void distribution, droplet deposition, liquid film entrainment and spacer grid behaviour. The benchmark specification requires participants to explain their modelling correlations between the measured critical power and the two-phase flow dominant processes.

It should be recognised that the purpose of this benchmark is not only the comparison of currently available computational approaches but above all the encouragement to develop novel next-generation approaches that focus on more microscopic processes. In this context, the sub-channel grade void fraction data are regarded as the macroscopic data and the digitised computer graphic images are the microscopic data, which provides the detailed void distribution within the sub-channel. This benchmark specification is supplemented by a CD-ROM with the complete NUPEC BWR Benchmark Database, which is distributed to all participants who have signed the confidentiality agreement.

1.3 Outline of the BFBT specification

Chapter 1 of this specification discusses the main objectives of the international OECD/NRC BFBT Benchmark. A definition of the benchmark phases and exercises is provided.

Chapter 2 discusses the NUPEC BWR BFBT facility and the specific methods used in the void distribution and critical power measurements.

Chapter 3 provides specifications of fuel assembly types and heater rods as well as spacer data and thermo-mechanical properties of structural materials.

Chapter 4 includes a description of the complete NUPEC BFBT Database that is released by JNES, Japan. The complete benchmark database for all cases defined in the test matrices is stored on the CD-ROM, which is provided to the participants by NEA/OECD in addition to this specification.

Chapter 5 defines the NUPEC BFBT data to be used for the benchmark exercises. In total, seven exercises of two phases will be performed in the framework of this benchmark.

Chapter 6 describes the requested output and the output format that the benchmark team will collect from the participants.

Appendix A explains proposed methods for accuracy and uncertainty analyses of the benchmark results.

1.4 Definition of benchmark phases

The test facility design and data from NUPEC includes both macroscopic and microscopic measurements. There are two separate phases, each consisting of different exercises. These phases and exercises are discussed below.

1.4.1 Phase I – Void distribution benchmark

The purpose of this benchmark phase is threefold:

1) to provide data for validation of numerical models of void distribution;

2) to provide data over a wide range of geometrical and operating conditions for the validation of void distribution models;

3) to provide data for development of mechanistic approaches widely applicable to the two-phase fluid phenomena inside fuel bundles.

Phase I includes four exercises:

- *Exercise 1* – steady-state sub-channel grade benchmark, where sub-channel, meso- and microscopic approaches can be used;
- *Exercise 2* – steady-state microscopic grade benchmark, where meso- and microscopic approaches and molecular dynamics can be utilised;
- *Exercise 3* – transient macroscopic grade benchmark, where a sub-channel approach can be applied;
- *Exercise 4* – uncertainty analysis of the void distribution benchmark.

1.4.2 Phase II – Critical power benchmark

The purpose of this benchmark is to develop truly mechanistic models for critical power prediction. Phase II includes three exercises:

- *Exercise 0* – steady-state pressure drop benchmark;
- *Exercise 1* – steady-state benchmark, which applies a one-dimensional approach with BT correlations and a sub-channel mechanistic approach;
- *Exercise 2* – transient benchmark, which applies a one-dimensional approach with BT correlations and a sub-channel mechanistic approach.

1.5 Benchmark team and sponsorship

About 30 experts from 20 organisations in 10 countries have confirmed their intention to participate. This international project is officially approved by METI, Japan, US NRC, and is endorsed by the OECD/NEA. The benchmark team is organised based on the collaboration between Japan and the USA as shown in Figure 1.5.1.

Figure 1.5.1 BFBT benchmark team

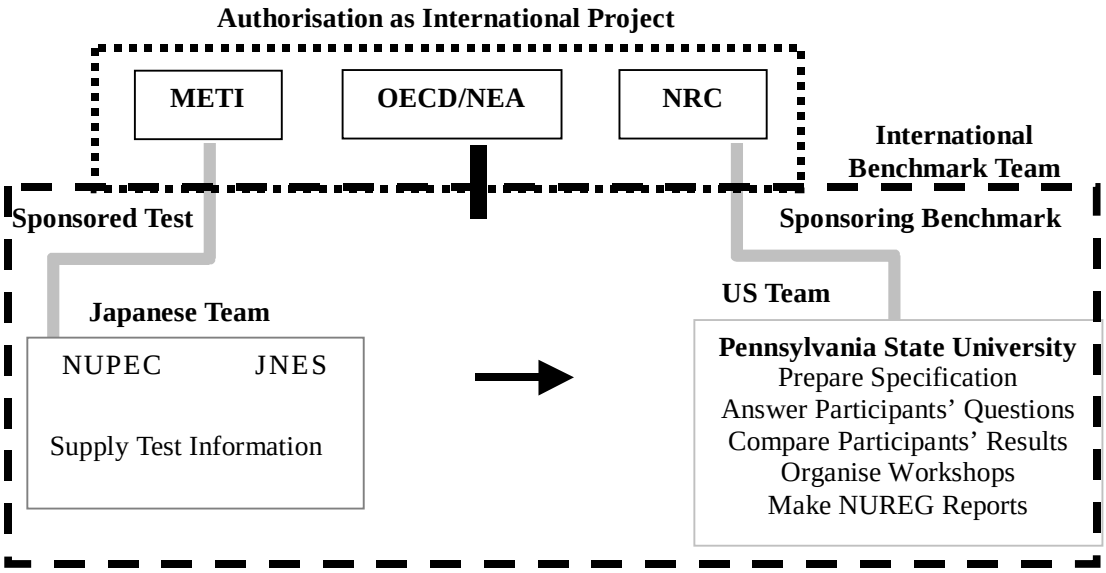

Chapter 2

TEST FACILITY

2.1 General

The void fraction distribution and critical power in a multi-rod assembly with a typical reactor power and fluid conditions has been measured in the NUPEC BWR BFBT facility. The facility is able to simulate the high-pressure, high-temperature fluid conditions found in BWRs. An electrically-heated rod bundle has been used to simulate a full-scale BWR fuel assembly.

2.2 Test loop

Figure 2.3.1 shows a diagram of the test loop. The main structural components are made of stainless steel (SUS304). Demineralised water is used as a cooling fluid. The maximum operating conditions for the facility are 10.3 MPa in pressure, 315°C in temperature, 12 MW in test power, and 75 t/h in flow rate. The test facility has the capability for a full range of steady-state testing over BWR operating conditions and can also simulate time-dependent characteristics of complicated BWR operational transients. Water is circulated by the circulation pump (1) and the coolant flow rate is controlled by the three valves (3) of different sizes. The inlet fluid temperature for the test section (5) is controlled by a direct-heating tubular pre-heater (4). Sub-cooled coolant flows upward into the test bundle (5), where it is heated and becomes a two-phase mixture. The steam is separated from the steam-water mixture in the separator (7) and is condensed using a spray of sub-cooled water in the steam drum (8). The condensed water is then returned to the circulation pump (1). The system pressure in both steady and transient state is controlled by spray lines (9), which have four different-sized valves. The pressuriser (6) controls the system pressure when the test assembly power is low. The spray pump (10) forces a spray into the steam-drum after water is cooled with two air-cooled heat exchangers (11). Based on this diagram, the test loop was operated covering the full range of BWR steady-state operating conditions.

2.3 Test section

The test section, shown in Figure 2.3.2, consists of a pressure vessel, a simulated flow channel, and electrodes. The simulated full-scale BWR fuel assembly was installed within the vessel. Two bundle types, a current 8×8 type and a high burn-up 8×8 type, were simulated. Here it should be noted that the terminology “current 8×8 design” refers to the late 1980s when the NUPEC BFBT database was collected. The dimensions for the different rod bundle arrays are summarised in Table 2.3.1. Chapter 3 of the BFBT specification provides detailed rod bundle geometry information. Each rod in the test assembly is indirectly electrically heated to simulate a reactor fuel rod. The cladding, the insulator and the heater were made of inconel, boron nitride and nichrome, respectively.

Figure 2.3.1. System diagram of test facility for NUPEC rod bundle test series

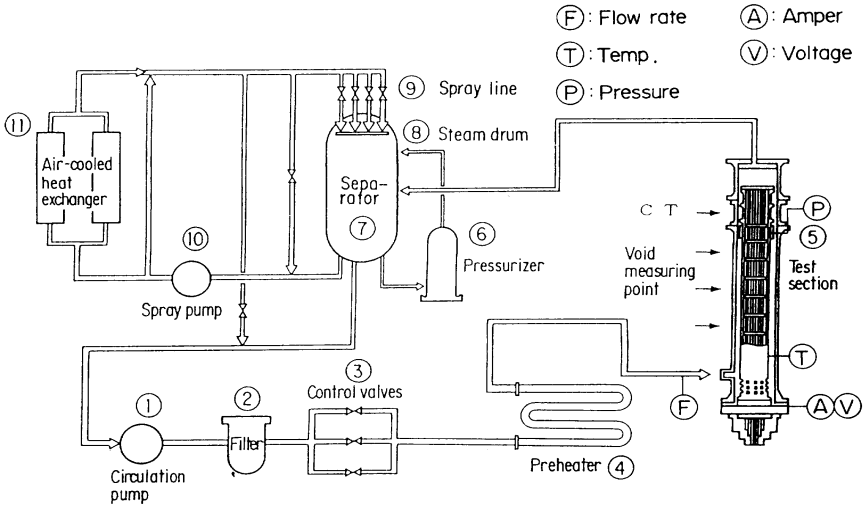

Figure 2.3.2. Cross-sectional view of test section

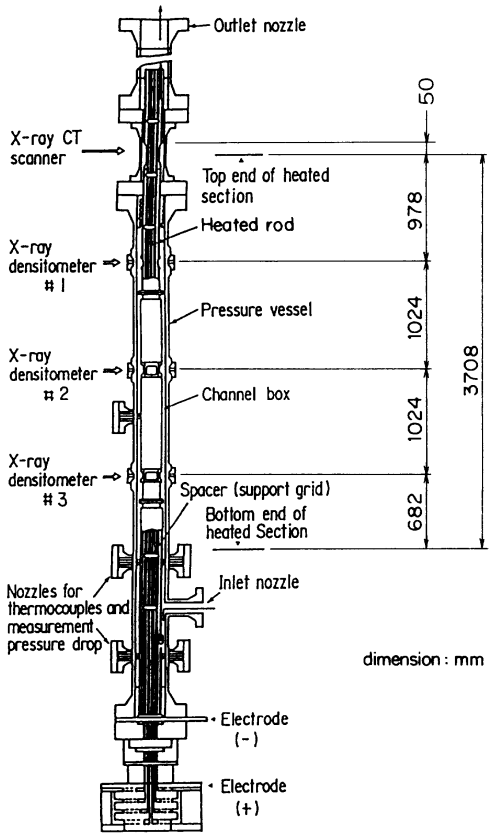

Table 2.3.1. Dimensions of BWR test bundles

Items	Current 8 × 8	High burn-up 8 × 8
Number of fuel rods	62	60
Outer diameter (mm)	12.3	12.3
Heated length (m)	3.7	3.7
Number of water rods (mm)	2	1
Outer diameter of water rod (mm)	15.0	34.0
Rod pitch (mm)	16.2	16.2
Width of channel box	132.5	132.5
Number of spacers	7	7
Spacer type	Grid	Ferrule

2.4 Void distribution measurement methods

As shown in Figure 2.4.1(a), two types of void distribution measurement systems were employed: an X-ray CT scanner and an X-ray densitometer.

Under steady-state conditions, fine mesh void distributions were measured using the X-ray CT scanner, which was located 50 mm above the heated length. The measurement system and the location are shown in Figure 2.4.1(a). The system consists of an X-ray tube and 512 detectors. Figure 2.4.1(b) shows the void fraction measuring section, where the pressure vessel was made of titanium (Ti). The channel wall and the cladding of the heater rods at this location are made of beryllium (Be) to minimise X-ray attenuation in the structure. In order to avoid the effect of the two-phase flow fluctuations, the collection of projection data was repeated and the results were time-averaged. The attained spatial resolution was as small as 0.3 mm × 0.3 mm.

The X-ray CT scanner is also used for transient void measurements called chordal averaged void fraction measurements. During the transient the X-ray CT scanner is not rotated but fixed. The data called “CT Chordal Averaged Void Fraction” is the value averaged over nine measurements taken during nine repetitions of the same transient.

The X-ray densitometer measurements were performed at several axial elevations. The channel box was made of beryllium (Be) and the heater rods had beryllium cladding of the same diameter as the Inconel portion of the heater rod. Figure 2.4.2 shows the void measurement directions of the X-ray densitometer. The chordal averaging is done from west to east (or x direction) and the order of data collection is from north to south (or y direction, y=1 to 9).

The void fraction measurement methods are shown in Figure 2.4.3.

The cross-sectional averaged transient void distributions were measured with the X-ray densitometer. During the transient void measurements the X-ray densitomer was fixed (not rotated) at a given axial position (Figure 2.4.2). The measurement was repeated nine times, changing the axial location of the densitometer along the heated length. The data is called “DENsitometer Chordal Averaged Void Fraction”. The DEN chordal averaged void fraction is the value averaged over these nine measurements.

Table 2.4.1 shows the basic specifications of the X-ray CT scanner. The X-ray beam is scanned over an object. An outline of the CT scanner principle is shown in Figure 2.4.1(c). While scanning, the

Figure 2.4.1. Void fraction measurement system

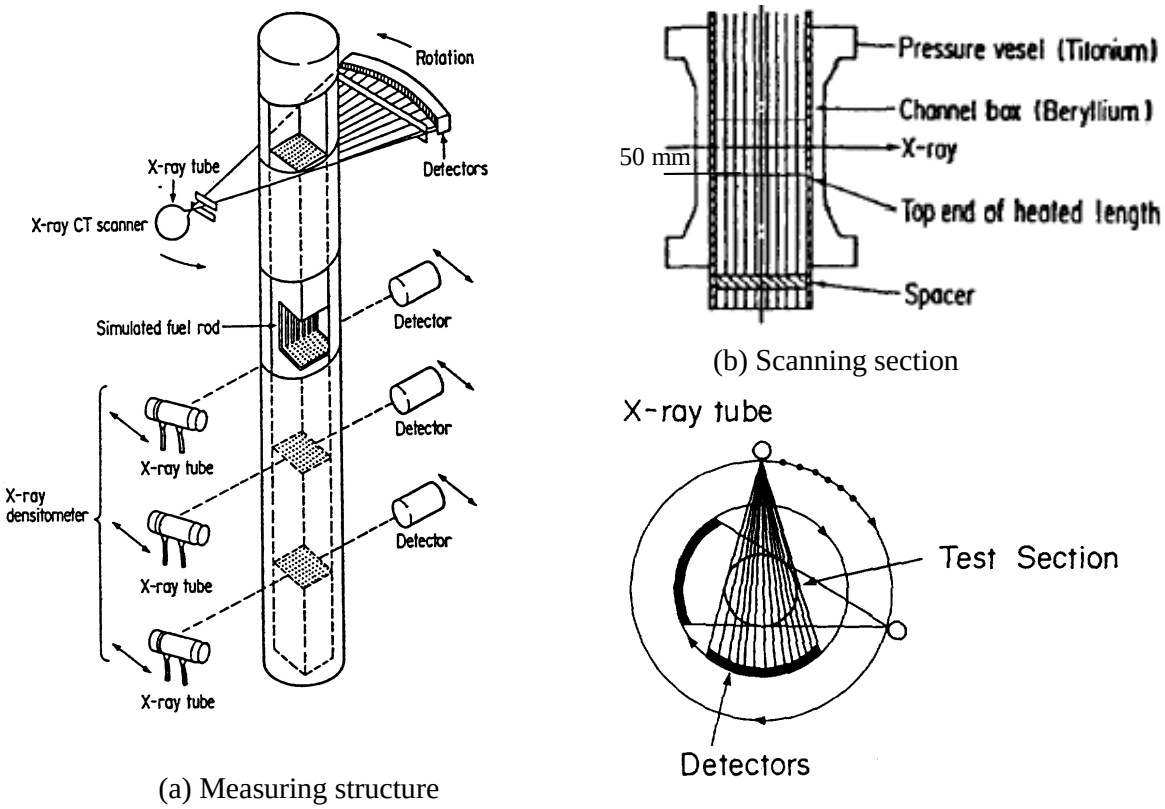

(a) Measuring structure

(b) Scanning section

(c) Scanning method

Figure 2.4.2. Void fraction measurement directions

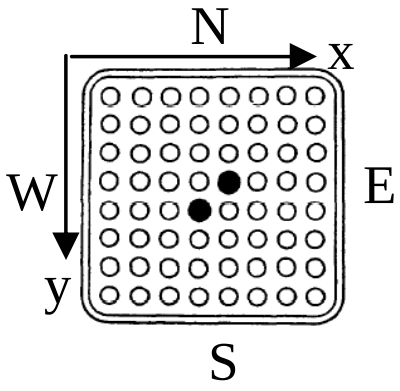

Figure 2.4.3. Void fraction measurement methods

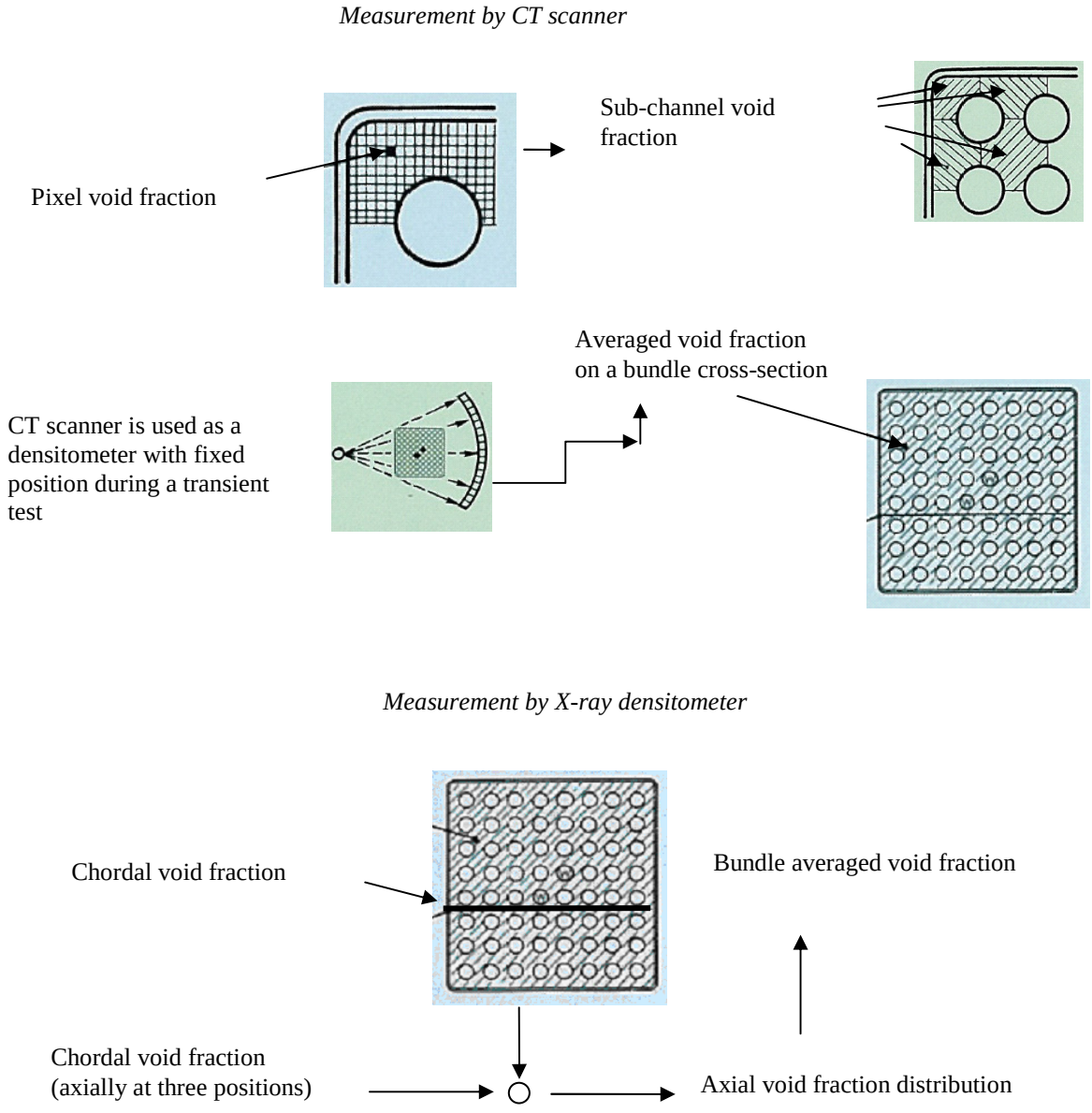

Table 2.4.1. Specification of X-ray CT scanner

Item	Specification
Method of scanning	360° rotation with pulse X-rays
Type of X-ray beam	Fan-shaped X-ray beam of 34° radiation angle
Voltage of X-ray tube	Max. 120 kV
Current	Max. 400 mA
Scanning time	15 s
Scanning region	D = 300 mm
Dimensions of reconstruction element	0.3 mm × 0.3 mm

fan-shaped X-ray beam is attenuated by the object and the attenuated beam is measured by the detectors. The X-ray intensity data recorded by the detectors is called the projection data. The complete 360° projection data are obtained for the object.

Table 2.4.2 shows the basic specifications of the X-ray densitometer.

Table 2.4.2. Specification of X-ray densitometer

Item	Specification
Method of measurement	Continuous X-ray at fixed position
Type of X-ray beam	Pencil type beam
Voltage of X-ray tube	Max. 160 kV
Current	Approx. 19 mA at 160 kV
Sampling time	Max. 60 s (variable)
Synchronisation	3 X-ray densitometers synchronise with X-ray CT scanner for data gathering

The distribution of the linear attenuation coefficient is obtained by reconstructing the projection data. The reconstruction technique is called a “filter back projection”, and has been widely used in the field of nuclear medicine.

All void fraction signals from the detectors are calibrated using a signal from a reference detector to improve the signal-to-noise ratio.

Before performing actual void fraction measurements, position co-ordinates are calibrated at room temperature with the test section empty. They are then repeated with the section filled with water and at operating temperature with non-boiling water. Frequent measurements through a standard absorber are made to correct any electronic drift.

Absolute and differential pressures were measured using diaphragm transducers. The inlet flow rate was measured using a turbine flow meter. The inlet sub-cooling was measured using double thermistors. The heater rods’ surface temperatures were monitored at positions just upstream of the spacers by chromel-alumel thermocouples, which were located in the heater rod cladding. The thermocouples have a diameter of 0.5 mm.

Table 2.4.3 shows the estimated measurement accuracy. Three types of void fraction measurements were carried out: a local void fraction on a 0.3 mm × 0.3 mm square pixel element; a sub-channel averaged void fraction, which is averaged over more than 400 pixel elements; and a cross–sectional averaged void fraction, which is averaged over more than 10^5 pixel elements. The accuracy of these void fraction measurements depends on the photon statistics of the X-ray source, the detector non-linearity, and the accuracy of the known fluid condition (temperature and pressure) measurements.

Five different types of bundle assembly design with different combinations of geometries and power shapes were tested in the void distribution experiments. BWR steady-state and transient conditions were simulated. Detailed information on the bundle assembly design and test conditions is presented in Chapters 3 and 4 (for the complete database) and 5 (for the benchmark exercises) of this specification.

The steady-state test series was performed using thermal-hydraulic conditions that envelope BWR bundle geometrical, power shape and two-phase flow parameters of actual plant steady-state operation.

Table 2.4.3. Estimated accuracy of main process parameters for void distribution measurements

Quantity	Accuracy
Pressure	1%
Flow	1%
Power	1.5%
Inlet fluid temperature	1.5° Celsius
X-ray CT scanner	
Local void fraction	8%
Sub-channel void fraction	3%
Cross-sectional void fraction	2%
Spatial resolution	0.3 mm × 0.3 mm
Scanning time	15 seconds
X-ray densitometer	
Sampling time	Max. 60 seconds

Both the X-ray CT scanner and the X-ray densitometer technique were used in the experiments. The range of test conditions was as follows: pressure – 1 ÷ 8.6 MPa; flow rate – 284 ÷ 1 988 kg/m^2-s; and exit quality – 1 ÷ 25%. In total, 476 measurement points were included.

Transient tests were performed to measure the cross-sectional averaged transient void fraction over a range of pressure, flow and power variations. The X-ray densitometer was used for these tests. The following four operational transients were simulated: turbine trip without bypass; one pump trip; re-circulation pump tripped; and malfunction of pressure control system (pressure increase). The four above events include the combined effects of pressure, flow and power with the resulting change in the bundle void distribution. In order to obtain the individual sensitivity of these process parameters, additional tests were performed in which only one of these three parameters was changed at a time.

2.5 Critical power measurement methods

The test loop used for the void distribution measurements (Figures 2.3.1 and 2.3.2) was also utilised for the critical power measurements. The test loop was operated under normal BWR operational conditions and transient conditions corresponding to one pump trip event and a turbine trip event.

The full-scale test bundle, simulating the 8 × 8 high burn-up fuel, was installed in the test section. Three combinations of radial and axial power shapes were tested: 1) beginning of cycle radial power pattern/cosine axial power shape (the so-called C2A pattern); 2) middle of cycle radial power pattern/ cosine axial power shape (C2B pattern); and 3) beginning of cycle radial power pattern/inlet peaked axial power shape (C3 pattern). The individual radial and axial power distributions for all three combinations are given in Chapter 3 of this specification.

The steady-state test series consisted of two parts: pressure drop measurements and critical power measurements. The pressure drop was measured under both single-phase and two-phase flow conditions that cover the normal operational behaviour. The range of each test condition is given in Chapter 4. In total, 151 measurement points, without pressure drop tests, were run during the critical power test.

The critical power was measured when slowly increasing the bundle power while monitoring the individual heater rod thermocouple signals. The critical power was defined when the peak rod surface temperature became 14°C higher than the steady-state temperature level before the dry-out occurred.

The dry-out was observed in the peak power rod located at the peripheral row adjacent to the channel box. The boiling transition was always observed just upstream of the spacer. The estimated accuracies of the major process parameters were equivalent to those in the void measurement tests as listed in Table 2.4.3.

The bundle pressure drop was monitored at several locations as depicted in Figure 2.5.1.

Figure 2.5.1. Location of pressure taps for critical power measurement

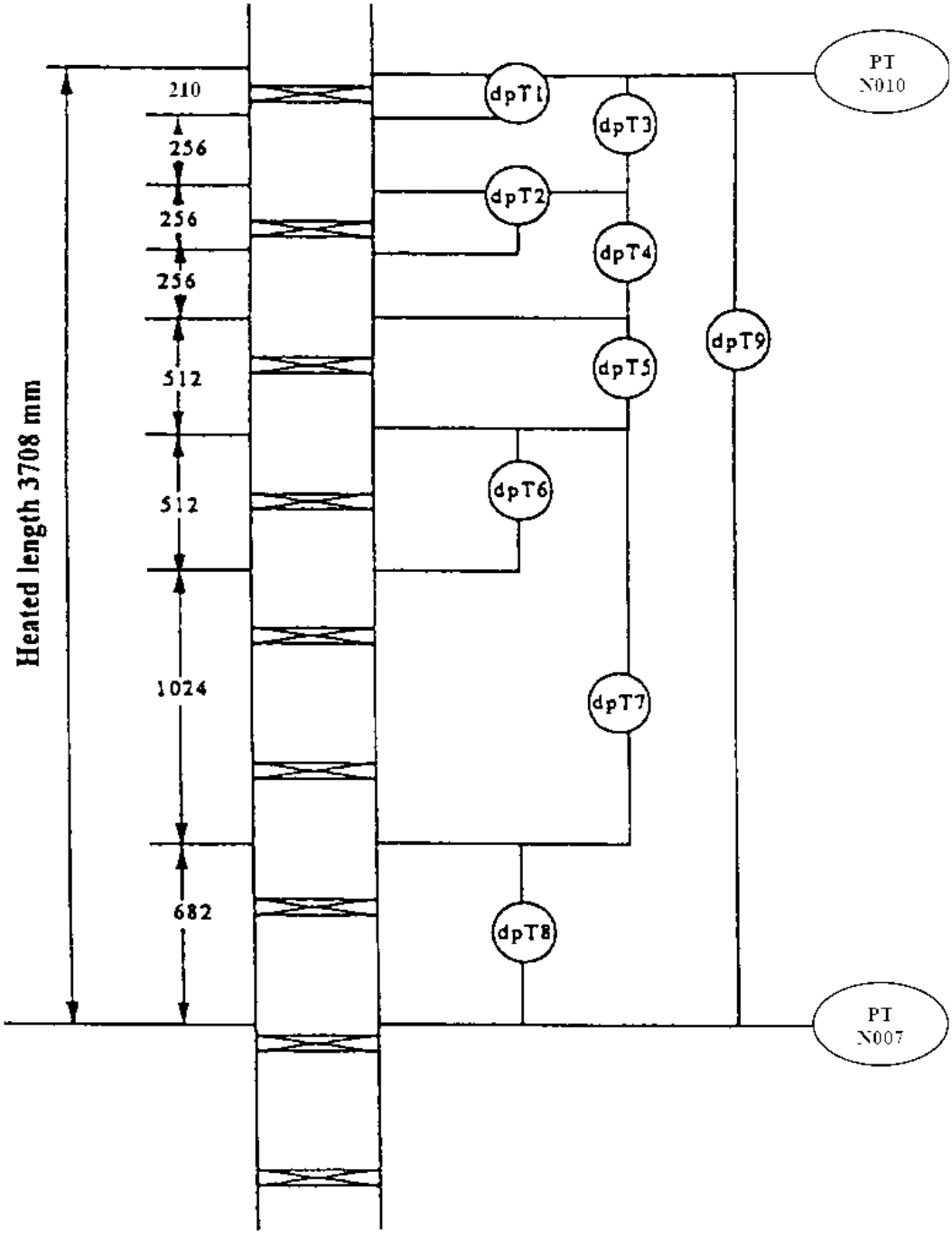

Figure 2.5.2 describes the definition of thermocouple position. Each thermocouple position is identified as follows: **Rod No. – Axial location – Rotational angle.** For example **16 – B – 270**

The rod surface temperature was also monitored at several locations as depicted in Figures 2.5.3 to 2.5.5.

Two typical BWR operational transients were simulated: 1) power transient: turbine trip event; and 2) flow transient: one recirculation pump trip event. The transient tests were separated into three types: license base transient tests, extreme scenario transient tests and post-boiling transition tests. The objective of the license base transient test series was confirmation that the boiling transition never occurs during these transients. In the extreme scenario transient test series, the initial power levels were increased to observe the boiling transition; the rod surface temperature was monitored. In the post-boiling transition test series, the rod surface temperature was measured under the quasi-steady-state condition beyond the boiling transition. The main purpose of this test series was quantification of the post-dry-out heat transfer coefficient.

The complete set of test conditions data for void distribution and critical power measurements are provided in Chapter 4 of this specification.

Figure 2.5.2. Definition of thermocouple position

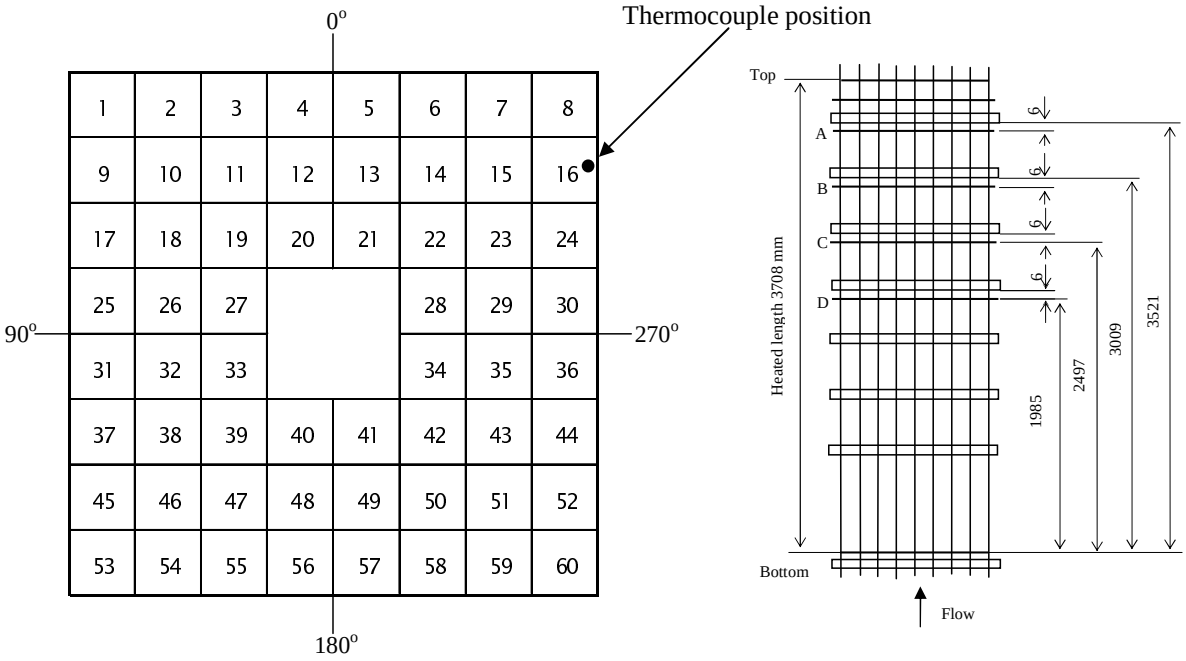

Rod no. Axial location (A-D section)

Figure 2.5.3. Location of thermocouples for critical power measurement (C2A)

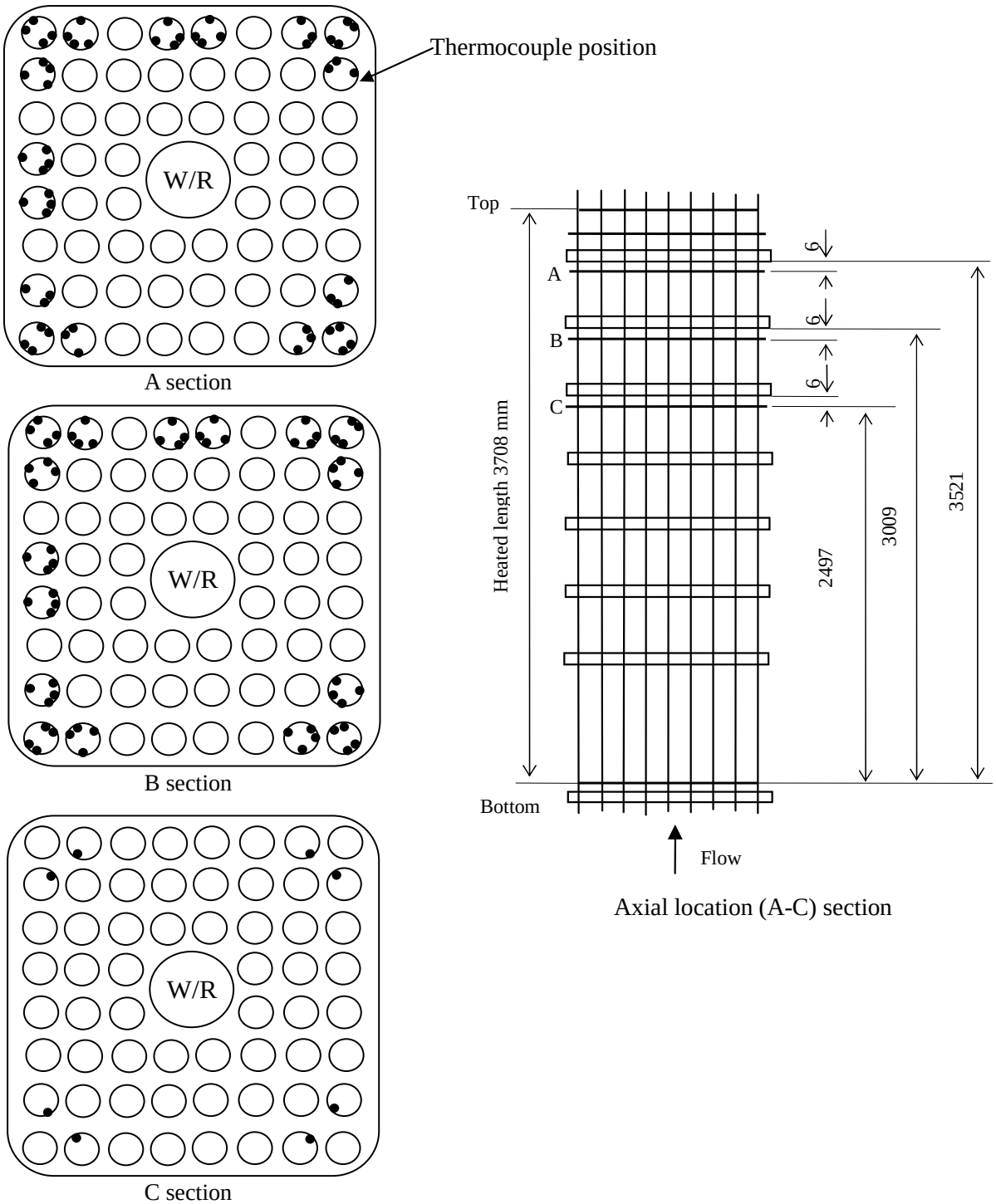

Figure 2.5.4. Location of thermocouples for critical power measurement (C2B)

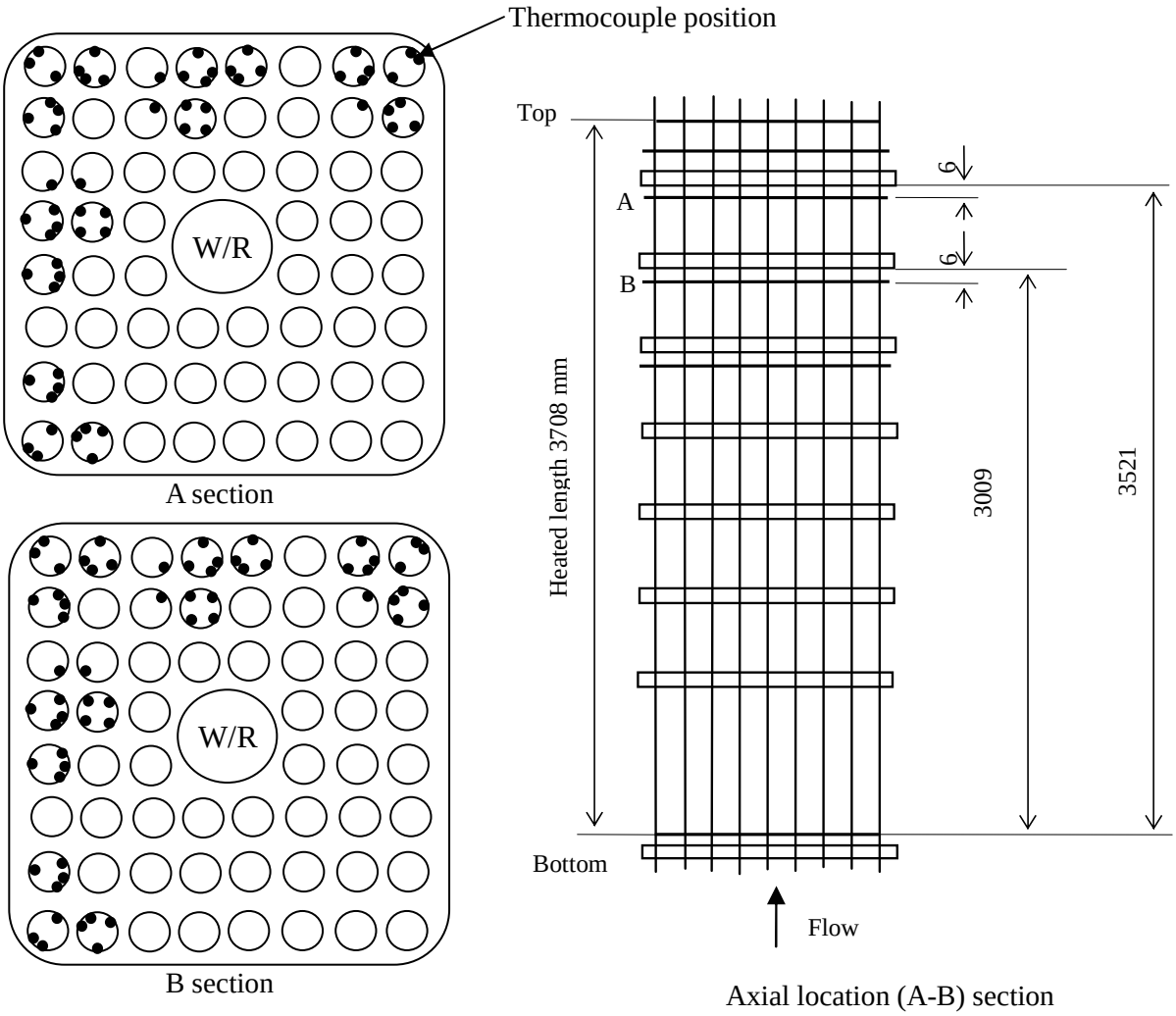

Figure 2.5.5. Location of thermocouples for critical power measurement (C3)

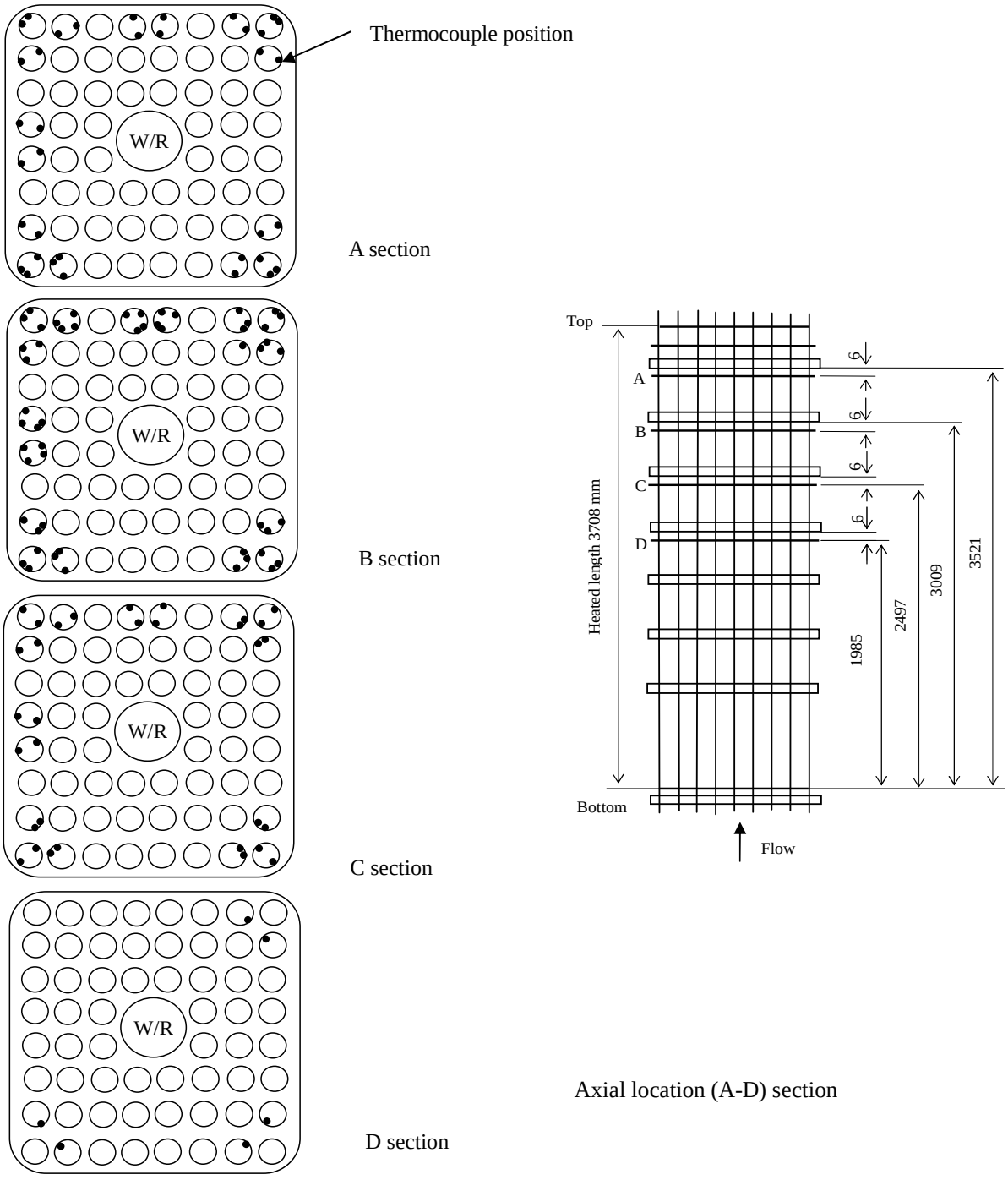

Chapter 3

FUEL ASSEMBLY DATA

3.1 General

This chapter provides the participants with geometry and material data for the BWR rod bundles utilised in the void distribution and critical power measurements. The power distribution patterns, radial and axial, as well as the tests conditions are described. Data for the fuel assemblies and spacers' dimensions, heater rods specifications and material properties are also given.

3.2 Assembly geometry data

Two types of BWR assemblies are simulated in a full length test facility, a current 8×8 fuel bundle and an 8×8 high burn-up bundle. A summary of bundles' dimension is already given in Chapter 2, Table 2.3.1. In total, five test assembly configurations with different geometry and power profiles were utilised for the void distribution and critical power measurements.

Table.3.2.1 summarises the assembly types (Type 0 to Type 4) used in the void distribution measurements.

Table 3.2.1. Test assembly and radial power distribution for void distribution measurements

Test assembly No.	0	1	2	3	4
Fuel Type	Current use 8x8 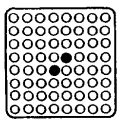				High burnup 8x8 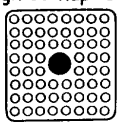
Planar power profile	Uniform	Simulated design profile	Simulated design profile	Simulated design profile	Simulated design profile
Axial power profile	Uniform	Cosine	Half-cosine	Inlet peak	Uniform
Heated length	Full	Full	Half	Full	Full
Axial powe distribution Axial → Power	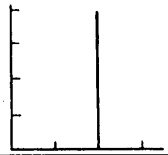	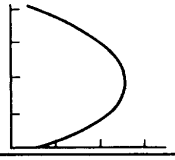	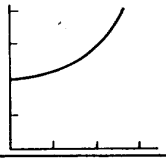	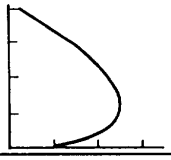	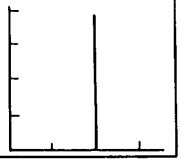

The *test assembly type 0* (as given in Table 3.2.1) has uniform radial and axial power distributions. Three sub-types of test bundle 0, namely 0-1, 0-2, and 0-3, were used to examine the effects of radial power distribution on the void fraction distribution by varying the number of unheated rods among them.

The radial arrangements of heated and unheated rods are shown in Figure 3.2.1. Test assembly 0-1 simulates a current BWR fuel assembly and has two unheated rods. Test assemblies 0-2 and 0-3 have four and nine unheated rods, respectively. Two water channels (rods) are present in all of these three sub-type test assemblies and they are counted as unheated rods.

Figure 3.2.1. Unheated rods arrangements in test assembly type 0

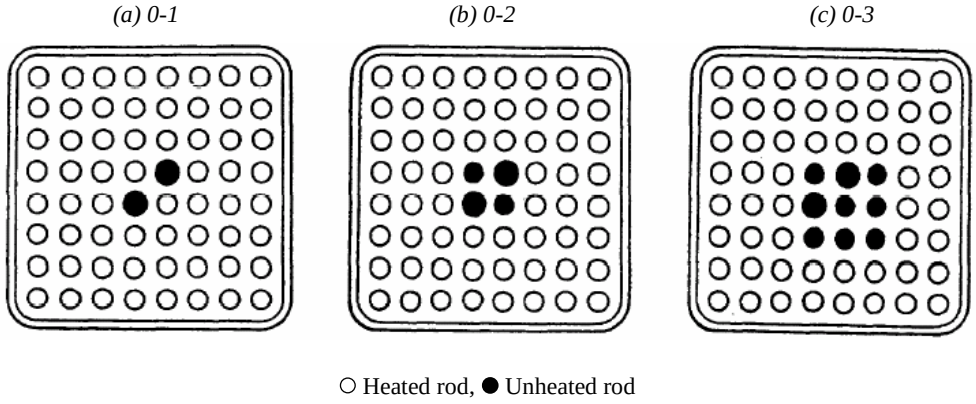

Test assembly types 1, 2, and 3 are like assembly type 0-1 with two unheated rods, but with different axial heated length (3 708 mm, 1 747 mm and 3 708 mm respectively) and different axial power shapes. These bundles have a design-simulated radial power profile which is shown in Table 3.2.2.

Table 3.2.2. Radial power shape of test assembly types 1 ÷ 3

1.15	1.30	1.15	1.30	1.30	1.15	1.30	1.15
1.30	0.45	0.89	0.89	0.89	0.45	1.15	1.30
1.15	0.89	0.89	0.89	0.89	0.89	0.45	1.15
1.30	0.89	0.89	0.89		0.89	0.89	1.15
1.30	0.89	0.89		0.89	0.89	0.89	1.15
1.15	0.45	0.89	0.89	0.89	0.89	0.45	1.15
1.30	1.15	0.45	0.89	0.89	0.45	1.15	1.30
1.15	1.30	1.15	1.15	1.15	1.15	1.30	1.15

The tabulated data for all the three non-uniform axial power shapes, shown in Table 3.2.1, are given in Table 3.2.3. Only the full length tests will be examined as part of the benchmark exercises.

The axial power distributions given in Table 3.2.3 are also shown in Figure 3.2.2(a) for the cosine shape and Figure 3.2.2(b) for the inlet peak shape. The heated length is divided into 24 steps (154.5 mm each) for both cosine and inlet peak shapes.

The radial power profile of assembly type 4 is given in Table 3.2.5.

Both the reference test bundles (test assembly 0) and the high burn-up test bundle (test assembly 4) have a uniform axial power distribution as indicated in Table 3.2.1. Here it should be highlighted that assembly type 4 has a uniform axial power profile only for the void distribution measurements.

Three combinations of high burn-up assemblies with different radial and axial power shapes, namely C2A, C2B and C3, were utilised for the critical power measurements. The combinations are summarised in Table 3.2.4. Assemblies C2A and C3 simulate the radial peaking condition at the beginning of operation while the assembly C2B simulates the radial peaking condition at the middle of operation.

The radial power profiles for the beginning of operation (type A) and for the middle of operation (type B) are given in Table 3.2.5. The axial power shapes, cosine and inlet-peaked, are shown in Figure 3.2.2 (values are the same as in Table 3.2.3).

Table 3.2.3. Axial power shape of different test assembly types

Node	Relative power		
	Cosine – test assembly 1, C2A, and C2B	**Half-cosine – test assembly 2**	**Inlet peak – test assembly 3 and C3**
(Bottom)			
1	0.46	0	0.53
2	0.58	0	0.83
3	0.69	0	1.00
4	0.79	0	1.17
5	0.88	0	1.28
6	0.99	0	1.34
7	1.09	0	1.37
8	1.22	0	1.39
9	1.22	0	1.40
10	1.34	0	1.39
11	1.34	0	1.37
12	1.40	0	1.34
13	1.40	0.46	1.28
14	1.34	0.58	1.21
15	1.34	0.69	1.10
16	1.22	0.79	1.00
17	1.22	0.88	0.89
18	1.09	0.99	0.79
19	0.99	1.09	0.71
20	0.88	1.22	0.64
21	0.79	1.22	0.58
22	0.69	1.34	0.53
23	0.58	1.34	0.46
24	0.46	1.40	0.40
(Top)			

Figure 3.2.2. Cosine and inlet peak axial power distribution patterns

(a) Cosine shape

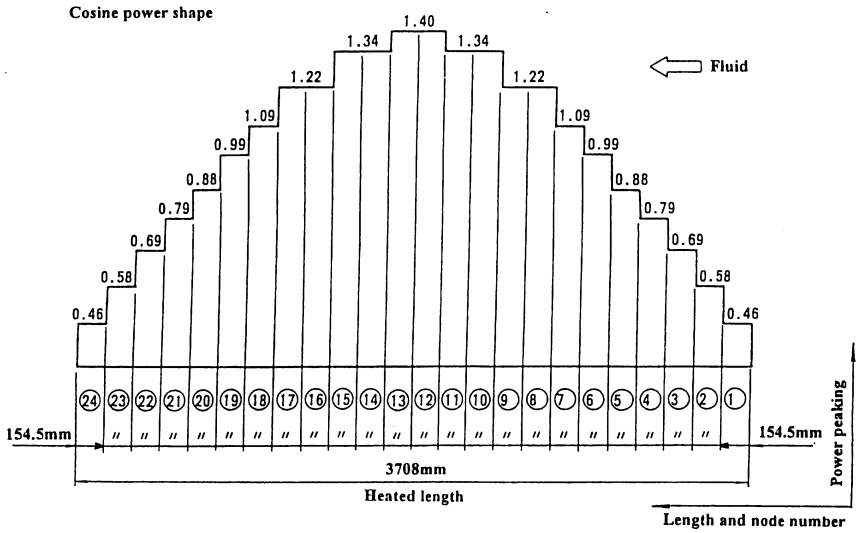

(b) Inlet peak shape

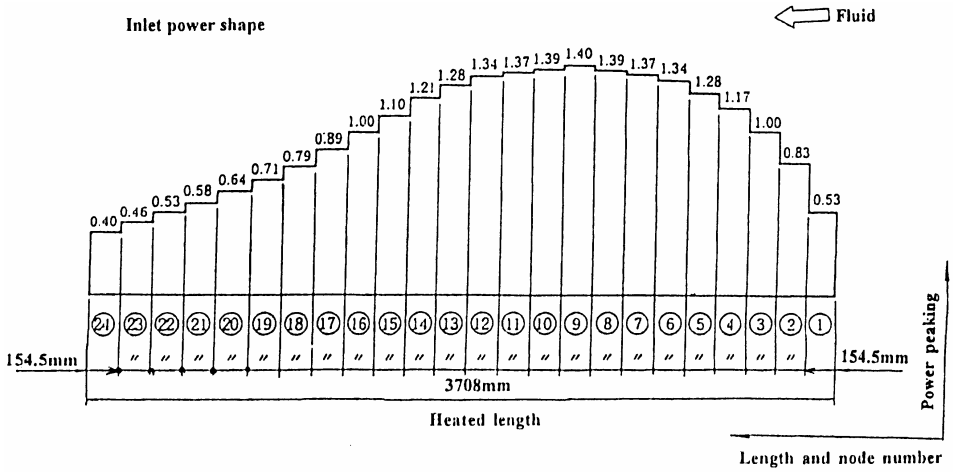

Table 3.2.4. Test assembly types for critical power measurements

Test item	Critical power test		
Test assembly	C2A	C2B	C3
Fuel type	High burn-up 8 × 8		
Axial power shape	Cosine	Cosine	Inlet peak
Radial power shape	A	B	A

A – Simulation pattern for beginning of operation.
B – Simulation pattern for middle of operation.

Table 3.2.5. Radial power shape of test assembly types for critical power measurements

A (for assembly 4, C2A, C3)

1.15	1.30	1.15	1.30	1.30	1.15	1.30	1.15
1.30	0.45	0.89	0.89	0.89	0.45	1.15	1.30
1.15	0.89	0.89	0.89	0.89	0.89	0.45	1.15
1.30	0.89	0.89			0.89	0.89	1.15
1.30	0.89	0.89			0.89	0.89	1.15
1.15	0.45	0.89	0.89	0.89	0.89	0.45	1.15
1.30	1.15	0.45	0.89	0.89	0.45	1.15	1.30
1.15	1.30	1.15	1.15	1.15	1.15	1.30	1.15

B (for assembly C2B)

0.99	1.18	0.99	1.18	1.18	0.99	1.18	0.99
1.18	0.75	0.99	1.18	0.99	0.75	0.99	1.18
0.99	0.99	0.99	0.99	0.99	0.99	0.75	0.99
1.18	1.18	0.99			0.99	0.99	0.99
1.18	0.99	0.99			0.99	0.99	0.99
0.99	0.75	0.99	0.99	0.99	0.99	0.75	0.99
1.18	0.99	0.75	0.99	0.99	0.75	0.99	0.99
0.99	1.18	0.99	0.99	0.99	0.99	0.99	0.99

Table 3.2.6 provides the geometry data for test bundles 0-1, 0-2 and 0-3 and specifies the power distribution patterns.

Table 3.2.6. Geometry and power shape of test assembly types 0-1, 0-2 and 0-3

Item	Data		
Assembly	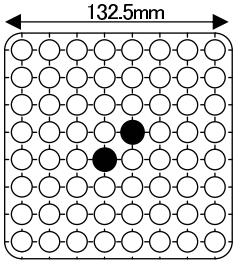 0-1	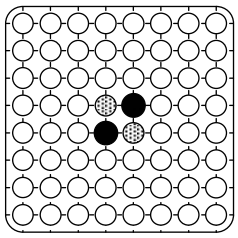 0-2	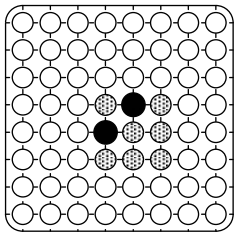 0-3
Simulated fuel assembly type		8 × 8	
Number of heated rods	62	60	55
Number of unheated rods	0	2	7
Heated rods outer diameter (mm)	12.3		
Heated rods pitch (mm)	16.2		
Axial heated length (mm)	3 708		

○ Heated rod, ❁ Unheated rod, ● Water rod – no flow in water rods

Table 3.2.6. Geometry and power shape of test assembly types 0-1, 0-2 and 0-3 (*cont.*)

Item	Data
Number of water rods	2
Water rods outer diameter (mm)	15.0
Channel box inner width (mm)	132.5
Channel box corner radius (mm)	8.0
In channel flow area (mm^2)	9 781
Spacer type	Grid
Number of spacers	7
Spacer pressure loss coefficients	1.2
Spacer location (mm)	455, 967, 1 479, 1 991, 2 503, 3 015, 3 527 (distance from bottom of heated length to spacer bottom face)
Radial power shape	Uniform
Axial power shape	Uniform

Table 3.2.7 provides the geometry and power shape information for bundles 1, 2 and 3. All the bundle designs use a spacer grid, which dimensions will be discussed in Section 3.4.

Table 3.2.7. Geometry and power shape of test assembly types 1, 2 and 3

Item	Data		
Assembly	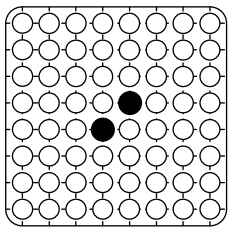 1	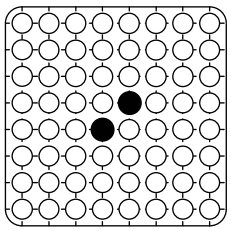 2	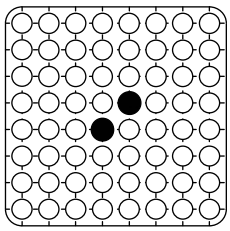 3
Simulated fuel assembly type		8 × 8	
Number of heated rods		62	
Heated rods outer diameter (mm)		12.3	
Heated rods pitch (mm)		16.2	
Axial heated length (mm)	3 708	1 747	3 708
Number of water rods		2	
Water rods outer diameter (mm)		15.0	
Channel box inner width (mm)		132.5	
Channel box corner radius (mm)		8.0	
In channel flow area (mm^2)		9 781	
Spacer type		Grid	
Number of spacers		7	
Spacer pressure loss coefficients		1.2	
Spacer location (mm)		455, 967, 1 479, 1 991, 2 503, 3 015, 3 527 (distance from bottom of heated length to spacer bottom face)	
Radial power shape		Simulation pattern for beginning of operation	
Axial power shape	Cosine	Half-cosine	Inlet peak

○ Heated rod, ❁ Unheated rod, ● Water rod – no flow in water rods

Assembly type 4, shown in Table 3.2.1, is designed as a high burn-up 8 × 8 fuel bundle, and has a large water rod at the bundle centre. Table 3.2.8 gives the geometry for this design. As indicated, there were four (4) different configurations tested for the high burn-up design. The grid used in these tests is a ferrule grid; it is discussed in Section 3.4.

Table 3.2.8. Geometry and power shape of test assembly types 4, C2A, C2B and C3

Item	Data			
Test assembly	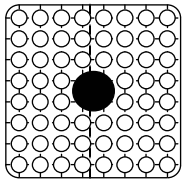			
	4	C2A	C2B	C3
Simulated fuel assembly type	High burn-up 8 × 8			
Number of heated rods	60			
Heated rods outer diameter (mm)	12.3			
Heated rods pitch (mm)	16.2			
Axial heated length (mm)	3708			
Number of water rods	1			
Water rods outer diameter (mm)	34.0			
Channel box inner width (mm)	132.5			
Channel box corner radius (mm)	8.0			
In channel flow area (mm^2)	9463			
Spacer type	Ferrule			
Number of spacers	7			
Spacer pressure loss coefficients	1.2			
Spacer location (mm)	455, 967, 1479, 1991, 2503, 3015, 3527 (distance from bottom of heated length to spacer bottom face)			
Radial power shape	A	A	B	A
Axial power shape	Uniform	Cosine	Cosine	Inlet-peak

○ Heated rod, ● Water rod – no flow in water rods
A: Simulation pattern for beginning of operation.
B: Simulation pattern for middle of operation.

3.3 Heater rod specification

Figure 3.3.1 shows the cross-sectional view of the heated rod. The rod is a single-ended, grounded electrical heater rod, which represents the nuclear fuel rod. The original geometry of the heater is spiral coil. This geometry treatment does not affect the steady-state calculation. For the transient the thermal time constant may affect the results. Therefore in addition to the demonstrated geometrical data, a thermal time constant of about 5 seconds is specified as a reference value. The heater rod structure is given in Table 3.3.1. The cladding, insulator and heater are made of inconel, boron nitride and nichrome, respectively. Gaps between heater, insulator and cladding could be assumed zero contact. The heated rod surface temperature is measured by chromel-alumel thermocouples, which have a diameter of 0.5 mm. Individual cladding thermocouples are embedded in the cladding surface. Axially, they are positioned mainly just upstream of the spacers. Each heated rod is joined to an X-ray transmission section, which has the same diameter as the heated rod but the cladding is made of beryllium (Be) for case of X-ray transmission.

Figure 3.3.1. Cross-sectional view of heater rod

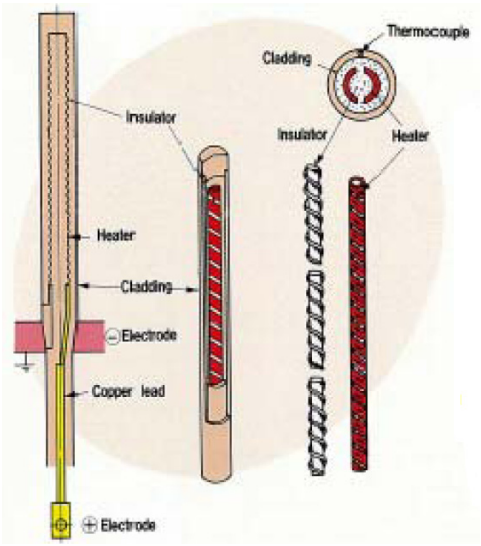

Table 3.3.1. Heater rod structure

Item		Data
Heater	Outer diameter (mm)	7.3
	Material	Nichrome
Insulator	Outer diameter (mm)	9.7
	Material	Boron nitride
Cladding	Thickness (mm)	1.3
	Material	Inconel 600/berylium

3.4 Thermo-mechanical properties

The thermo-mechanical properties listed below are based on the MATPRO model used in TRAC code [8]. Updated values of the coil properties will be provided as they become available.

3.4.1 Properties of nichrome

It is assumed that nichrome coils have similar properties as those of constantan.

- *Density*
  A constant value of 8 393.4 kg/m^3 is used.

- *Specific heat*
  The specific heat is $c_p = 110 T_f^{0.2075}$, where c_p is the specific heat (J/kg.K) and T_f is the temperature (F).

- *Thermal conductivity*
  The thermal conductivity is k = 29.18 + 2.683 × $10^{-3}(T_f - 100)$, where k is the thermal conductivity (W/m.K) and T_f is the temperature (F).

3.4.2 Properties of boron nitride

- *Density*
  A constant value of 2 002 kg/m^3 is used.

- *Specific heat*
  The specific heat is $c_p = 760.59 + 1.7955T_f - 8.6704 \times 10^{-4} T_f^2 + 1.5896 \times 10^{-7} T_f^3$, where c_p is the specific heat (J/kg.K) and T_f is the temperature (F).

- *Thermal conductivity*
  The boron-nitride thermal-conductivity calculation, based on a conversion to SI units of a curve fit is $k = 25.27 - 1.365 \times 10^{-3} T_f$, where k is the thermal conductivity (W/m.K) and T_f is the temperature (F).

3.4.3 Properties of Inconel 600

- *Density*
  The density is $\rho = 16.01846 \times \left(5.261008 \times 10^2 - 1.345453 \times 10^{-2} T_f - 1.194357 \times 10^{-7} T_f^2\right)$, where ρ is the density (kg/m^3) and T_f is the temperature (F).

- *Specific heat*
  The specific heat is $c_p = 4186.8 \times (0.1014 + 4.378952 \times 10^{-5} T_f - 2.046138 \times 10^{-8} T_f^2 + 3.418111 \times 10^{-11} T_f^3 - 2.060318 \times 10^{-13} T_f^4 + 3.682836 \times 10^{-16} T_f^5 - 2.458648 \times 10^{-19} T_f^6 + 5.597571 \times 10^{-23} T_f^7)$, where c_p is the specific heat (J/kg.K) and T_f is the temperature (F).

- *Thermal conductivity*
  The thermal conductivity is $k = 1.729577 \times (8.011332 + 4.643719 \times 10^{-3} T_f + 1.872857 \times 10^{-6} T_f^2 - 3.914512 \times 10^{-9} T_f^3 + 3.475513 \times 10^{-12} T_f^4 - 9.936696 \times 10^{-16} T_f^5$, where k is the thermal conductivity (W/m.K) and T_f is the temperature (F).

Since no information on the heat loss is available in the NUPEC BFBT database, an adiabatic condition is suggested for the benchmark.

3.5 Spacer data

Spacer grids are used to support fuel rods in nuclear reactor fuel assemblies. These grids interact with the flow and heat transfer in a number of ways. It is known that they generally have a beneficial effect on critical heat flux (CHF) in typical nuclear reactor assemblies. However, the enhancement obtained depends on the geometrical characteristics of the spacer grids as well as on the parameter range in terms of pressure, local mass velocity and quality. Spacer grids decrease the flow cross-sectional area locally and thereby increase the local pressure drop and heat transfer coefficients. They may have special geometrical features to promote turbulence, the effect of which may propagate further downstream. Spacer grids may provide a larger surface area on which to collect the entrained liquid droplets, which may cause increase in the local fluid film flow rate under sub-CHF conditions and may lead to rewetting of the fuel rod cladding under post-CHF conditions.

There are two types of spacers used in the NUPEC BFBT experiments – ferrule type and grid type. The grid type spacers are applied to the 8×8 assemblies (assembly types 0, 1, 2, and 3). The ferrule type is applied to the high burn-up 8×8 assemblies (assembly types 4, C2A, C2B and C3).

Figure 3.5.1 shows different view of grid spacer design. Since this is not a design drawing some disparity from the symmetry on the rod arrangement could occur. The rod arrangement should be considered as homogeneous.

Figure 3.5.2 shows different views of the ferrule spacer, which was used for the high burn-up fuel assembly design. These figures and the data for both spacer designs were provided by JNES of Japan.

Using the JNES spacers' data, the spacer grid and ferrule grid dimensions were estimated in co-operation with the OECD NEA, as described below. The numerical data was extracted and scaled from the figures using SigmaScan Pro 5.0 software. The graphical reconstruction was based on the extracted data using 3DsMax 5, PhotoShop and Paint Shop Pro 7. The precision of the process used is estimated to be between 2% and 5% (1σ) depending on the size of the object measured (the smaller the object, the higher the uncertainty, as the smaller items are not always exactly to scale). It should be noted that the graphics made available might have been slightly deformed through the different copying processes therefore it is difficult to be precise on the uncertainty of the data provided. The estimated dimensions and 3-D views of the spacers are depicted in Figures 3.5.3 through 3.5.16.

An estimate of the ferrule grid dimensions was performed at PSU. The results are shown in Figure 3.5.17.

Here it should be noted that the uncertainties in the spacer grid dimensions, as provided in Figure 3.5.3, lead to modelling problems (for example, the water rod has bigger diameter than the distance between grid straps). The participants are welcome to perform more realistic estimations of the spacer grid dimensions. However, if requested PSU can provide such estimate.

In this specification, only bundle average spacer pressure loss coefficients are provided (see Tables 3.2.6 through 3.2.8). Depending on the participants' computer code, and using the provided spacer data, each participant may choose the sub-channel grids loss coefficients or other required input values.

The PSU will provide best-estimate individual sub-channel loss coefficients, based on the spacer grid information as provided by JNES, for each spacer design. The method used to perform these estimates as well as the best-estimate values will be provided to the participants for their consideration.

Figure 3.5.1. Schematic of the grid spacer (dimensions in mm)

(a) Top view

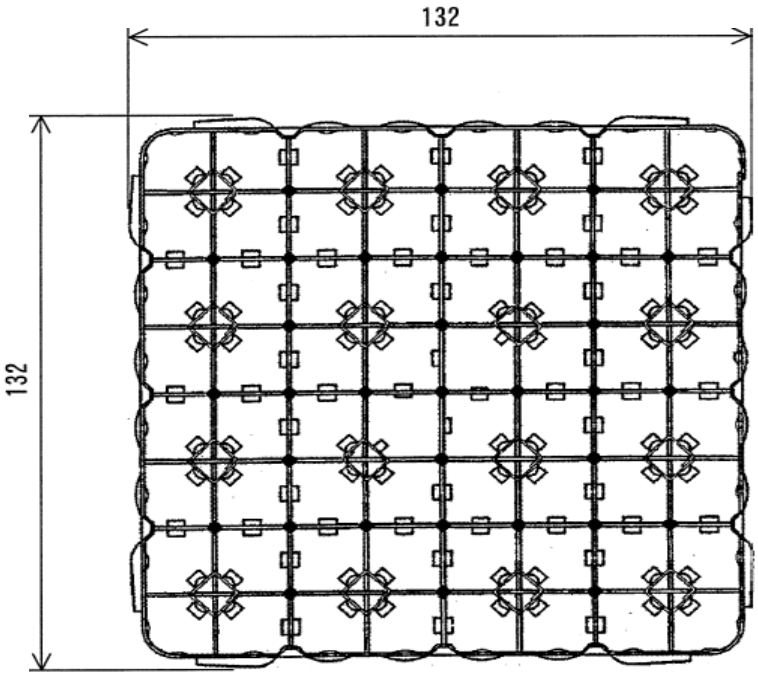

(b) Side view

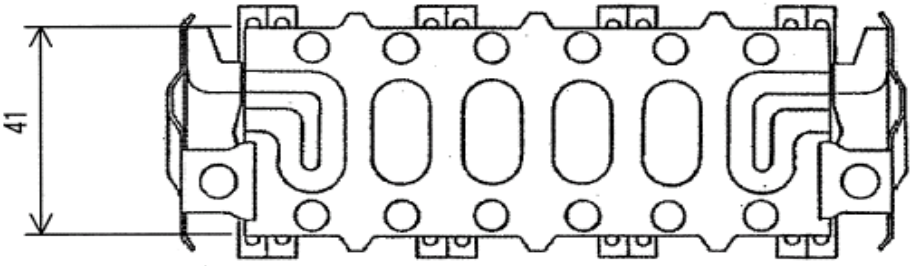

(c) Elementary structure

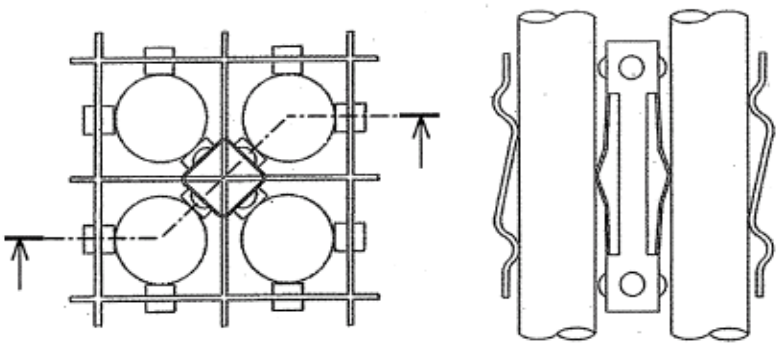

Figure 3.5.2. Schematic of ferrule spacer design (dimensions in mm)

(a) Top view

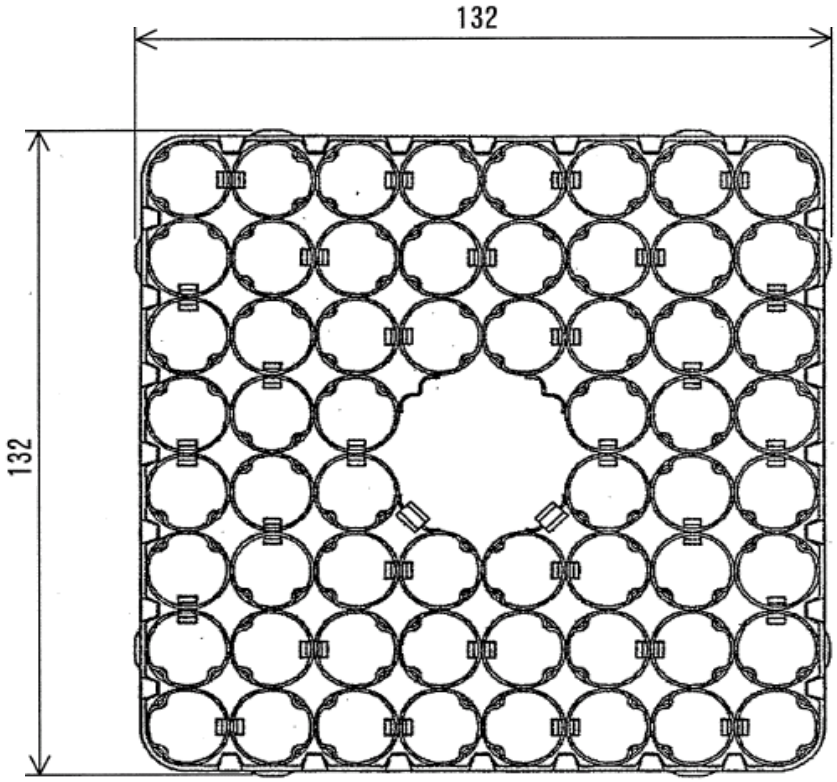

(b) Side view

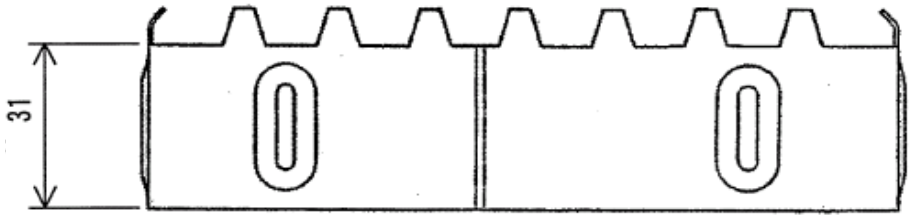

(c) Elementary structure

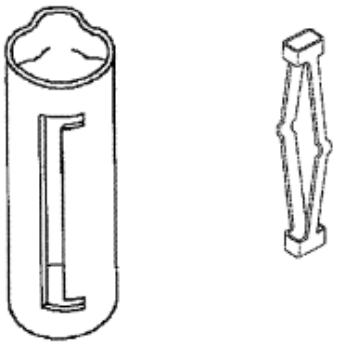

Figure 3.5.3. Grid spacer – dimensions

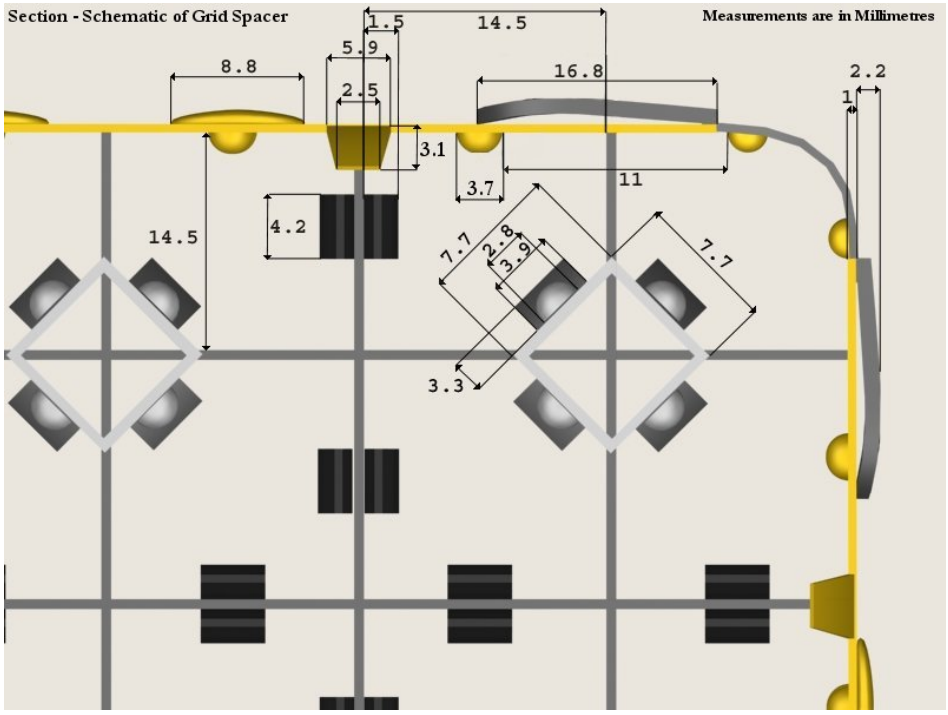

Figure 3.5.4. Grid spacer – dimensions

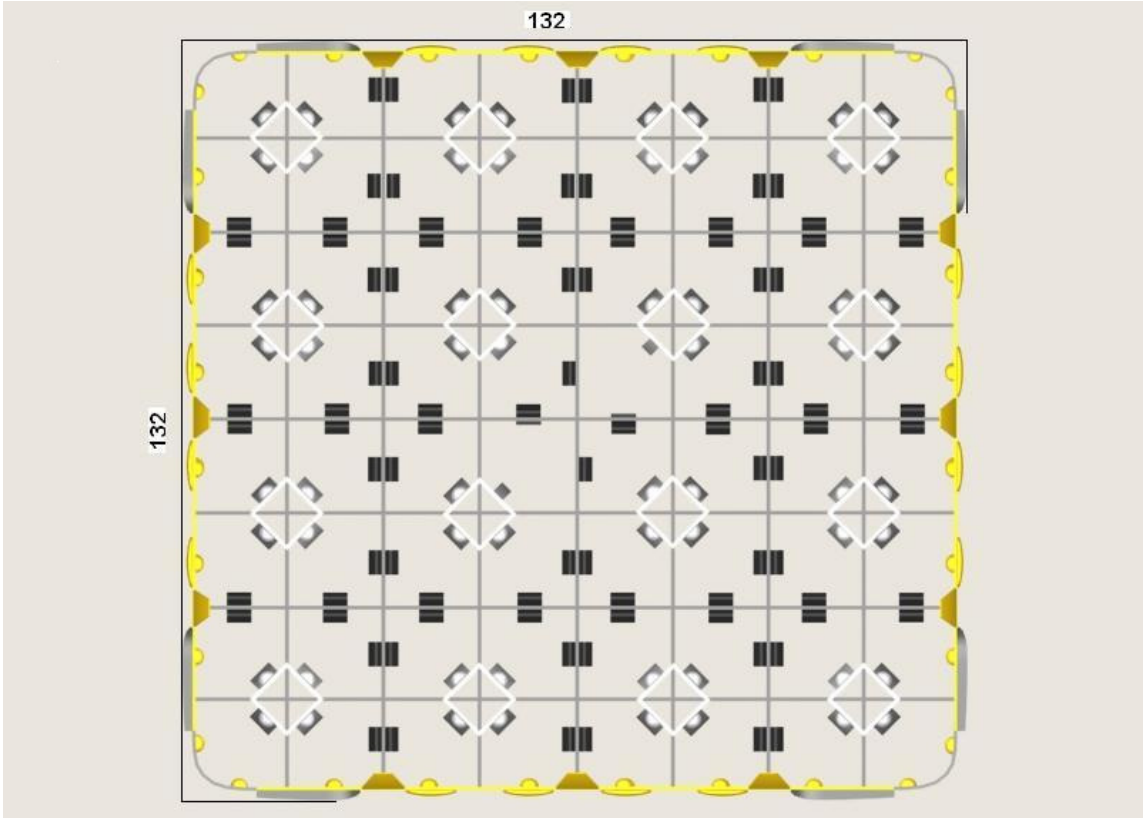

Figure 3.5.5. Grid spacer – central view

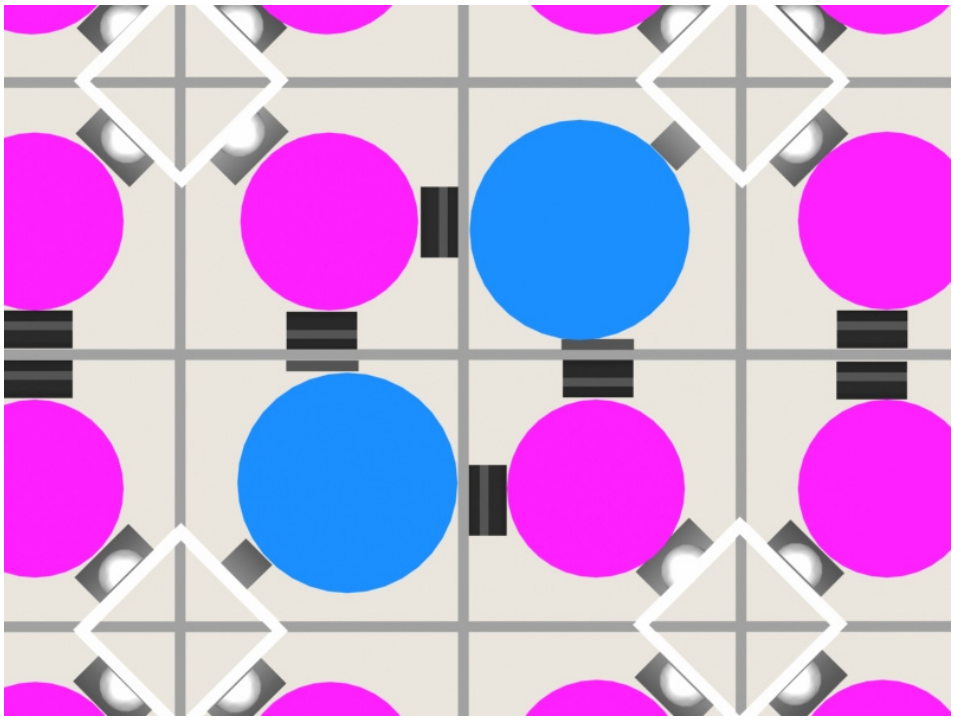

Figure 3.5.6. Grid spacer – 3-D bottom view

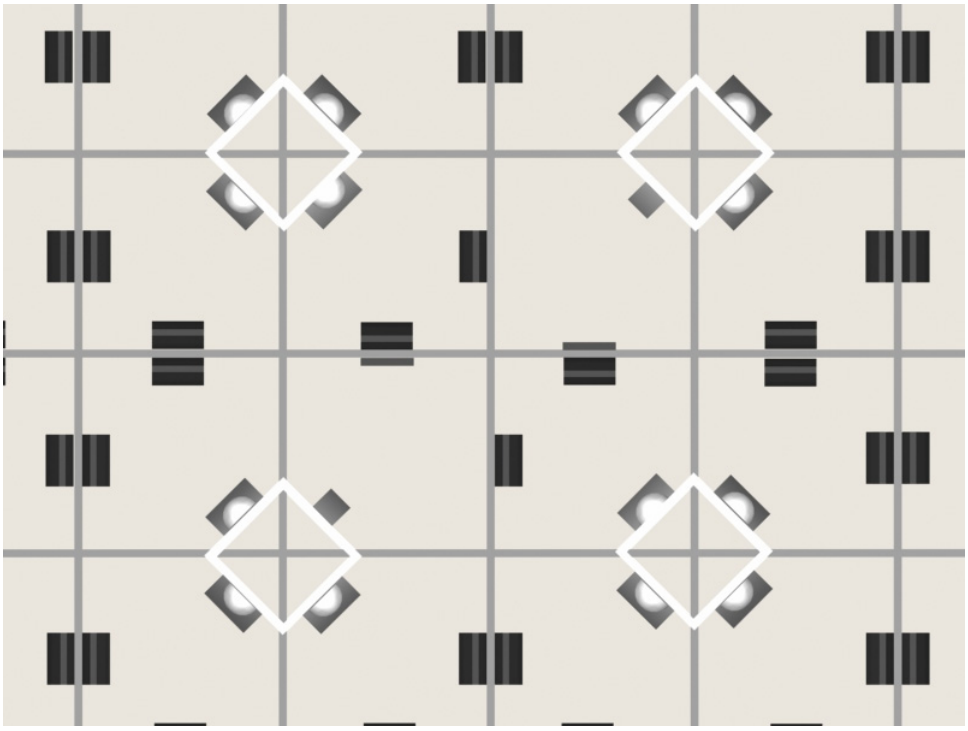

Figure 3.5.7. Grid spacer – 3-D view

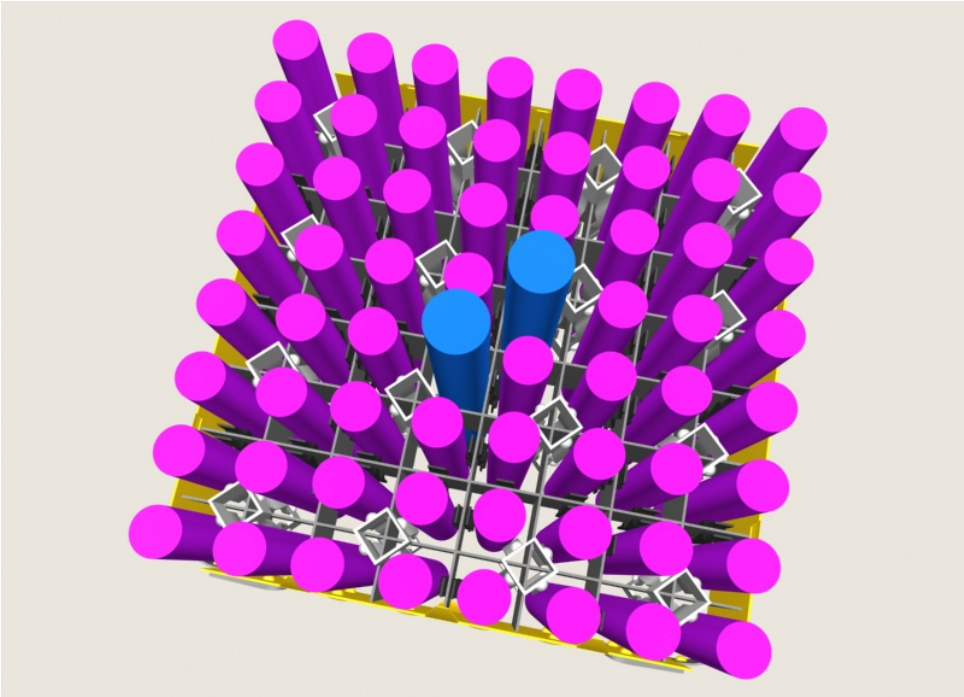

Figure 3.5.8. Grid spacer – 3-D view

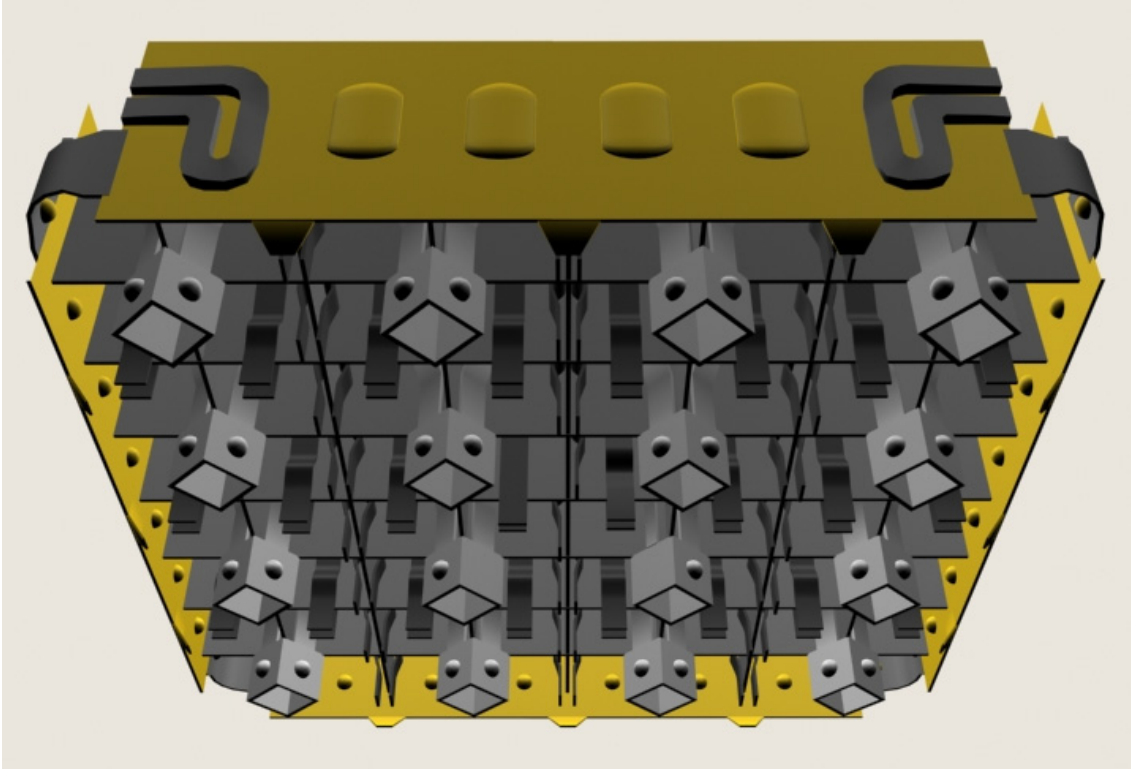

Figure 3.5.9. Grid spacer – 3-D view

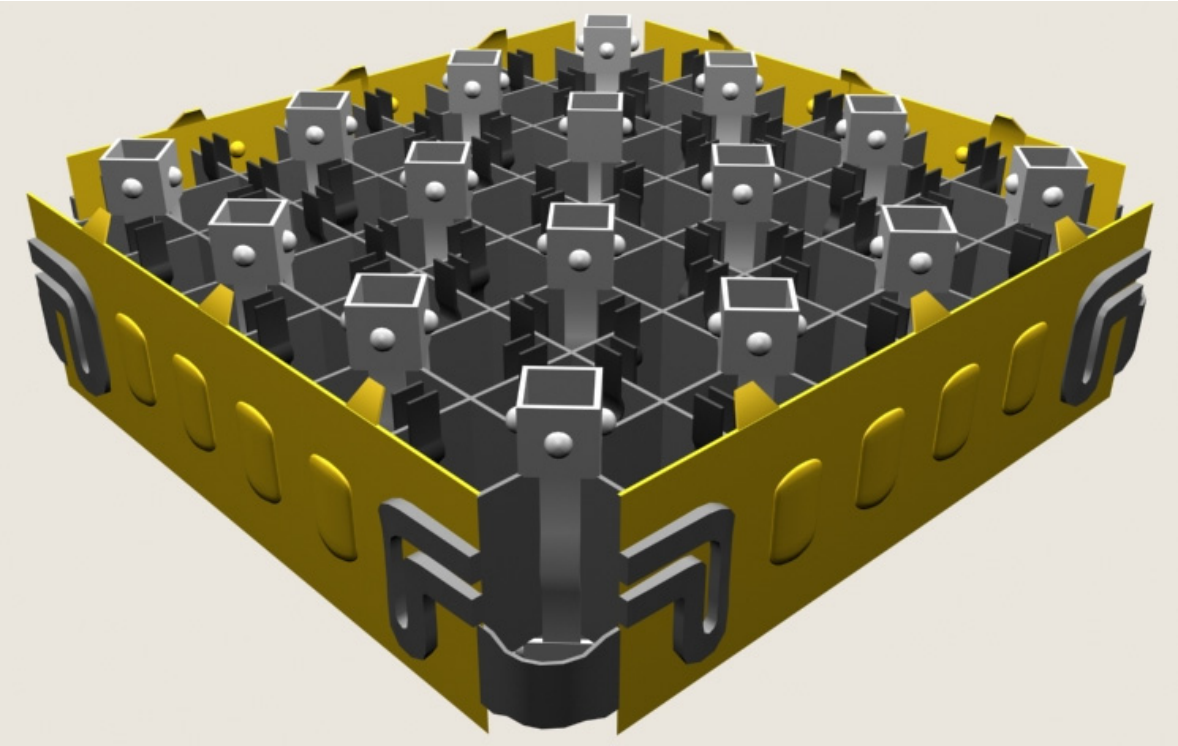

Figure 3.5.10. Grid spacer – 3-D view

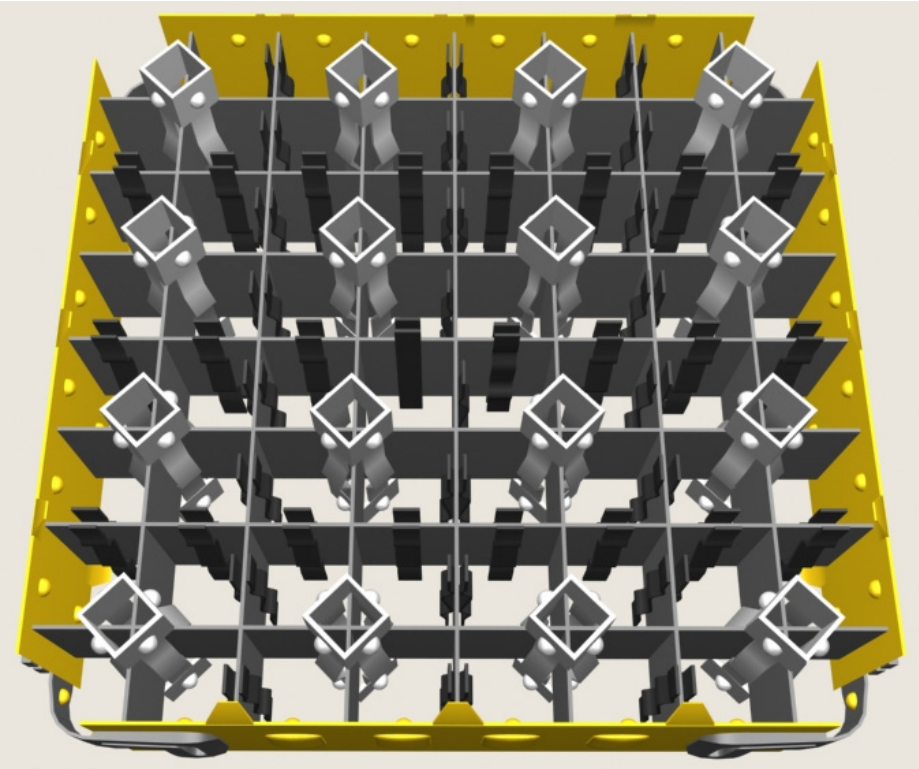

Figure 3.5.11. Grid spacer – side view

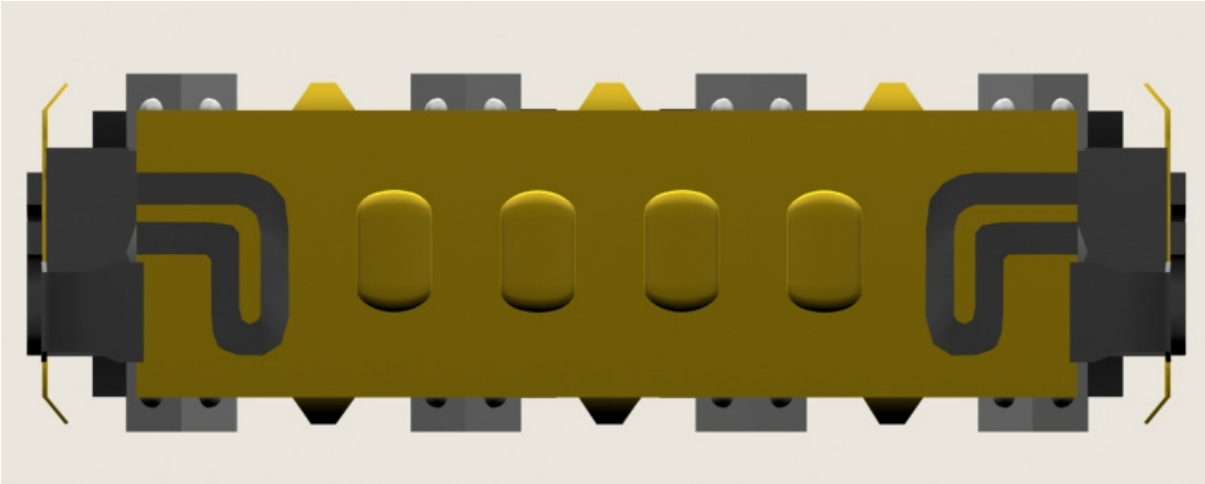

Figure 3.5.12. Ferrule spacer design – dimensions

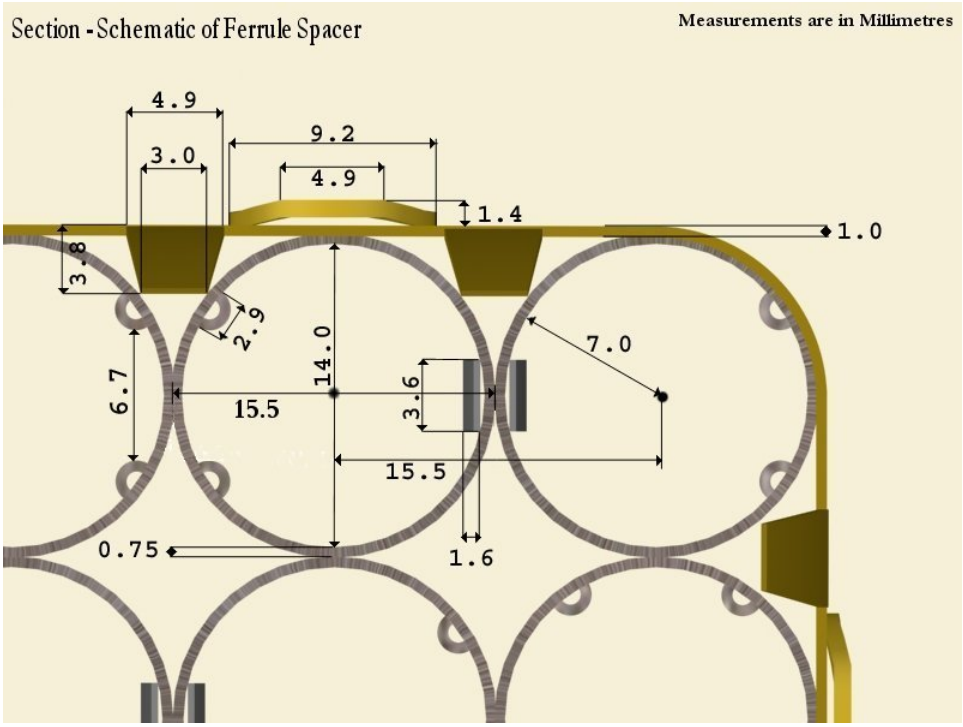

Figure 3.5.13. Ferrule spacer – 3-D view

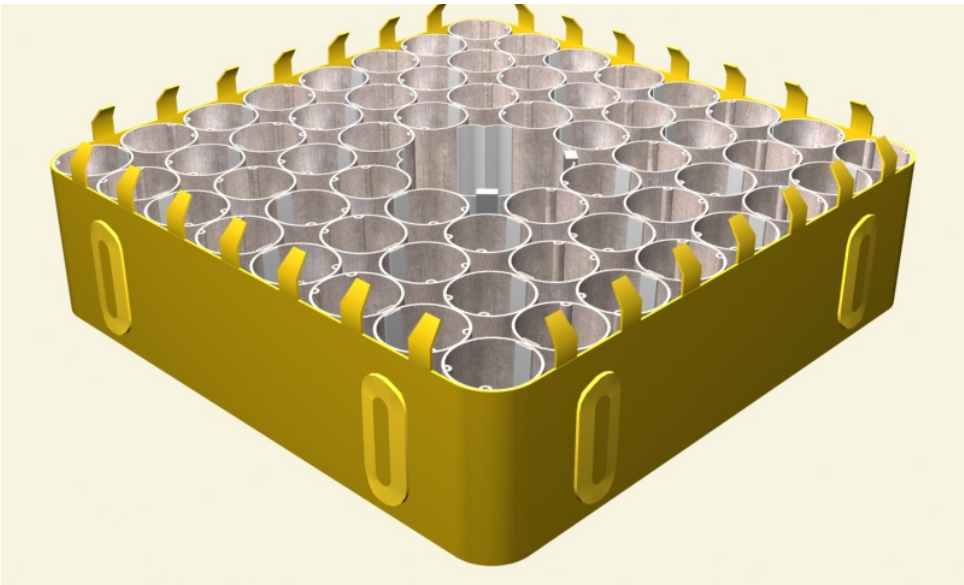

Figure 3.5.14. Ferrule spacer – 3-D view

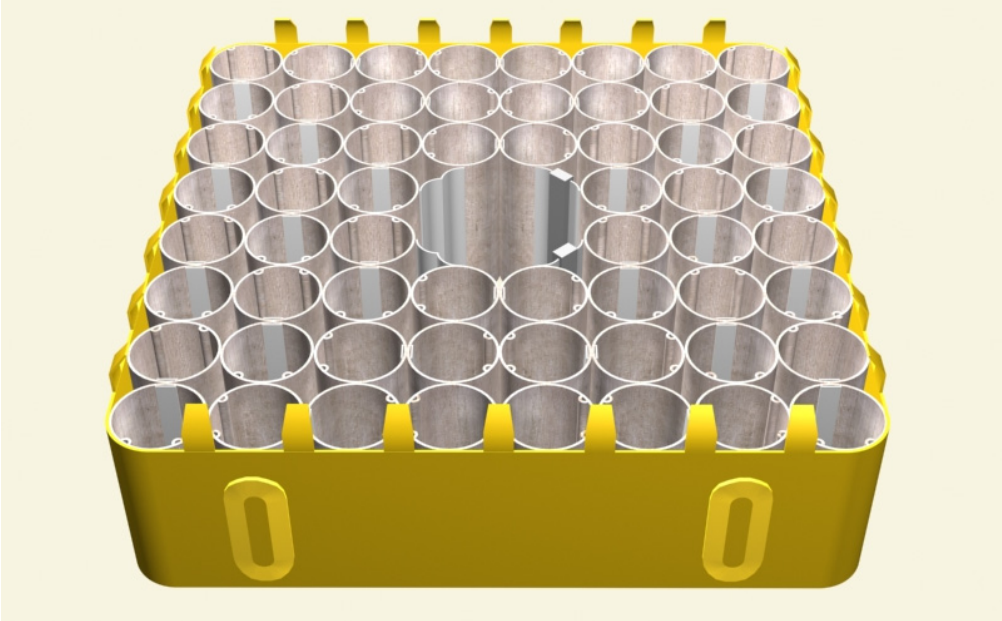

Figure 3.5.15. Ferrule spacer – side view

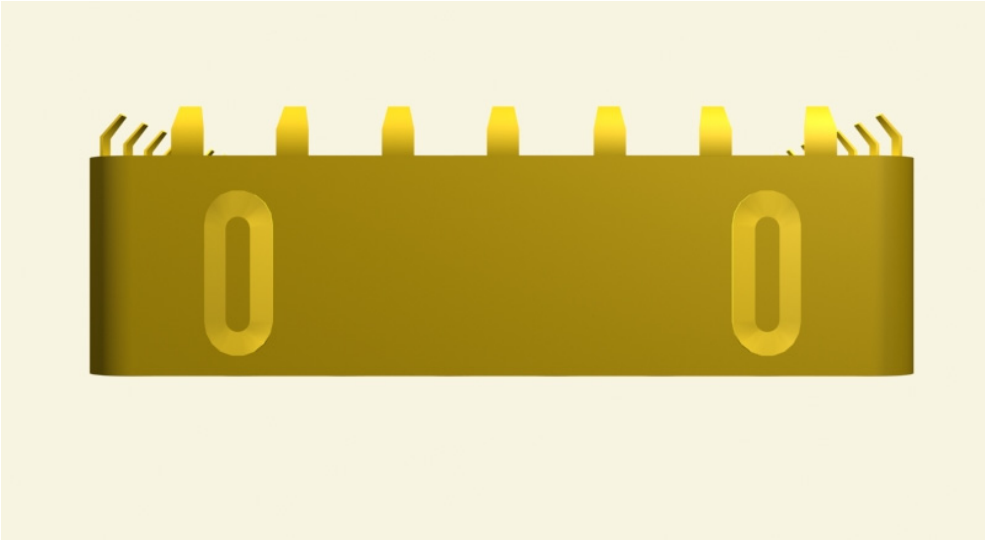

Figure 3.5.16. Ferrule spacer – top view

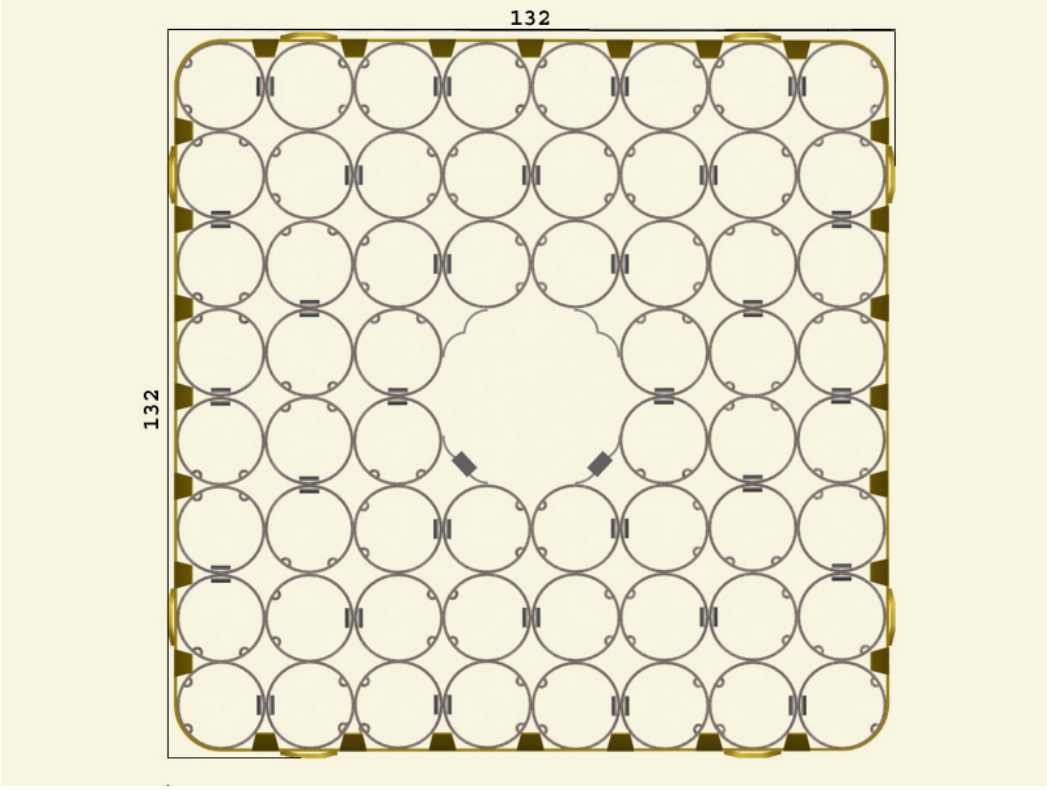

Figure 3.5.17. Schematic of ferrule spacer

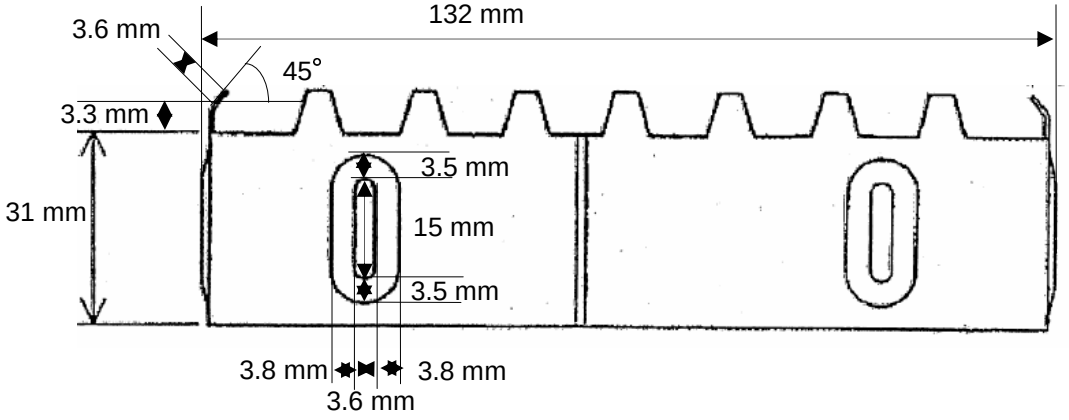

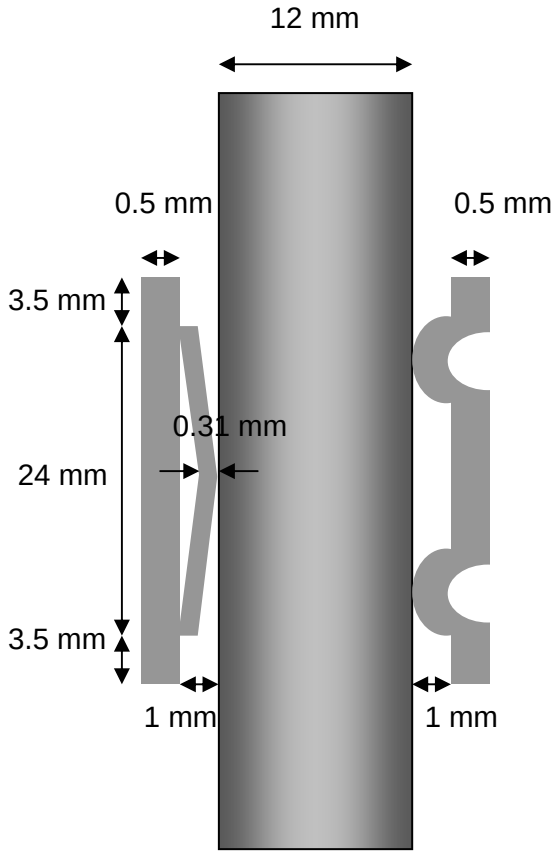

Chapter 4

BENCHMARK DATABASE

4.1 Introduction

A significant amount of data has been collected in the NUPEC BWR full-size mock-up test series. This chapter describes the complete NUPEC BFBT benchmark database. The data is summarised in Table 4.1.1.

Table 4.1.1. NUPEC BFBT database

Void distribution measurements	**No. of data sets**
Steady state void distribution measurements	392
Transient void distribution measurements	2
Critical power measurements	**No. of data sets**
Single-phase pressure drop measurements	36
Two-phase pressure drop measurements	33
Steady-state critical power measurements	151
Transient critical power measurements	4

Test cases selected for comparative analysis in the framework of the OECD/NRC BFBT benchmark will be described in Chapter 5.

4.2 Void distribution measurements

The boundary conditions for the steady-state void distribution measurements are given in Table 4.2.1.

Table 4.2.2 represents a summary of the experimental and process data for different types of assemblies. “Process data” is a terminology used in the original BFBT database for the actual values in time.

The test matrix of steady-state void distributions is given in Table 4.2.3 for each assembly type and design.

The full set of experimental and process conditions of the steady-state void distribution measurements is provided in Tables 4.2.4 through 4.2.17.

Table 4.2.1. Steady-state void distribution measurement conditions

Assembly	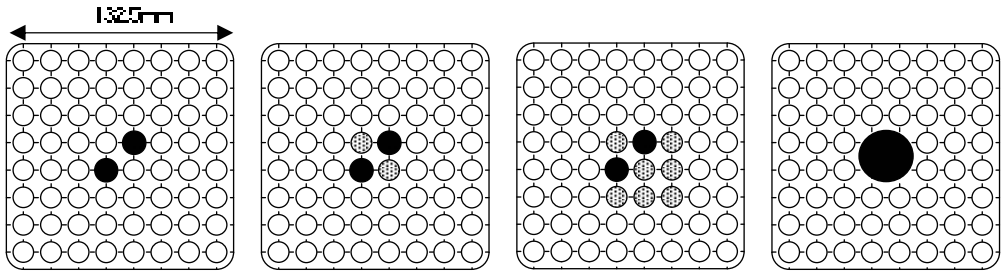 0-1, 1, 2, 3 0-2 0-3 4	
Boundary conditions	Pressure (MPa) Flow rate (t/h) Inlet sub-cooling (kJ/kg) Exit quality (%)	7.2 55 50.2 2 5 8 12 18 25
Data	Void distribution matrix in sub-channel mesh size Void distribution matrix in 0.3 × 0.3 mm mesh size (512 × 512 = 262K pixels) Corresponding boundary conditions	
No. of cases	Data supplied cases Exercise cases	392 Sub-channel: 15 Microscopic: 4

Exit quality: Thermal equilibrium quality.

Table 4.2.2. Summary experimental and process data for different types of assemblies

Assembly type	Tables representing experimental data	Tables representing process data
0-1	4.2.4	4.2.5
0-2	4.2.6	4.2.7
0-3	4.2.8	4.2.9
1	4.2.10	4.2.11
2	4.2.12	4.2.13
3	4.2.14	4.2.15
4	4.2.16	4.2.17

Table 4.2.3. Test matrix of steady-state void distribution measurements

Assembly	Pressure (Mpa)	Inlet sub-cooling (kJ/kg)	Flow rate (t/h)	Exit quality (%)						No. of data
				2	5	8	12	18	25	
0-1	1.0	50.2	10	X	X	X	X	–	–	13
			30	X	X	X	X	–	–	
			55	X	X	W	X	–	–	
	3.9		10	X	X	X	X	X	X	19
			30	X	X	X	X	X	X	
			55	X	X	X	X	X	W	
	7.2	20.9	45	–	X	–	X	–	–	36
		50.2	10	X	X	X	X	X	X	
			20	X	X	X	X	X	X	
			30	X	X	X	X	X	X	
			55	W	E1	W	E1	W	E1	
			70	X	X	X	X	X	–	
		126	55	–	X	–	X	–	–	
	8.6	50.2	10	X	X	X	X	X	X	18
			30	X	X	X	X	X	X	
			55	X	X	X	X	W	–	
0-2	3.9	50.2	55	X	X	X	X	X	W	28
	7.2		10	X	X	X	X	X	X	
			30	X	X	X	X	X	X	
			55	W	E1	W	E1	W	E1	
			70	X	X	X	X	X	–	
	8.6		55	X	X	X	X	W	–	
0-3	3.9	50.2	55	X	X	X	X	X	W	28
	7.2		10	X	X	X	X	X	X	
			30	X	X	X	X	X	X	
			55	W	E1	W	E1	W	E1	
			70	X	X	X	X	X	–	
	8.6		55	X	X	X	X	W	–	
1	1.0	50.2	10	X	X	X	X	–	–	13
			30	X	X	X	X	–	–	
			55	X	E4	W	X	–	–	
	3.9		10	X	X	X	X	X	X	19
			30	X	X	X	X	X	X	
			55	X	E4	X	X	X	W	
	7.2	20.9	45	–	X	–	X	–	–	36
		50.2	10	X	E4	X	X	X	X	
			20	X	E4	X	X	X	X	
			30	X	X	X	X	X	X	
			55	W,E4	E1, E4	W	E1, E4	W	E1, E4	
			70	X	E4	X	X	X	–	
		126	55	E4	X	–	X	–	–	
	8.6	50.2	10	X	X	X	X	X	X	18
			30	X	X	X	X	X	X	
			55	X	E4	X	X	W	–	

X: test case, W: duplicated test case, E1: Exercise 1 case, E2: Exercise 2 case, E4: Exercise 4 case.

Table 4.2.3. Test matrix of steady-state void distribution measurements (*cont.*)

Assembly	Pressure (Mpa)	Inlet sub-cooling (kJ/kg)	Flow rate (t/h)	Exit quality (%)						No. of data
				2	5	8	12	18	25	
2	3.9	50.2	10	X	X	X	X	–	X	14
			30	X	X	X	X	–	–	
			55	X	X	X	X	–	–	
	7.2		10	X	X	X	X	–	X	23
			20	X	X	X	X	–	X	
			30	X	X	X	X	–	X	
			55	X	X	X	W	–	–	
			70	X	X	X	–	–	–	
	8.6		10	X	X	X	X	–	X	13
			30	X	X	X	X	–	–	
			55	X	X	W	–	–	–	
3	3.9	50.2	55	X	X	X	X	X	W	28
	7.2		10	X	X	X	X	X	X	
			30	X	X	X	X	X	X	
			55	W	X	W	X	W	X	
			70	X	X	X	X	X	–	
	8.6		55	X	X	X	X	W	–	
4	1.0	50.2	10	X	X	X	X	–	–	13
			30	X	X	X	X	–	–	
			55	X	X	W	X	–	–	
	3.9		10	X	X	X	X	X	X	19
			30	X	X	X	X	X	X	
			55	X	X	X	X	X	W	
	7.2	20.9	45	–	X	–	X	–	–	36
		50.2	10	X	X	X	X	X	X	
			20	X	X	X	X	X	X	
			30	X	X	X	X	X	X	
			55	W,E2	E1, E2	W	E1, E2	W	E1, E2	
			70	X	X	X	X	X	–	
		126	55	–	X	–	X	–	–	
	8.6	50.2	10	X	X	X	X	X	X	18
			30	X	X	X	X	X	X	
			55	X	X	X	X	W	–	

X: Test case, W: Duplicated test case, E1: Exercise 1 case, E2: Exercise 2 case.

Table 4.2.4. Experimental conditions for steady-state void distribution measurement data – assembly 0-1

Experiment conditions	Pressure (MPa)	Flow rate (t/h)	Inlet sub-cooling (kJ/kg)	Outlet quality (%)	Experimental cases
Test 0011-01	0.981	10	50.2	1	–
Test 0011-02	0.981	10	50.2	3	–
Test 0011-03	0.981	10	50.2	5	–
Test 0011-04	0.981	10	50.2	12	–
Test 0011-05	0.981	30	50.2	1	–
Test 0011-06	0.981	30	50.2	3	–
Test 0011-07	0.981	30	50.2	5	–
Test 0011-08	0.981	30	50.2	12	–
Test 0011-09	0.981	55	50.2	1	–
Test 0011-10	0.981	55	50.2	3	–
Test 0011-11	0.981	55	50.2	5	Duplicated test
Test 0011-12	0.981	55	50.2	5	Duplicated test
Test 0011-13	0.981	55	50.2	12	–
Test 0011-14	3.923	10	50.2	2	–
Test 0011-15	3.923	10	50.2	5	–
Test 0011-16	3.923	10	50.2	8	–
Test 0011-17	3.923	10	50.2	12	–
Test 0011-18	3.923	10	50.2	18	–
Test 0011-19	3.923	10	50.2	25	–
Test 0011-20	3.923	30	50.2	2	–
Test 0011-21	3.923	30	50.2	5	–
Test 0011-22	3.923	30	50.2	8	–
Test 0011-23	3.923	30	50.2	12	–
Test 0011-24	3.923	30	50.2	18	–
Test 0011-25	3.923	30	50.2	25	–
Test 0011-26	3.923	55	50.2	2	–
Test 0011-27	3.923	55	50.2	5	–
Test 0011-28	3.923	55	50.2	8	–
Test 0011-29	3.923	55	50.2	12	–
Test 0011-30	3.923	55	50.2	18	–
Test 0011-31	3.923	55	50.2	25	Duplicated test
Test 0011-32	3.923	55	50.2	25	Duplicated test
Test 0011-33	7.159	10	50.2	2	–
Test 0011-34	7.159	10	50.2	5	–
Test 0011-35	7.159	10	50.2	8	–
Test 0011-36	7.159	10	50.2	12	–
Test 0011-37	7.159	10	50.2	18	–
Test 0011-38	7.159	10	50.2	25	–
Test 0011-39	7.159	20	50.2	2	–
Test 0011-40	7.159	20	50.2	5	–
Test 0011-41	7.159	20	50.2	8	–
Test 0011-42	7.159	20	50.2	12	–
Test 0011-43	7.159	20	50.2	18	–

Table 4.2.4. Experimental conditions for steady-state void distribution measurement data – assembly 0-1 (*cont.*)

Experiment conditions	Pressure (MPa)	Flow rate (t/h)	Inlet sub-cooling (kJ/kg)	Outlet quality (%)	Experimental cases
Test 0011-44	7.159	20	50.2	25	–
Test 0011-45	7.159	30	50.2	2	–
Test 0011-46	7.159	30	50.2	5	–
Test 0011-47	7.159	30	50.2	8	–
Test 0011-48	7.159	30	50.2	12	–
Test 0011-49	7.159	30	50.2	18	–
Test 0011-50	7.159	30	50.2	25	–
Test 0011-51	7.159	55	20.9	5	–
Test 0011-52	7.159	55	20.9	12	–
Test 0011-53	7.159	55	50.2	2	Duplicated test
Test 0011-54	7.159	55	50.2	2	Duplicated test
Test 0011-55	7.159	55	50.2	5	E1
Test 0011-56	7.159	55	50.2	8	–
Test 0011-57	7.159	55	50.2	8	–
Test 0011-58	7.159	55	50.2	12	E1
Test 0011-59	7.159	55	50.2	18	Duplicated test
Test 0011-60	7.159	55	50.2	18	Duplicated test
Test 0011-61	7.159	55	50.2	25	E1
Test 0011-62	7.159	55	125.6	5	–
Test 0011-63	7.159	55	125.6	12	–
Test 0011-64	7.159	70	50.2	2	–
Test 0011-65	7.159	70	50.2	5	–
Test 0011-66	7.159	70	50.2	8	–
Test 0011-67	7.159	70	50.2	12	–
Test 0011-68	7.159	70	50.2	18	–
Test 0011-69	8.63	10	50.2	2	–
Test 0011-70	8.63	10	50.2	5	–
Test 0011-71	8.63	10	50.2	8	–
Test 0011-72	8.63	10	50.2	12	–
Test 0011-73	8.63	10	50.2	18	–
Test 0011-74	8.63	10	50.2	25	–
Test 0011-75	8.63	30	50.2	2	–
Test 0011-76	8.63	30	50.2	5	–
Test 0011-77	8.63	30	50.2	8	–
Test 0011-78	8.63	30	50.2	12	–
Test 0011-79	8.63	30	50.2	18	–
Test 0011-80	8.63	30	50.2	25	–
Test 0011-81	8.63	55	50.2	2	–
Test 0011-82	8.63	55	50.2	5	–
Test 0011-83	8.63	55	50.2	8	–
Test 0011-84	8.63	55	50.2	12	–
Test 0011-85	8.63	55	50.2	18	Duplicated test
Test 0011-86	8.63	55	50.2	18	Duplicated test

E1: Exercise 1 case.

Table 4.2.5. Process conditions for steady-state void distribution measurement data – assembly 0-1

Process conditions	Pressure (MPa)	Flow rate (t/h)	Inlet sub-cooling (kJ/kg)	Power (MW)	Experimental cases
Test 0011-01	0.992	10.16	51.7	0.21	–
Test 0011-02	0.981	10.20	49.2	0.32	–
Test 0011-03	0.978	10.17	48.5	0.43	–
Test 0011-04	0.985	10.17	47.8	0.81	–
Test 0011-05	1.005	30.11	54.1	0.59	–
Test 0011-06	1.010	30.07	54.5	0.92	–
Test 0011-07	0.994	29.97	50.9	1.25	–
Test 0011-08	1.015	30.16	53.4	2.43	–
Test 0011-09	1.006	54.89	56.6	1.08	–
Test 0011-10	1.072	54.72	65.5	1.68	–
Test 0011-11	1.055	54.79	62.2	2.28	Duplicated test
Test 0011-12	1.058	54.84	62.8	2.28	Duplicated test
Test 0011-13	1.220	54.75	90.5	4.47	–
Test 0011-14	3.975	10.13	57.8	0.23	–
Test 0011-15	3.916	10.15	49.9	0.40	–
Test 0011-16	3.914	10.16	49.0	0.54	–
Test 0011-17	3.964	10.17	53.4	0.70	–
Test 0011-18	3.903	10.39	46.9	1.01	–
Test 0011-19	3.887	10.16	48.1	1.33	–
Test 0011-20	3.931	30.10	50.2	0.71	–
Test 0011-21	3.937	30.08	52.1	1.16	–
Test 0011-22	3.943	30.04	52.4	1.56	–
Test 0011-23	3.949	30.06	53.4	2.13	–
Test 0011-24	3.958	29.74	51.7	3.01	–
Test 0011-25	3.971	29.54	46.6	3.99	–
Test 0011-26	3.959	54.71	53.9	1.29	–
Test 0011-27	3.952	54.71	53.0	2.08	–
Test 0011-28	3.950	54.82	52.8	2.84	–
Test 0011-29	4.038	54.78	57.2	3.91	–
Test 0011-30	3.991	54.82	53.1	5.49	–
Test 0011-31	4.046	54.75	56.7	7.32	Duplicated test
Test 0011-32	4.030	54.78	54.1	7.32	Duplicated test
Test 0011-33	7.175	10.14	53.3	0.23	–
Test 0011-34	7.158	10.19	50.5	0.34	–
Test 0011-35	7.142	10.25	48.2	0.48	–
Test 0011-36	7.140	10.29	47.2	0.64	–
Test 0011-37	7.152	10.19	52.5	0.88	–
Test 0011-38	7.141	10.20	50.4	1.16	–
Test 0011-39	7.158	20.70	52.4	0.45	–
Test 0011-40	7.144	20.19	49.6	0.71	–
Test 0011-41	7.199	20.34	56.6	0.94	–
Test 0011-42	7.162	20.22	53.2	1.29	–

Table 4.2.5. Process conditions for steady-state void distribution measurement data – assembly 0-1 (*cont.*)

Process conditions	Pressure (MPa)	Flow rate (t/h)	Inlet sub-cooling (kJ/kg)	Power (MW)	Experimental cases
Test 0011-43	7.16	20.14	52.4	1.78	–
Test 0011-44	7.152	20.20	50.4	2.35	–
Test 0011-45	7.141	30.18	51.4	0.68	–
Test 0011-46	7.154	30.17	50.1	1.05	–
Test 0011-47	7.164	29.65	50.0	1.42	–
Test 0011-48	7.172	29.60	50.2	1.92	–
Test 0011-49	7.180	30.16	50.5	2.65	–
Test 0011-50	7.178	30.17	48.6	3.52	–
Test 0011-51	7.148	54.73	20.2	1.47	–
Test 0011-52	7.185	54.74	19.7	3.06	–
Test 0011-53	7.180	54.47	51.5	1.24	Duplicated test
Test 0011-54	7.173	54.18	52.3	1.22	Duplicated test
Test 0011-55	7.180	54.03	52.6	1.90	E1
Test 0011-56	7.168	54.83	51.6	2.57	–
Test 0011-57	7.158	54.84	49.8	2.59	–
Test 0011-58	7.172	54.90	51.0	3.51	E1
Test 0011-59	7.189	54.96	50.2	4.87	Duplicated test
Test 0011-60	7.184	54.85	52.1	4.86	Duplicated test
Test 0011-61	7.210	54.79	50.9	6.44	E1
Test 0011-62	7.214	54.89	129.9	3.06	–
Test 0011-63	7.188	54.91	125.2	4.67	–
Test 0011-64	7.184	69.91	53.0	1.56	–
Test 0011-65	7.179	69.84	52.7	2.43	–
Test 0011-66	7.190	69.85	53.5	3.3	–
Test 0011-67	7.182	69.93	51.4	4.45	–
Test 0011-68	7.188	69.98	50.4	6.20	–
Test 0011-69	8.624	10.23	59.7	0.24	–
Test 0011-70	8.618	10.25	58.2	0.35	–
Test 0011-71	8.635	10.18	51.4	0.46	–
Test 0011-72	8.641	10.15	49.5	0.62	–
Test 0011-73	8.635	10.15	50.7	0.86	–
Test 0011-74	8.631	10.13	49.4	1.10	–
Test 0011-75	8.639	29.93	51.8	0.67	–
Test 0011-76	8.631	29.94	49.9	1.02	–
Test 0011-77	8.638	30.26	49.6	1.37	–
Test 0011-78	8.628	30.19	49.2	1.83	–
Test 0011-79	8.661	30.06	49.5	2.52	–
Test 0011-80	8.633	29.52	45.7	3.33	–
Test 0011-81	8.636	54.52	50.3	1.21	–
Test 0011-82	8.655	54.35	51.9	1.84	–
Test 0011-83	8.656	54.85	57.5	2.48	–

E1: Exercise 1 case.

Table 4.2.6. Experimental conditions for steady-state void distribution measurement data – assembly 0-2

Experimental conditions	Pressure (MPa)	Flow rate (t/h)	Inlet sub-cooling (kJ/kg)	Outlet quality (%)	Experimental cases
Test 0021-01	3.923	55	50.2	5	–
Test 0021-02	3.923	55	50.2	12	–
Test 0021-03	7.159	10	50.2	2	–
Test 0021-04	7.159	10	50.2	5	–
Test 0021-05	7.159	10	50.2	8	–
Test 0021-06	7.159	10	50.2	12	–
Test 0021-07	7.159	10	50.2	18	–
Test 0021-08	7.159	10	50.2	25	–
Test 0021-09	7.159	30	50.2	2	–
Test 0021-10	7.159	30	50.2	5	–
Test 0021-11	7.159	30	50.2	8	–
Test 0021-12	7.159	30	50.2	12	–
Test 0021-13	7.159	30	50.2	18	–
Test 0021-14	7.159	30	50.2	25	–
Test 0021-15	7.159	55	50.2	2	–
Test 0021-16	7.159	55	50.2	5	E1
Test 0021-17	7.159	55	50.2	8	–
Test 0021-18	7.159	55	50.2	12	E1
Test 0021-19	7.159	55	50.2	18	–
Test 0021-20	7.159	55	50.2	18	–
Test 0021-21	7.159	55	50.2	25	E1
Test 0021-22	7.159	70	50.2	2	–
Test 0021-23	7.159	70	50.2	5	–
Test 0021-24	7.159	70	50.2	8	–
Test 0021-25	7.159	70	50.2	12	–
Test 0021-26	7.159	70	50.2	18	–
Test 0021-27	8.630	55	50.2	5	–
Test 0021-28	8.630	55	50.2	12	–

E1: Exercise 1 case.

Table 4.2.7. Process conditions for steady-state void distribution measurement data – assembly 0-2

Process conditions	Pressure (MPa)	Flow Rate (t/h)	Inlet Sub-cooling (kJ/kg)	Power (MW)	Experimental cases
Test 0021-01	3.939	54.80	50.8	2.07	–
Test 0021-02	3.923	54.87	52.3	3.91	–
Test 0021-03	7.164	10.32	54.6	0.25	–
Test 0021-04	7.158	10.25	53.2	0.36	–
Test 0021-05	7.162	10.32	53.3	0.49	–
Test 0021-06	7.157	10.38	51.1	0.64	–
Test 0021-07	7.155	10.31	47.0	0.90	–
Test 0021-08	7.150	10.31	47.0	1.17	–
Test 0021-09	7.165	30.30	52.4	0.67	–
Test 0021-10	7.160	30.31	51.1	1.05	–
Test 0021-11	7.168	30.17	53.0	1.42	–
Test 0021-12	7.171	30.16	52.2	1.91	–
Test 0021-13	7.170	30.17	49.0	2.66	–
Test 0021-14	7.180	30.15	47.8	3.55	–
Test 0021-15	7.163	54.73	52.3	1.23	–
Test 0021-16	7.190	54.85	54.0	1.91	E1
Test 0021-17	7.165	54.83	51.1	2.59	–
Test 0021-18	7.171	54.90	59.8	3.51	E1
Test 0021-19	7.167	54.90	49.4	4.86	–
Test 0021-20	7.164	54.82	51.5	4.85	–
Test 0021-21	7.179	54.90	51.4	6.45	E1
Test 0021-22	7.174	69.54	51.9	1.56	–
Test 0021-23	7.201	69.88	52.9	2.44	–
Test 0021-24	7.218	69.82	52.0	3.31	–
Test 0021-25	7.184	69.81	53.1	4.45	–
Test 0021-26	7.158	69.78	50.0	6.21	–
Test 0021-27	8.625	55.06	54.3	1.85	–
Test 0021-28	8.650	54.96	53.0	3.33	–

E1: Exercise 1 case.

Table 4.2.8. Experimental conditions for steady-state void distribution measurement data – assembly 0-3

Experiment conditions	Pressure (MPa)	Flow rate (t/h)	Inlet sub-cooling (kJ/kg)	Outlet quality (%)	Experimental cases
Test 0031-01	3.923	55	50.2	5	–
Test 0031-02	3.923	55	50.2	12	–
Test 0031-03	7.159	10	50.2	2	–
Test 0031-04	7.159	10	50.2	5	–
Test 0031-05	7.159	10	50.2	8	–
Test 0031-06	7.159	10	50.2	12	–
Test 0031-07	7.159	10	50.2	18	–
Test 0031-08	7.159	10	50.2	25	–
Test 0031-09	7.159	30	50.2	2	–
Test 0031-10	7.159	30	50.2	5	–
Test 0031-11	7.159	30	50.2	8	–
Test 0031-12	7.159	30	50.2	12	–
Test 0031-13	7.159	30	50.2	18	–
Test 0031-14	7.159	30	50.2	25	–
Test 0031-15	7.159	55	50.2	2	–
Test 0031-16	7.159	55	50.2	5	E1
Test 0031-17	7.159	55	50.2	8	–
Test 0031-18	7.159	55	50.2	12	E1
Test 0031-19	7.159	55	50.2	18	Duplicated test
Test 0031-20	7.159	55	50.2	18	Duplicated test
Test 0031-21	7.159	55	50.2	25	E1
Test 0031-22	7.159	70	50.2	2	–
Test 0031-23	7.159	70	50.2	5	–
Test 0031-24	7.159	70	50.2	8	–
Test 0031-25	7.159	70	50.2	12	–
Test 0031-26	7.159	70	50.2	18	–
Test 0031-27	8.630	55	50.2	5	–
Test 0031-28	8.630	55	50.2	12	–

E1: Exercise 1 case.

Table 4.2.9. Process conditions for steady-state void distribution measurement data – assembly 0-3

Process conditions	Pressure (MPa)	Flow rate (t/h)	Inlet sub-cooling (kJ/kg)	Power (MW)	Experimental cases
Test 0031-01	3.961	54.20	52.4	2.09	–
Test 0031-02	3.928	54.76	50.4	3.92	–
Test 0031-03	7.150	10.26	53.9	0.24	–
Test 0031-04	7.145	10.29	53.7	0.36	–
Test 0031-05	7.143	10.34	51.7	0.48	–
Test 0031-06	7.142	10.35	51.8	0.65	–
Test 0031-07	7.141	10.24	49.4	0.90	–
Test 0031-08	7.136	10.24	48.6	1.18	–
Test 0031-09	7.150	29.36	52.1	0.67	–
Test 0031-10	7.150	30.72	52.1	1.05	–
Test 0031-11	7.149	30.44	50.4	1.42	–
Test 0031-12	7.149	30.20	51.7	1.92	–
Test 0031-13	7.161	30.19	50.2	2.66	–
Test 0031-14	7.156	30.17	48.2	3.53	–
Test 0031-15	7.170	54.97	52.3	1.23	–
Test 0031-16	7.180	54.96	52.4	1.92	E1
Test 0031-17	7.160	54.78	50.5	2.59	–
Test 0031-18	7.179	54.79	50.0	3.52	E1
Test 0031-19	7.168	54.83	50.8	4.88	Duplicated tests
Test 0031-20	7.157	54.83	49.6	4.86	Duplicated tests
Test 0031-21	7.171	54.90	49.4	6.45	E1
Test 0031-22	7.189	69.35	53.5	1.56	–
Test 0031-23	7.152	69.73	51.2	2.42	–
Test 0031-24	7.170	69.82	52.4	3.30	–
Test 0031-25	7.177	69.81	51.9	4.46	–
Test 0031-26	7.195	69.90	50.7	6.20	–
Test 0031-27	8.662	54.96	55.9	1.84	–
Test 0031-28	8.662	54.87	53.9	3.34	–

E1: Exercise 1 case.

Table 4.2.10. Experimental conditions for steady-state void distribution measurement data – assembly 1

Experimental conditions	Pressure (MPa)	Flow rate (t/h)	Inlet sub-cooling (kJ/kg)	Outlet quality (%)	Experimental cases
Test 1071-01	0.981	10	50.2	1	–
Test 1071-02	0.981	10	50.2	3	–
Test 1071-03	0.981	10	50.2	5	–
Test 1071-04	0.981	10	50.2	12	–
Test 1071-05	0.981	30	50.2	1	–
Test 1071-06	0.981	30	50.2	3	–
Test 1071-07	0.981	30	50.2	5	–
Test 1071-08	0.981	30	50.2	12	–
Test 1071-09	0.981	55	50.2	1	–
Test 1071-10	0.981	55	50.2	3	–
Test 1071-11	0.981	55	50.2	5	Duplicated test
Test 1071-12	0.981	55	50.2	5	Duplicated test, E4
Test 1071-13	0.981	55	50.2	12	–
Test 1071-14	3.923	10	50.2	2	–
Test 1071-15	3.923	10	50.2	5	–
Test 1071-16	3.923	10	50.2	8	–
Test 1071-17	3.923	10	50.2	12	–
Test 1071-18	3.923	10	50.2	18	–
Test 1071-19	3.923	10	50.2	25	–
Test 1071-20	3.923	30	50.2	2	–
Test 1071-21	3.923	30	50.2	5	–
Test 1071-22	3.923	30	50.2	8	–
Test 1071-23	3.923	30	50.2	12	–
Test 1071-24	3.923	30	50.2	18	–
Test 1071-25	3.923	30	50.2	25	–
Test 1071-26	3.923	55	50.2	2	–
Test 1071-27	3.923	55	50.2	5	E4
Test 1071-28	3.923	55	50.2	8	–
Test 1071-29	3.923	55	50.2	12	–
Test 1071-30	3.923	55	50.2	18	–
Test 1071-31	3.923	55	50.2	25	Duplicated test
Test 1071-32	3.923	55	50.2	25	Duplicated test
Test 1071-33	7.159	10	50.2	2	–
Test 1071-34	7.159	10	50.2	5	E4
Test 1071-35	7.159	10	50.2	8	–
Test 1071-36	7.159	10	50.2	12	–
Test 1071-37	7.159	10	50.2	18	–
Test 1071-38	7.159	10	50.2	25	–
Test 1071-39	7.159	20	50.2	2	–
Test 1071-40	7.159	20	50.2	5	E4
Test 1071-41	7.159	20	50.2	8	–
Test 1071-42	7.159	20	50.2	12	–

E4: Exercise 4 case.

Table 4.2.10. Experimental conditions for steady-state void distribution measurement data – assembly 1 (*cont.*)

Experimental conditions	Pressure (MPa)	Flow rate (t/h)	Inlet sub-cooling (kJ/kg)	Outlet quality (%)	Experimental cases
Test 1071-43	7.159	20	50.2	18	–
Test 1071-44	7.159	20	50.2	25	–
Test 1071-45	7.159	30	50.2	2	–
Test 1071-46	7.159	30	50.2	5	–
Test 1071-47	7.159	30	50.2	8	–
Test 1071-48	7.159	30	50.2	12	–
Test 1071-49	7.159	30	50.2	18	–
Test 1071-50	7.159	30	50.2	25	–
Test 1071-51	7.159	55	20.9	5	–
Test 1071-52	7.159	55	20.9	12	–
Test 1071-53	7.159	55	50.2	2	Duplicated test, E4
Test 1071-54	7.159	55	50.2	2	Duplicated test
Test 1071-55	7.159	55	50.2	5	E1, E4
Test 1071-56	7.159	55	50.2	8	–
Test 1071-57	7.159	55	50.2	8	
Test 1071-58	7.159	55	50.2	12	E1, E4
Test 1071-59	7.159	55	50.2	18	Duplicated test
Test 1071-60	7.159	55	50.2	18	Duplicated test
Test 1071-61	7.159	55	50.2	25	E1, E4
Test 1071-62	7.159	55	125.6	5	E4
Test 1071-63	7.159	55	125.6	12	–
Test 1071-64	7.159	70	50.2	2	–
Test 1071-65	7.159	70	50.2	5	E4
Test 1071-66	7.159	70	50.2	8	–
Test 1071-67	7.159	70	50.2	12	–
Test 1071-68	7.159	70	50.2	18	–
Test 1071-69	8.63	10	50.2	2	–
Test 1071-70	8.63	10	50.2	5	–
Test 1071-71	8.63	10	50.2	8	–
Test 1071-72	8.63	10	50.2	12	–
Test 1071-73	8.63	10	50.2	18	–
Test 1071-74	8.63	10	50.2	25	–
Test 1071-75	8.63	30	50.2	2	–
Test 1071-76	8.63	30	50.2	5	–
Test 1071-77	8.63	30	50.2	8	–
Test 1071-78	8.63	30	50.2	12	–
Test 1071-79	8.63	30	50.2	18	–
Test 1071-80	8.63	30	50.2	25	–
Test 1071-81	8.63	55	50.2	2	–
Test 1071-82	8.63	55	50.2	5	E4
Test 1071-83	8.63	55	50.2	8	–
Test 1071-84	8.63	55	50.2	12	–
Test 1071-85	8.63	55	50.2	18	Duplicated test
Test 1071-86	8.63	55	50.2	18	Duplicated test

E1: Exercise 1 case, E4: Exercise 4 case.

Table 4.2.11. Process conditions for steady-state void distribution measurement data – assembly 1

Process conditions	Pressure (MPa)	Flow rate (t/h)	Inlet sub-cooling (kJ/kg)	Power (MW)	Experimental cases
Test 1071-01	0.981	10.14	48.2	0.23	–
Test 1071-02	0.96	10.14	44.3	0.32	–
Test 1071-03	0.967	10.14	46.3	0.43	–
Test 1071-04	0.966	10.14	45.1	0.82	–
Test 1071-05	0.969	29.99	45.7	0.60	–
Test 1071-06	0.989	29.99	49.4	0.94	–
Test 1071-07	1.002	30.02	51.6	1.26	–
Test 1071-08	0.987	30.01	51.0	2.43	–
Test 1071-09	1.066	54.71	66.3	1.09	–
Test 1071-10	1.092	54.88	71.4	1.70	–
Test 1071-11	1.104	55.00	74.0	2.31	Duplicated test
Test 1071-12	1.016	54.92	56.2	2.32	Duplicated test, E4
Test 1071-13	1.234	54.84	88.5	6.32	–
Test 1071-14	3.914	10.13	50.4	0.25	–
Test 1071-15	3.913	10.12	49.5	0.39	–
Test 1071-16	3.918	10.11	49.8	0.53	–
Test 1071-17	3.916	10.15	47.2	0.73	–
Test 1071-18	3.912	10.13	49.1	1.01	–
Test 1071-19	3.901	10.14	47.2	1.34	–
Test 1071-20	3.930	29.25	49.4	0.72	–
Test 1071-21	3.931	30.01	50.0	1.14	–
Test 1071-22	3.925	29.97	50.3	1.58	–
Test 1071-23	3.943	30.02	51.0	2.14	–
Test 1071-24	3.928	29.89	49.6	3.00	–
Test 1071-25	3.944	29.97	50.5	4.00	–
Test 1071-26	3.924	54.69	50.3	1.31	–
Test 1071-27	3.944	54.71	50.7	2.09	E4
Test 1071-28	3.916	54.82	48.9	2.87	–
Test 1071-29	3.930	54.70	50.1	3.91	–
Test 1071-30	3.934	54.77	50.1	5.51	–
Test 1071-31	3.964	54.73	52.1	7.35	Duplicated test
Test 1071-32	3.952	54.82	50.9	7.34	Duplicated test
Test 1071-33	7.223	10.22	57.3	0.24	–
Test 1071-34	7.164	10.22	49.5	0.36	E4
Test 1071-35	7.16	10.18	51.4	0.47	–
Test 1071-36	7.148	10.12	49.4	0.65	–
Test 1071-37	7.148	10.22	49.2	0.89	–
Test 1071-38	7.130	10.20	51.5	1.18	–
Test 1071-39	7.173	19.99	64.3	0.46	–
Test 1071-40	7.161	20.00	63.6	0.70	E4
Test 1071-41	7.141	20.03	56.1	0.95	–
Test 1071-42	7.150	20.00	50.9	1.29	–

E4: Exercise 4 case.

Table 4.2.11. Process conditions for steady-state void distribution measurement data – assembly 1 (*cont.*)

Process conditions	Pressure (MPa)	Flow rate (t/h)	Inlet sub-cooling (kJ/kg)	Power (MW)	Experimental cases
Test 1071-43	7.167	20.05	52.5	1.8	–
Test 1071-44	7.150	20.05	50.5	2.37	–
Test 1071-45	7.155	29.86	51.6	0.68	–
Test 1071-46	7.15	29.83	52.2	1.04	–
Test 1071-47	7.156	29.97	51.7	1.42	–
Test 1071-48	7.169	30.01	51.3	1.92	–
Test 1071-49	7.171	29.93	51.8	2.66	–
Test 1071-50	7.173	29.95	51.3	3.52	–
Test 1071-51	7.182	54.87	21.5	1.47	–
Test 1071-52	7.202	54.81	21.1	3.08	–
Test 1071-53	7.185	54.58	52.2	1.23	Duplicated test, E4
Test 1071-54	7.171	54.43	52.4	1.23	Duplicated test
Test 1071-55	7.191	54.61	52.8	1.92	E1, E4
Test 1071-56	7.203	54.64	54.0	2.60	–
Test 1071-57	7.166	54.60	52.3	2.58	–
Test 1071-58	7.158	55.07	50.3	3.52	E1, E4
Test 1071-59	7.177	54.74	51.3	4.88	Duplicated test
Test 1071-60	7.182	54.98	51.8	4.88	Duplicated test
Test 1071-61	7.200	54.65	51.8	6.48	E1, E4
Test 1071-62	7.147	54.85	124.6	3.07	E4
Test 1071-63	7.194	54.75	128.4	4.67	–
Test 1071-64	7.176	69.23	52.7	1.56	–
Test 1071-65	7.195	69.49	53.9	2.45	E4
Test 1071-66	7.206	69.33	54.0	3.31	–
Test 1071-67	7.196	69.61	53.2	4.47	–
Test 1071-68	7.197	69.50	52.6	6.21	–
Test 1071-69	8.609	10.00	51.3	0.22	–
Test 1071-70	8.604	10.01	46.8	0.34	–
Test 1071-71	8.603	10.01	50.1	0.47	–
Test 1071-72	8.614	10.19	52.1	0.62	–
Test 1071-73	8.622	10.18	51.0	0.86	–
Test 1071-74	8.608	10.16	46.6	1.13	–
Test 1071-75	8.635	29.71	51.6	0.65	–
Test 1071-76	8.625	29.95	47.3	1.02	–
Test 1071-77	8.615	30.27	50.3	1.36	–
Test 1071-78	8.627	29.95	50.3	1.83	–
Test 1071-79	8.619	29.95	50.4	2.54	–
Test 1071-80	8.624	29.99	51.6	3.35	–
Test 1071-81	8.629	54.03	47.4	1.22	–
Test 1071-82	8.633	54.69	51.7	1.85	E4
Test 1071-83	8.653	54.50	54.8	2.50	–
Test 1071-84	8.659	54.57	55.2	3.34	–
Test 1071-85	8.681	54.61	56.0	4.64	Duplicated test
Test 1071-86	8.667	54.60	53.3	4.63	Duplicated test

E1: Exercise 1 case, E4: Exercise 4 case.

Table 4.2.12. Experimental conditions for steady-state void distribution measurement data – assembly 2

Experimental conditions	Pressure (MPa)	Flow rate (t/h)	Inlet sub-cooling (kJ/kg)	Quality (%)	Experimental cases
Test 2081-01	3.923	10	50.2	2	–
Test 2081-02	3.923	10	50.2	5	–
Test 2081-03	3.923	10	50.2	8	–
Test 2081-04	3.923	10	50.2	12	–
Test 2081-05	3.923	10	50.2	15	–
Test 2081-06	3.923	30	50.2	2	–
Test 2081-07	3.923	30	50.2	5	–
Test 2081-08	3.923	30	50.2	8	–
Test 2081-09	3.923	30	50.2	12	–
Test 2081-10	3.923	55	50.2	2	–
Test 2081-11	3.923	55	50.2	5	–
Test 2081-12	3.923	55	50.2	8	–
Test 2081-13	3.923	55	50.2	12	Duplicated test
Test 2081-14	3.923	55	50.2	12	Duplicated test
Test 2081-15	7.159	10	50.2	2	–
Test 2081-16	7.159	10	50.2	5	–
Test 2081-17	7.159	10	50.2	8	–
Test 2081-18	7.159	10	50.2	12	–
Test 2081-19	7.159	10	50.2	15	–
Test 2081-20	7.159	20	50.2	2	–
Test 2081-21	7.159	20	50.2	5	–
Test 2081-22	7.159	20	50.2	8	–
Test 2081-23	7.159	20	50.2	12	–
Test 2081-24	7.159	20	50.2	15	–
Test 2081-25	7.159	30	50.2	2	–
Test 2081-26	7.159	30	50.2	5	–
Test 2081-27	7.159	30	50.2	8	–
Test 2081-28	7.159	30	50.2	12	–
Test 2081-29	7.159	30	50.2	15	–
Test 2081-30	7.159	55	50.2	2	–
Test 2081-31	7.159	55	50.2	5	–
Test 2081-32	7.159	55	50.2	8	–
Test 2081-33	7.159	55	50.2	12	Duplicated test
Test 2081-34	7.159	55	50.2	12	Duplicated test
Test 2081-35	7.159	70	50.2	2	–
Test 2081-36	7.159	70	50.2	5	–
Test 2081-37	7.159	70	50.2	8	–
Test 2081-38	8.630	10	50.2	2	–
Test 2081-39	8.630	10	50.2	5	–
Test 2081-40	8.630	10	50.2	8	–
Test 2081-41	8.630	10	50.2	12	–
Test 2081-42	8.630	10	50.2	15	–
Test 2081-43	8.630	30	50.2	2	–

Table 4.2.12. Experimental conditions for steady-state void distribution measurement data – assembly 2 (*cont.*)

Experimental conditions	Pressure (MPa)	Flow rate (t/h)	Inlet sub-cooling (kJ/kg)	Quality (%)	Experimental cases
Test 2081-44	8.63	30	50.2	5	–
Test 2081-45	8.63	30	50.2	8	–
Test 2081-46	8.63	30	50.2	12	–
Test 2081-47	8.63	55	50.2	2	–
Test 2081-48	8.63	55	50.2	5	–
Test 2081-49	8.63	55	50.2	8	Duplicated test
Test 2081-50	8.63	55	50.2	8	Duplicated test

Table 4.2.13. Process conditions for steady-state void distribution measurement data – assembly 2

Process	Pressure	Flow rate	Inlet sub-cooling	Power	Experimental
Test 2081-01	3.923	10.10	51.1	0.25	–
Test 2081-02	3.916	10.09	51.1	0.39	–
Test 2081-03	3.914	10.08	50.7	0.53	–
Test 2081-04	3.928	10.13	56.7	0.74	–
Test 2081-05	3.926	10.11	57.0	0.87	–
Test 2081-06	3.944	29.97	56.7	0.73	–
Test 2081-07	3.943	29.96	56.7	1.15	–
Test 2081-08	3.902	29.93	48.1	1.57	–
Test 2081-09	3.915	30.00	48.3	2.15	–
Test 2081-10	3.921	54.70	49.6	1.30	–
Test 2081-11	3.937	54.67	51.0	2.03	–
Test 2081-12	3.993	54.77	53.9	2.87	–
Test 2081-13	4.017	54.71	56.9	3.94	Duplicated test
Test 2081-14	4.012	54.76	55.9	3.94	Duplicated test
Test 2081-15	7.158	10.10	50.9	0.23	–
Test 2081-16	7.146	10.08	51.7	0.37	–
Test 2081-17	7.150	10.09	52.0	0.49	–
Test 2081-18	7.151	10.10	51.4	0.66	–
Test 2081-19	7.151	10.10	51.4	0.78	–
Test 2081-20	7.148	19.99	48.9	0.45	–
Test 2081-21	7.145	19.97	49.3	0.69	–
Test 2081-22	7.146	20.07	51.1	0.95	–
Test 2081-23	7.147	20.05	50.3	1.28	–
Test 2081-24	7.149	20.03	49.7	1.53	–
Test 2081-25	7.145	29.90	52.0	0.69	–
Test 2081-26	7.155	29.91	51.4	1.06	–
Test 2081-27	7.162	29.94	51.1	1.43	–
Test 2081-28	7.167	29.94	51.0	1.93	–
Test 2081-29	7.154	29.91	50.6	2.28	–
Test 2081-30	7.175	54.6	52.5	1.24	–
Test 2081-31	7.177	54.55	51.5	1.91	–

Table 4.2.13. Process conditions for steady-state void distribution measurement data – assembly 2 (*cont.*)

Process conditions	Pressure (MPa)	Flow rate (t/h)	Inlet sub-cooling (kJ/kg)	Power (MW)	Experimental cases
Test 2081-32	7.177	54.61	51.5	2.61	–
Test 2081-33	7.163	54.65	50.9	3.54	Duplicated test
Test 2081-34	7.163	54.65	51.7	3.53	Duplicated test
Test 2081-35	7.164	69.49	52.7	1.56	–
Test 2081-36	7.197	69.61	54.6	2.44	–
Test 2081-37	7.218	69.66	53.1	3.32	–
Test 2081-38	8.630	10.14	53.6	0.23	–
Test 2081-39	8.626	10.14	55.8	0.34	–
Test 2081-40	8.624	10.12	55.1	0.47	–
Test 2081-41	8.620	10.08	59.9	0.62	–
Test 2081-42	8.629	10.03	60.5	0.75	–
Test 2081-43	8.632	29.91	52.1	0.67	–
Test 2081-44	8.635	29.89	61.8	1.02	–
Test 2081-45	8.620	29.97	51.5	1.36	–
Test 2081-46	8.610	30.08	50.1	1.82	–
Test 2081-47	8.632	54.12	51.4	1.20	–
Test 2081-48	8.620	54.37	50.9	1.84	–
Test 2081-49	8.658	54.66	52.1	2.50	Duplicated test
Test 2081-50	8.657	54.63	52.6	2.49	Duplicated test

Table 4.2.14. Experimental conditions for steady-state void distribution measurement data – assembly 3

Experimental conditions	Pressure (MPa)	Flow rate (t/h)	Inlet sub-cooling (kJ/kg)	Quality (%)	Experimental cases
Test 3091-01	3.923	55	50.2	5	–
Test 3091-02	3.923	55	50.2	12	–
Test 3091-03	7.159	10	50.2	2	–
Test 3091-04	7.159	10	50.2	5	–
Test 3091-05	7.159	10	50.2	8	–
Test 3091-06	7.159	10	50.2	12	–
Test 3091-07	7.159	10	50.2	18	–
Test 3091-08	7.159	10	50.2	25	–
Test 3091-09	7.159	30	50.2	2	–
Test 3091-10	7.159	30	50.2	5	–
Test 3091-11	7.159	30	50.2	8	–
Test 3091-12	7.159	30	50.2	12	–
Test 3091-13	7.159	30	50.2	18	–
Test 3091-14	7.159	30	50.2	25	–
Test 3091-15	7.159	55	50.2	2	–
Test 3091-16	7.159	55	50.2	5	–
Test 3091-17	7.159	55	50.2	8	–
Test 3091-18	7.159	55	50.2	12	–

Table 4.2.14. Experimental conditions for steady-state void distribution measurement data – assembly 3 (*cont.*)

Experimental conditions	Pressure (MPa)	Flow rate (t/h)	Inlet sub-cooling (kJ/kg)	Quality (%)	Experimental cases
Test 3091-19	7.159	55	50.2	18	Duplicated test
Test 3091-20	7.159	55	50.2	18	Duplicated test
Test 3091-21	7.159	55	50.2	25	–
Test 3091-22	7.159	70	50.2	2	–
Test 3091-23	7.159	70	50.2	5	–
Test 3091-24	7.159	70	50.2	8	–
Test 3091-25	7.159	70	50.2	12	–
Test 3091-26	7.159	70	50.2	18	–
Test 3091-27	8.630	55	50.2	5	–
Test 3091-28	8.630	55	50.2	12	–

Table 4.2.15. Process conditions for steady-state void distribution measurement data – assembly 3

Process conditions	Pressure (MPa)	Flow rate (t/h)	Inlet sub-cooling (kJ/kg)	Power (MW)	Experimental cases
Test 3091-01	3.928	54.50	50.7	2.09	–
Test 3091-02	3.923	54.71	48.7	3.93	–
Test 3091-03	7.161	10.09	58.9	0.23	–
Test 3091-04	7.148	10.11	57.0	0.36	–
Test 3091-05	7.142	10.12	54.1	0.48	–
Test 3091-06	7.141	10.09	53.1	0.63	–
Test 3091-07	7.140	10.11	51.9	0.89	–
Test 3091-08	7.136	10.10	50.0	1.18	–
Test 3091-09	7.151	29.92	56.3	0.68	–
Test 3091-10	7.156	29.94	55.9	1.05	–
Test 3091-11	7.158	29.95	53.7	1.42	–
Test 3091-12	7.161	29.95	53.8	1.92	–
Test 3091-13	7.150	29.86	51.7	2.67	–
Test 3091-14	7.141	29.87	52.1	3.55	–
Test 3091-15	7.163	54.60	51.9	1.25	–
Test 3091-16	7.155	54.53	51.9	1.92	–
Test 3091-17	7.187	54.66	55.6	2.60	–
Test 3091-18	7.205	54.64	56.6	3.52	–
Test 3091-19	7.191	54.54	52.7	4.89	Duplicated test
Test 3091-20	7.194	54.62	52.9	4.89	Duplicated test
Test 3091-21	7.193	54.67	52.8	6.47	
Test 3091-22	7.164	69.24	52.1	1.57	
Test 3091-23	7.207	69.59	57.8	2.44	
Test 3091-24	7.168	69.48	53.1	3.32	
Test 3091-25	7.192	69.45	53.0	4.47	
Test 3091-26	7.200	69.56	53.1	6.19	
Test 3091-27	8.627	54.65	52.8	1.84	
Test 3091-28	8.642	54.72	52.2	3.34	

Table 4.2.16. Experimental conditions for steady-state void distribution measurement data – assembly 4

Experimental conditions	Pressure (MPa)	Flow rate (t/h)	Inlet sub-cooling (kJ/kg)	Outlet quality (%)	Experimental cases
Test 4101-01	0.981	10	50.2	1	–
Test 4101-02	0.981	10	50.2	3	–
Test 4101-03	0.981	10	50.2	5	–
Test 4101-04	0.981	10	50.2	12	–
Test 4101-05	0.981	30	50.2	1	–
Test 4101-06	0.981	30	50.2	3	–
Test 4101-07	0.981	30	50.2	5	–
Test 4101-08	0.981	30	50.2	12	–
Test 4101-09	0.981	55	50.2	1	–
Test 4101-10	0.981	55	50.2	3	–
Test 4101-11	0.981	55	50.2	5	Duplicated test
Test 4101-12	0.981	55	50.2	5	Duplicated test
Test 4101-13	0.981	55	50.2	12	–
Test 4101-14	3.923	10	50.2	2	–
Test 4101-15	3.923	10	50.2	5	–
Test 4101-16	3.923	10	50.2	8	–
Test 4101-17	3.923	10	50.2	12	–
Test 4101-18	3.923	10	50.2	18	–
Test 4101-19	3.923	10	50.2	25	–
Test 4101-20	3.923	30	50.2	2	–
Test 4101-21	3.923	30	50.2	5	–
Test 4101-22	3.923	30	50.2	8	–
Test 4101-23	3.923	30	50.2	12	–
Test 4101-24	3.923	30	50.2	18	–
Test 4101-25	3.923	30	50.2	25	–
Test 4101-26	3.923	55	50.2	2	–
Test 4101-27	3.923	55	50.2	5	–
Test 4101-28	3.923	55	50.2	8	–
Test 4101-29	3.923	55	50.2	12	–
Test 4101-30	3.923	55	50.2	18	–
Test 4101-31	3.923	55	50.2	25	Duplicated test
Test 4101-32	3.923	55	50.2	25	Duplicated test
Test 4101-33	7.159	10	50.2	2	–
Test 4101-34	7.159	10	50.2	5	–
Test 4101-35	7.159	10	50.2	8	–
Test 4101-36	7.159	10	50.2	12	–
Test 4101-37	7.159	10	50.2	18	–
Test 4101-38	7.159	10	50.2	25	–
Test 4101-39	7.159	20	50.2	2	–
Test 4101-40	7.159	20	50.2	5	–
Test 4101-41	7.159	20	50.2	8	–
Test 4101-42	7.159	20	50.2	12	–

Table 4.2.16 Experimental conditions for steady-state void distribution measurement data – assembly 4 (*cont.*)

Experimental conditions	Pressure (MPa)	Flow rate (t/h)	Inlet sub-cooling (kJ/kg)	Outlet quality (%)	Experimental cases
Test 4101-43	7.159	20	50.2	18	–
Test 4101-44	7.159	20	50.2	25	–
Test 4101-45	7.159	30	50.2	2	–
Test 4101-46	7.159	30	50.2	3	–
Test 4101-47	7.159	30	50.2	8	–
Test 4101-48	7.159	30	50.2	12	–
Test 4101-49	7.159	30	50.2	18	–
Test 4101-50	7.159	30	50.2	25	–
Test 4101-51	7.159	55	20.9	5	–
Test 4101-52	7.159	55	20.9	12	–
Test 4101-53	7.159	55	50.2	2	Duplicated test
Test 4101-54	7.159	55	50.2	2	Duplicated test, E2
Test 4101-55	7.159	55	50.2	5	E1, E2
Test 4101-56	7.159	55	50.2	8	Duplicated test
Test 4101-57	7.159	55	50.2	8	Duplicated test
Test 4101-58	7.159	55	50.2	12	E1, E2
Test 4101-59	7.159	55	50.2	18	–
Test 4101-60	7.159	55	50.2	18	–
Test 4101-61	7.159	55	50.2	25	E1, E2
Test 4101-62	7.159	55	125.6	5	–
Test 4101-63	7.159	55	125.6	12	–
Test 4101-64	7.159	70	50.2	2	–
Test 4101-65	7.159	70	50.2	5	–
Test 4101-66	7.159	70	50.2	8	–
Test 4101-67	7.159	70	50.2	12	–
Test 4101-68	7.159	70	50.2	18	–
Test 4101-69	8.630	10	50.2	2	–
Test 4101-70	8.630	10	50.2	5	–
Test 4101-71	8.630	10	50.2	8	–
Test 4101-72	8.630	10	50.2	12	–
Test 4101-73	8.630	10	50.2	18	–
Test 4101-74	8.630	10	50.2	25	–
Test 4101-75	8.630	30	50.2	2	–
Test 4101-76	8.630	30	50.2	5	–
Test 4101-77	8.630	30	50.2	8	–
Test 4101-78	8.630	30	50.2	12	–
Test 4101-79	8.630	30	50.2	18	–
Test 4101-80	8.630	30	50.2	25	–
Test 4101-81	8.630	55	50.2	2	–
Test 4101-82	8.630	55	50.2	5	–
Test 4101-83	8.630	55	50.2	8	–
Test 4101-84	8.630	55	50.2	12	–
Test 4101-85	8.630	55	50.2	18	Duplicated test
Test 4101-86	8.630	55	50.2	18	Duplicated test

E1: Experiment 1 case, E2: Experiment 2 case.

Table 4.2.17. Process conditions for steady-state void distribution measurement data – assembly 4

Process conditions	Pressure (MPa)	Flow rate (t/h)	Inlet sub-cooling (kJ/kg)	Power (MW)	Experimental cases
Test 4101-01	0.995	10.12	54.1	0.22	–
Test 4101-02	0.994	10.12	53.3	0.32	–
Test 4101-03	0.978	10.12	50.7	0.43	–
Test 4101-04	0.973	10.20	43.9	0.82	–
Test 4101-05	1.002	30.00	55.4	0.60	–
Test 4101-06	1.008	30.01	56.4	0.93	–
Test 4101-07	1.006	30.00	55.0	1.26	–
Test 4101-08	1.042	30.02	62.5	2.43	–
Test 4101-09	0.984	54.99	50.6	1.08	–
Test 4101-10	1.021	54.95	58.6	1.70	–
Test 4101-11	1.096	54.85	71.1	2.31	Duplicate test
Test 4101-12	1.079	54.80	67.9	2.31	Duplicate test
Test 4101-13	1.224	55.01	92.5	4.46	–
Test 4101-14	3.937	10.11	53.6	0.26	–
Test 4101-15	3.932	10.10	52.0	0.39	–
Test 4101-16	3.936	10.13	53.1	0.53	–
Test 4101-17	3.925	10.14	51.4	0.72	–
Test 4101-18	3.919	10.14	51.5	1.00	–
Test 4101-19	3.936	10.12	52.5	1.34	–
Test 4101-20	3.940	29.98	52.2	0.72	–
Test 4101-21	3.942	29.99	52.2	1.14	–
Test 4101-22	3.931	29.97	50.8	1.57	–
Test 4101-23	3.937	29.97	51.5	2.14	–
Test 4101-24	3.943	29.93	51.7	3.00	–
Test 4101-25	3.943	29.92	50.9	4.01	–
Test 4101-26	3.955	54.78	52.5	1.30	–
Test 4101-27	3.982	54.73	54.6	2.09	–
Test 4101-28	3.918	54.71	50.6	2.88	–
Test 4101-29	3.917	54.68	50.3	3.92	–
Test 4101-30	3.961	54.71	52.7	5.50	–
Test 4101-31	3.991	54.75	54.8	7.33	Duplicate test
Test 4101-32	3.988	54.77	54.6	7.33	Duplicate test
Test 4101-33	7.152	10.12	52.6	0.25	–
Test 4101-34	7.155	10.12	53.4	0.36	–
Test 4101-35	7.150	10.12	51.8	0.48	–
Test 4101-36	7.145	10.10	51.7	0.65	–
Test 4101-37	7.146	10.12	51.6	0.89	–
Test 4101-38	7.150	10.12	51.6	1.19	–
Test 4101-39	7.147	20.05	51.5	0.45	–
Test 4101-40	7.144	20.03	52.0	0.70	–
Test 4101-41	7.134	20.03	50.5	0.96	–
Test 4101-42	7.138	20.03	52.0	1.29	–

Table 4.2.17. Process conditions for steady-state void distribution measurement data – assembly 4 (*cont.*)

Process conditions	Pressure (MPa)	Flow rate (t/h)	Inlet sub-cooling (kJ/kg)	Power (MW)	Experimental cases
Test 4101-43	7.138	20.06	50.5	1.79	–
Test 4101-44	7.141	20.09	50.6	2.36	–
Test 4101-45	7.167	29.94	52.2	0.69	–
Test 4101-46	7.163	29.93	51.2	1.06	–
Test 4101-47	7.132	29.94	50.6	1.43	–
Test 4101-48	7.165	29.91	51.2	1.93	–
Test 4101-49	7.168	29.94	51.2	2.67	–
Test 4101-50	7.176	29.91	50.3	3.55	–
Test 4101-51	7.162	54.52	22.4	1.46	–
Test 4101-52	7.209	54.52	24.8	3.07	–
Test 4101-53	7.181	54.65	52.8	1.24	Duplicate test
Test 4101-54	7.186	54.63	52.7	1.23	Duplicate test, E2
Test 4101-55	7.195	54.59	52.9	1.92	E1, E2
Test 4101-56	7.175	54.62	51.8	2.59	Duplicate test
Test 4101-57	7.174	54.58	52.4	2.60	Duplicate test
Test 4101-58	7.152	54.58	50.6	3.52	E1, E2
Test 4101-59	7.190	54.57	52.1	4.88	–
Test 4101-60	7.178	54.62	50.5	4.89	–
Test 4101-61	7.180	54.65	52.5	6.48	E1, E2
Test 4101-62	7.190	54.84	127.5	3.07	–
Test 4101-63	7.217	54.80	128.1	4.68	–
Test 4101-64	7.159	69.53	53.6	1.57	–
Test 4101-65	7.160	69.53	52.8	2.44	–
Test 4101-66	7.202	69.69	52.9	3.32	–
Test 4101-67	7.248	69.58	54.6	4.48	–
Test 4101-68	7.275	69.56	56.0	6.22	–
Test 4101-69	8.638	10.08	52.5	0.23	–
Test 4101-70	8.628	10.08	51.0	0.34	–
Test 4101-71	8.628	10.09	51.2	0.45	–
Test 4101-72	8.617	10.08	52.4	0.62	–
Test 4101-73	8.611	10.10	52.4	0.86	–
Test 4101-74	8.606	10.10	51.9	1.11	–
Test 4101-75	8.641	29.88	53.8	0.67	–
Test 4101-76	8.644	29.93	53.6	1.01	–
Test 4101-77	8.633	29.93	53.4	1.37	–
Test 4101-78	8.638	29.93	53.6	1.83	–
Test 4101-79	8.614	29.89	51.1	2.52	–
Test 4101-80	8.631	29.88	51.8	3.34	–
Test 4101-81	8.636	54.60	51.5	1.20	–
Test 4101-82	8.635	54.54	52.9	1.85	–
Test 4101-83	8.666	54.62	53.2	2.49	–
Test 4101-84	8.68	54.66	53.2	3.35	–
Test 4101-85	8.700	54.61	53.8	4.62	Duplicate test
Test 4101-86	8.705	54.59	54.2	4.62	Duplicate test

E1: Experiment 1 case, E2: Experiment 2 case.

Among the major operational transients, the following four events were simulated, each one of them having a specific impact on the void distribution:

- turbine trip without bypass;
- re-circulation pump trip;
- re-circulation pump stick;
- malfunction of pressure control system (pressure increase).

The conditions for the transient void distribution measurements are given in Table 4.2.18. The test matrix of transient void distributions is given in Table 4.2.19 and the test numbers are given in Table 4.2.20.

The cases denoted in the tables with E1, E2, E3 and E4 are the ones selected for analysis in Exercises 1 to 4 of Phase I of the BFBT benchmark.

Figures 4.2.1 through 4.2.4 demonstrate power, flow rate, pressure and inlet temperature time variations during turbine trip transient for assembly type 4.

Figures 4.2.5 through 4.2.8 demonstrate power, flow rate, inlet pressure and inlet temperature time variations during the pump trip transient for assembly type 4.

Table 4.2.18. Transient void distribution measurement conditions

Assembly	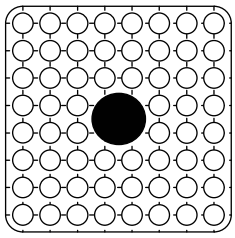 4	
Rated initial conditions	Pressure (MPa) Power (MW) Flow rate (t/h) Inlet temperature (Celsius) Outlet quality (%)	7.16 4.5 55 279 18
Transients	Turbine trip without bypass Re-circulation pump trip	
Data	Time histories of cross-sectional averaged void fraction in each axial level during transients Corresponding boundary conditions during transients	
No. of cases	Data supplied cases Exercise cases	2

Table 4.2.19. Test matrix of transient void distribution measurements

Assembly	Initial conditions					Transients	Exercise cases	No. of cases
	Pressure (MPa)	Power (MW)	Flow rate (t/h)	Inlet temperature (Celsius)	Outlet quality (%)			
4	7.16	4.5	55	279	18	Turbine trip w/o bypass	E3	2
						Re-circulation pump trip	E3	

E3: Exercise 3 case.

Table 4.2.20. Test number of transient void distribution measurements

Test no.	Assembly	Initial conditions					Transients	Exercise cases
		Pressure (MPa)	Power (MW)	Flow rate (t/h)	Inlet temperature (Celsius)	Outlet quality (%)		
4102-001~009	4	7.16	4.5	55	279	18	Turbine trip w/o bypass	E3
4102-019~027	4	7.2	4.5	55	279	18	Re-circulation pump trip	E3

E3: Exercise 3 case.

Figure 4.2.1. Turbine trip transient void distribution experimental boundary conditions, assembly type 4 – power

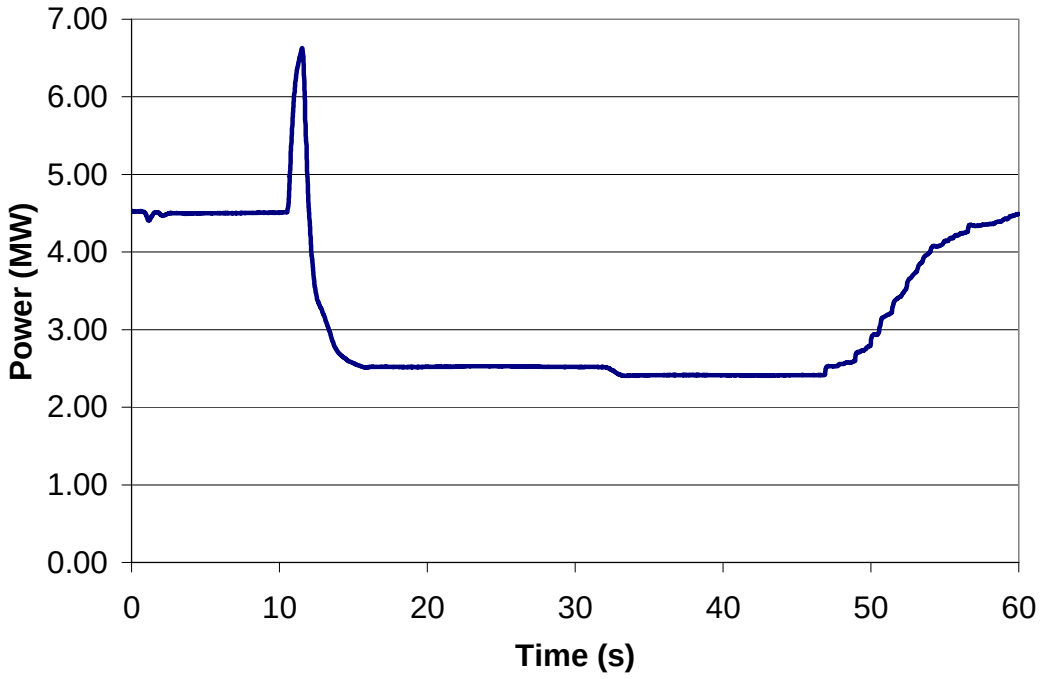

Figure 4.2.2. Turbine trip transient void distribution experimental boundary conditions, assembly type 4 – flow rate

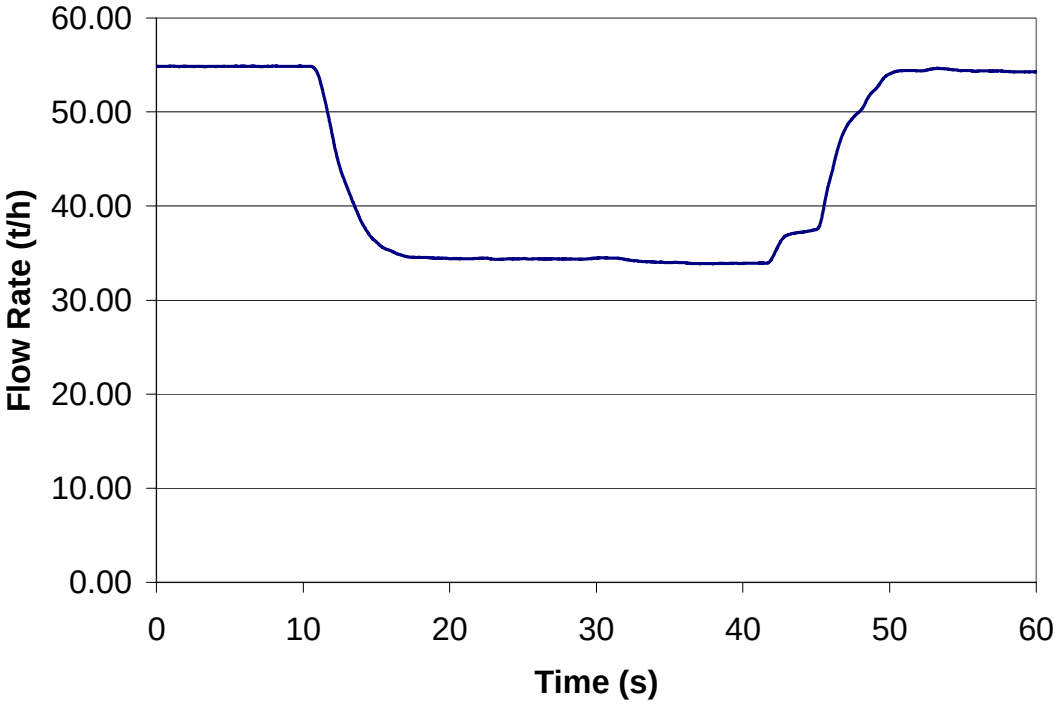

Figure 4.2.3. Turbine trip transient void distribution experimental boundary conditions, assembly type 4 – inlet pressure

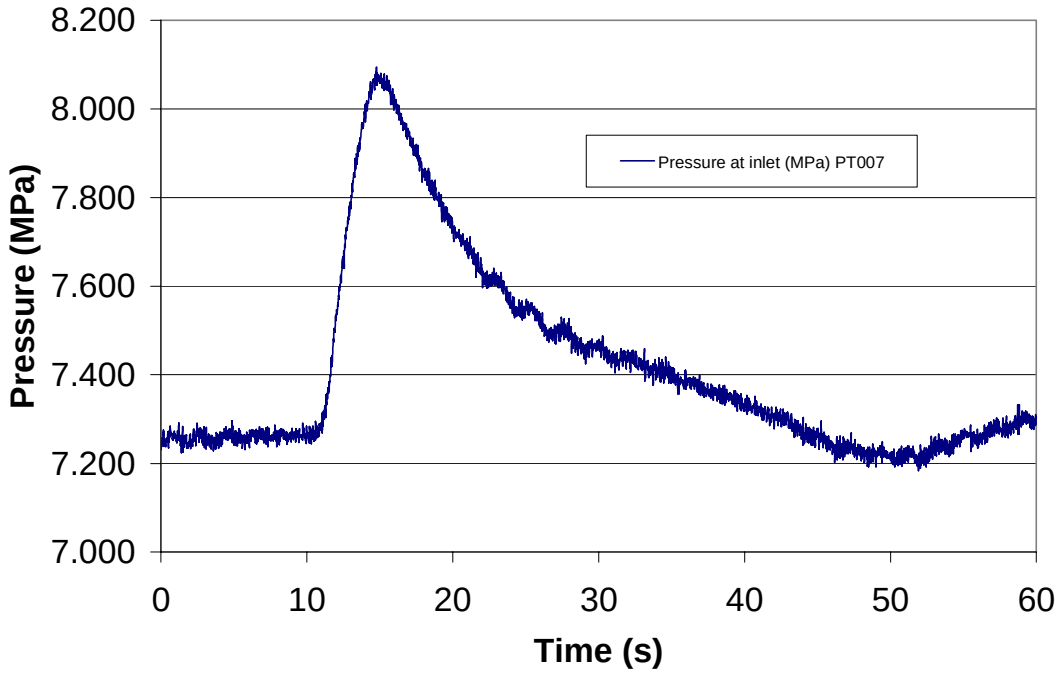

Figure 4.2.4. Turbine trip transient void distribution experimental boundary conditions, assembly type 4 – inlet temperature

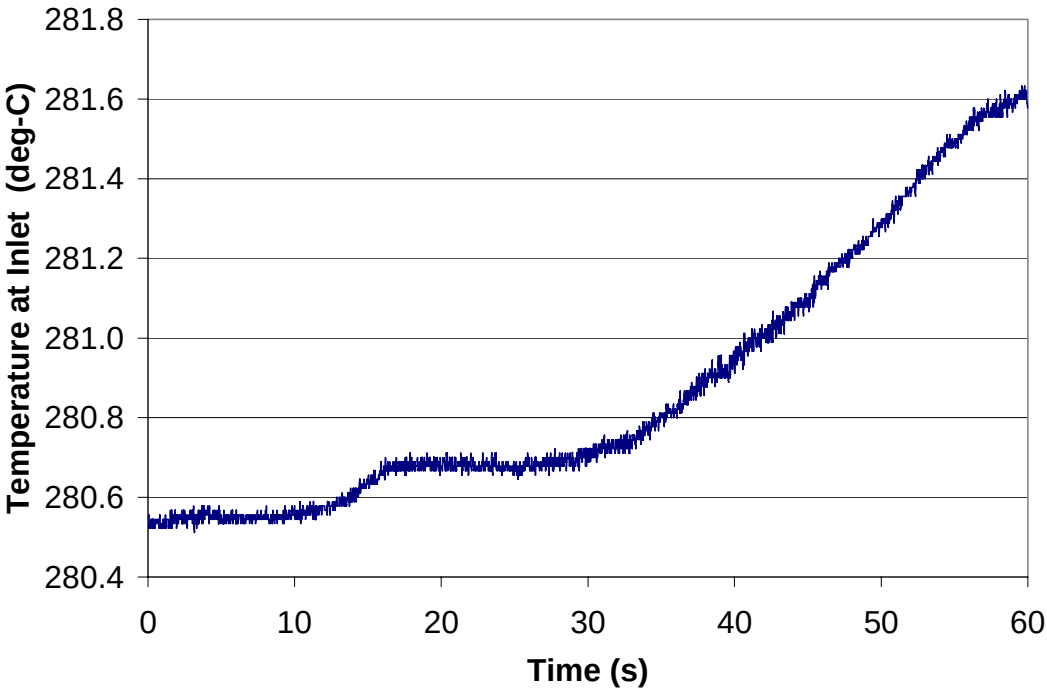

Figure 4.2.5. Pump trip transient void distribution experimental boundary conditions, assembly type 4 – power

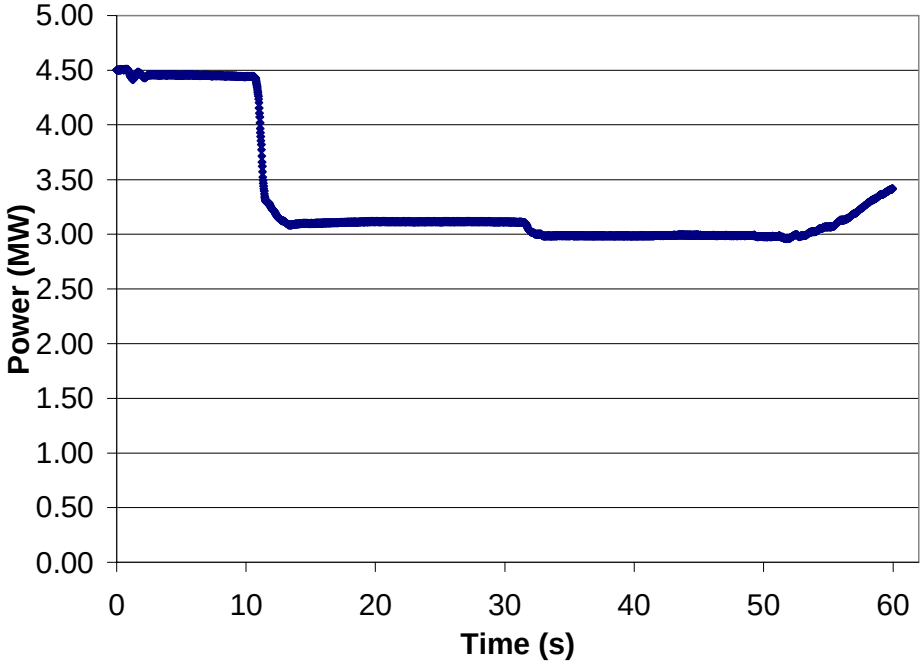

Figure 4.2.6. Pump trip transient void distribution experimental boundary conditions, assembly type 4 – flow rate

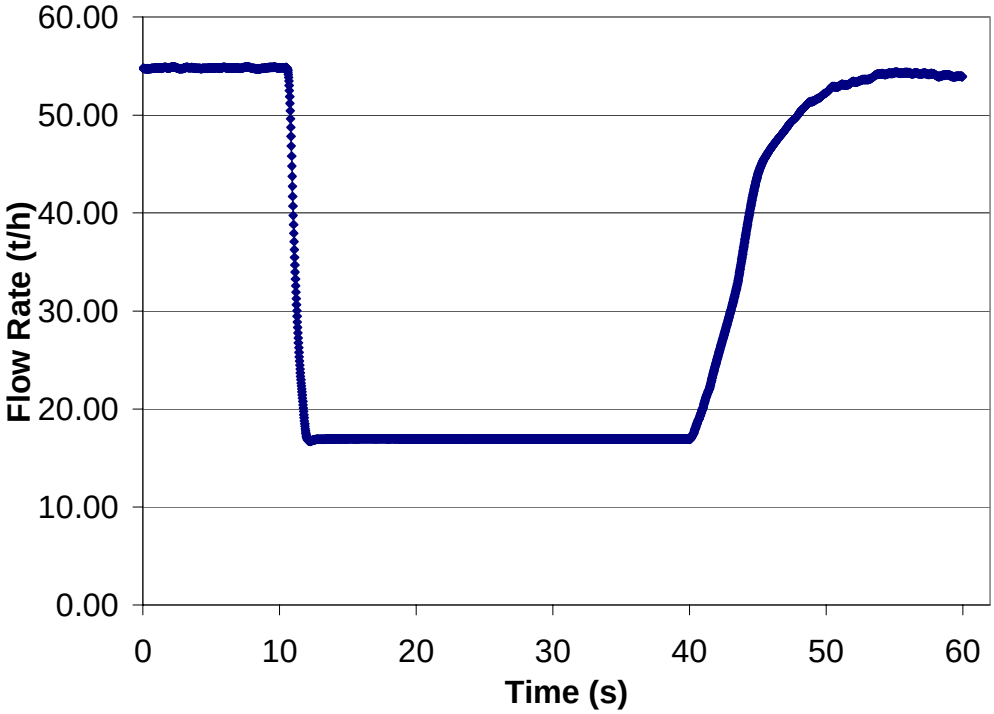

Figure 4.2.7. Pump trip transient void distribution experimental boundary conditions, assembly type 4 – inlet pressure

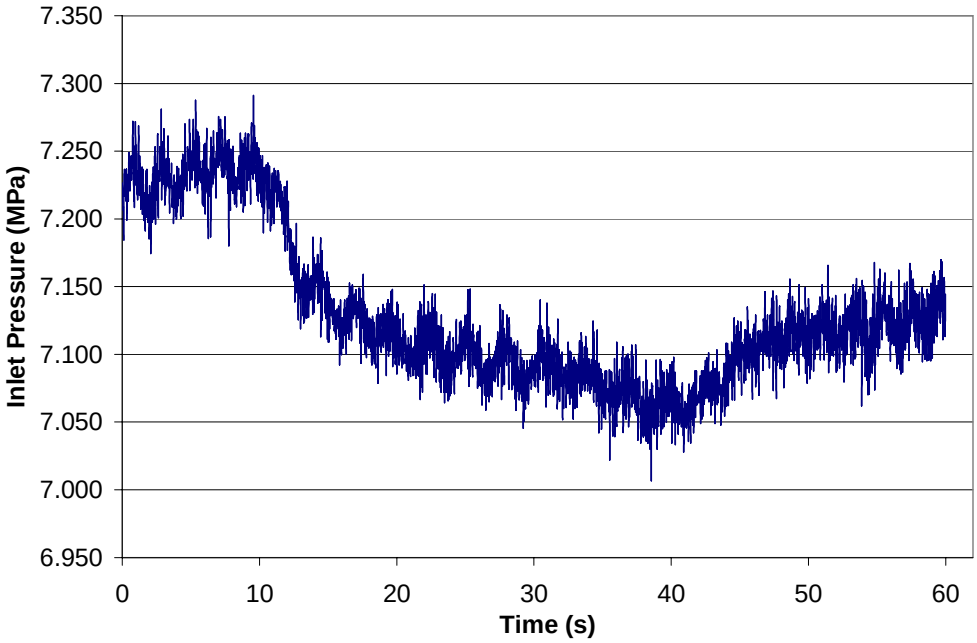

Figure 4.2.8. Pump trip transient void distribution experimental boundary conditions, assembly type 4 – inlet temperature

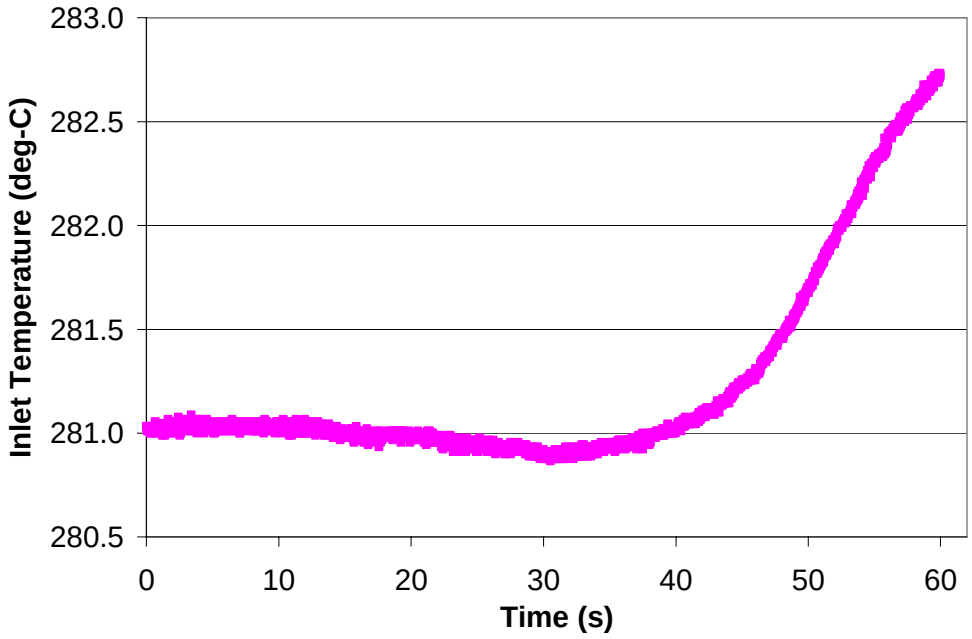

4.3 Critical power measurements

The conditions for the single-phase pressure drop measurements are given in Table 4.3.1. Measurements were performed utilising the test assembly type 4. Table 4.3.2 shows the test matrix for single-phase pressure drop measurements and Table 4.3.3 contains an example of single-phase pressure drop data.

The conditions for the two-phase pressure drop measurement are provided in Table 4.3.4. A high burn-up 8×8 rod bundle with configuration C2A was used in these tests. Table 4.3.5 shows the test matrix for two-phase pressure drop measurements and Table 4.3.6 demonstrates an example of the two-phase pressure drop data.

The conditions for the steady-state critical power measurement are provided in Table 4.3.7. Three different high burn-up designs were utilised: C2A, C2B and C3. The test matrix of steady-state critical power measurement is shown in Table 4.3.8 and the measurement data is given in Tables 4.3.9, 4.3.10 and 4.3.11 for assembly types C2A, C2B and C3, respectively.

The transient boiling transition measurement conditions are given in Table 4.3.12. High burn-up designs C2A and C3 were utilised. Two transients, a turbine trip and a pump trip, were simulated. The test matrix of transient boiling transition measurements is provided in Table 4.3.13. The test numbers of transient boiling transition measurements are shown in Table 4.3.14.

The cases denoted in the tables with E0, E1 and E2 are the ones selected for analysis in Exercises 0, 1 and 2 respectively, of the BFBT benchmark Phase II.

Figures 4.3.1 through 4.3.3 demonstrate different boundary conditions as a function of time during the turbine trip transient for assembly type C2A.

Figures 4.3.4 through 4.3.6 demonstrate different boundary conditions as a function of time during the pump trip transient for assembly type C2A.

Figures 4.3.7 through 4.3.9 demonstrate different boundary conditions as a function of time during the turbine trip transient for assembly type C3.

Figures 4.3.10 through 4.3.12 demonstrate different boundary conditions as a function of time during the pump trip transient for assembly type C3.

Table 4.3.1. Single-phase pressure drop measurement conditions

Assembly	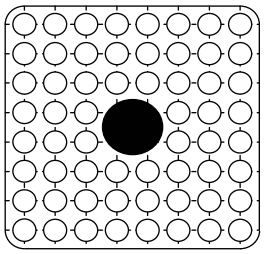 C2A	
Boundary conditions	Pressure (MPa) Flow rate (t/h)	0.2, 1, 7.2 10 15 20 25 30 35 40 45 55 60 65 70
Data	Pressure drop along with axial heated length Corresponding boundary conditions	
No. of cases	Data supplied cases Exercise cases	36 10
Concerned issues	Single-phase pressure drop from bottom to top of heated length	

Table 4.3.2. Test matrix of single-phase pressure drop measurements

Assembly	**Pressure (MPa)**	**Flow rate (t/h)**												**No. of data**
		10	15	20	25	30	35	40	45	55	60	65	70	
C2A	0.1	X	X	X	X	X	X	X	X	X	X	X	X	36
	1.0	X	X	X	X	X	X	X	X	X	X	X	X	
	7.2	X	X	E0	E0	E0	E0	E0	E0	E0	E0	E0	E0	

X: Test case, E0: Exercise 0 case.

Table 4.3.3. Example of single-phase pressure drop measurement data

Test number	Outlet pressure (MPa)	Inlet temperature (deg-C)	Flow rate (t/h)	Reynolds number $\times 10^4$	dp301 (kPa)	dp302 (kPa)	dp303 (kPa)	dp304 (kPa)	dp305 (kPa)	dp306 (kPa)	dp307 (kPa)	dp308 (kPa)	dp309 (kPa)
P70001	0.2	34.4	9.9	0.51	0.11	0.12	0.14	0.17	0.16	0.16	0.44	0.21	1.09
P70002	0.2	38.5	14.5	0.8	0.18	0.21	0.25	0.28	0.28	0.29	0.82	0.33	1.92
P70003	0.2	39.8	19.9	1.13	0.31	0.36	0.41	0.48	0.47	0.49	1.47	0.49	3.27
P70004	0.2	38.4	24.9	1.38	0.46	0.53	0.61	0.69	0.69	0.71	2.14	0.71	4.8
P70005	0.2	35.9	29.8	1.57	0.63	0.73	0.85	0.96	0.96	0.98	2.95	1.01	6.65
…	…	…	…	…	…	…	…	…	…	…	…	…	…
…	…	…	…	…	…	…	…	…	…	…	…	…	…
…	…	…	…	…	…	…	…	…	…	…	…	…	…
…	…	…	…	…	…	…	…	…	…	…	…	…	…
…	…	…	…	…	…	…	…	…	…	…	…	…	…
….	…..	….	….	….	….	….	….	….	….	….	….	….	….
P70033	7.15	284.7	55	21.86	2.06	2.3	2.55	2.87	2.91	2.96	8.85	3.22	20.43
P70034	7.15	284.8	59.7	23.74	2.41	2.69	2.99	3.35	3.39	3.46	10.36	3.76	23.87
P70035	7.16	284.6	64.8	25.76	2.81	3.14	3.46	3.9	3.95	4.03	12.05	4.37	27.77
P70036	7.15	284.8	69.9	27.79	3.25	3.63	3.99	4.5	4.55	4.65	13.89	5.04	32.03

Table 4.3.4. Two-phase pressure drop measurement conditions

Assembly	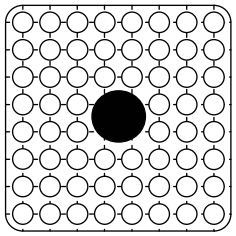 C2A	
Boundary conditions	Pressure (MPa) Flow rate (t/h) Inlet sub-cooling (kJ/kg) Exit quality (%)	7.2 8.6 20 45 55 70 50.2 7 10 15 20 25
Data	Pressure drop along with axial heated length Corresponding boundary conditions	
No. of cases	Data supplied cases Exercise cases	33 22

Exit quality: Thermal equilibrium quality.

Table 4.3.5 Test matrix of two-phase pressure drop measurements

Assembly	Pressure (MPa)	Flow rate (t/h)	Inlet sub-cooling (kJ/kg)	Exit quality (%)					No. of data
				7	10	15	20	25	
C2A	7.2	20	50.2	E0	X	E0	X	E0,W	21
		45		E0	X	E0	X	E0	
		55		E0	X	E0	X	E0,W	
		70		E0	X	E0	X	–	
	8.6	20	50.2	E0	–	E0	–	E0	12
		45		E0	–	E0	–	E0	
		55		E0	–	E0	–	E0,W	
		70		E0	–	E0	–	–	

X: Test case, W: Duplicated test case, E0: Exercise 0 case.

Table 4.3.6. Example of two-phase pressure drop measurement data

Test number	Outlet pressure (MPa)	Inlet temperature (deg-C)	Inlet sub-cooling (kJ/kg)	Flow rate (t/h)	Power (MW)	Outlet quality (%)	dp301 (kPa)	dp302 (kPa)	dp303 (kPa)	dp304 (kPa)	dp305 (kPa)	dp306 (kPa)	dp307 (kPa)	dp308 (kPa)	dp309 (kPa)
P60001	7.16	277.3	53.3	20.2	0.863	6.7	1.15	1.96	2.53	3.48	3.66	3.93	12.27	5.5	27.4
P60002	7.16	277.6	51.8	20.1	1.117	9.9	1.28	2.02	2.58	3.45	3.56	3.76	11.98	5.49	27.02
P60003	7.16	277.8	50.8	20.1	1.521	14.8	1.54	2.22	2.81	3.61	3.63	3.69	11.72	5.5	27.22
P60004	7.16	277.6	51.3	20.2	1.951	19.9	1.85	2.51	3.11	3.94	3.84	3.79	11.69	5.5	28.1
P60005	7.16	277.7	51.1	20	2.357	24.9	2.1	2.81	3.43	4.26	4.11	3.97	11.84	5.47	29.16
P60006	7.16	277.8	50.8	20.1	2.366	24.9	2.11	2.82	3.44	4.32	4.17	3.99	11.89	5.49	29.26
P60007	7.17	277.8	51.1	55	2.375	7	5.59	6.7	8.11	9.55	9.06	8.4	22.84	8.25	57.89
…	…	…	…	…	…	…	…	…	…	…	…	…	…	…	…
…	…	…	…	…	…	…	…	…	…	…	…	…	…	…	…
…	…	…	…	…	…	…	…	…	…	…	…	…	…	…	…
…	…	…	…	…	…	…	…	…	…	…	…	…	…	…	…
…	…	…	…	…	…	…	…	…	…	…	…	…	…	…	…
P60030	8.64	291.2	51.4	70.2	5.076	14.9	12.39	14.28	16.19	18.14	17.16	15.33	37.62	10.4	100.77
P60031	8.64	290.9	53	45.1	1.869	6.9	3.49	4.5	5.5	6.78	6.36	6.42	18.29	7.09	44.32
P60032	8.63	291.2	51.3	45.2	3.262	14.9	5.42	6.62	7.63	9.34	8.47	8.02	21.35	7.28	54.32
P60033	8.63	291.2	51.6	45.1	5.021	24.9	7.61	9.31	10.28	12.62	11.5	10.49	26.21	7.54	68.44

Table 4.3.7. Steady-state critical power measurement conditions

Assembly	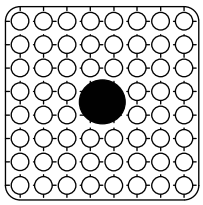 C2A	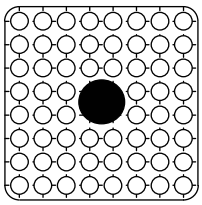 C2B	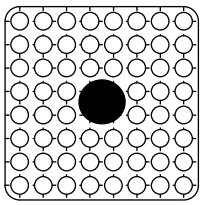 C3
Boundary conditions	Pressure (MPa) Flow rate (t/h) Inlet sub-cooling (kJ/kg)	5.5 7.2 8.6 10 20 30 45 55 60 65 25 50 84 104 126	
Data	Critical power, location of boiling transition Corresponding boundary conditions		
No. of cases	Data supplied cases Exercise cases	151 44	

E1: Exercise 1 case.

Table 4.3.8. Test matrix of steady-state critical power measurements

Assembly	Pressure (MPa)	Flow rate (t/h)	Inlet sub-cooling (kJ/kg)					No. of data
			25	50	84	104	126	
C2A	5.5	20	X	E1, W	X	–	X	20
		45	X	E1	X	–	X	
		55	E1, W	E1, W	E1, W	–	E1	
		65	X	E1	X	–	X	
	7.2	10	X	X	X	X	X	35
		20	X	E1, W	X	X	X	
		30	X	E1	X	X	X	
		45	X	E1	X	X	X	
		55	E1, W	E1, W	E1	E1,W	E1	
		60	X	E1	X	X	X	
		65	X	E1	X	X	X	
	8.6	20	X	E1, W	X	–	X	20
		45	X	E1	X	–	X	
		55	E1, W	E1, W	E1, W	–	E1	
		65	X	E1	X	–	X	
C2B	7.2	10	X	X	X	X	X	36
		20	X	E1	X	X	X	
		30	X	E1	X	X	X	
		45	X	E1	X	X	X	
		55	E1	E1, W	E1	E1	E1	
		60	X	E1	X	X	X	
		65	X	E1	X	X	X	
C3	7.2	10	X	X	X	X	X	36
		20	X	E1	X	X	X	
		30	X	E1	X	X	X	
		45	X	E1	X	X	X	
		55	E1	E1, W	E1	E1	E1	
		60	X	E1	X	X	X	
		65	X	E1	X	X	X	

X: Test case, W: Duplicated test case, E1: Exercise 1 case.

Table 4.3.9. Steady-state critical power measurements data – assembly type C2A

Test number	Outlet pressure (MPa)	Flow rate (t/h)	Inlet sub-cooling (kJ/kg)	Experimental cases
SA505500	5.49	20.16	50.95	Duplicated test, E1
SA505501	5.49	20.10	51.35	Duplicated test
SA505600	5.51	20.12	84.79	–
SA505800	5.50	20.19	129.38	–
SA505900	5.49	20.14	26.04	–
SA510500	5.48	55.06	56.41	Duplicated test, E1
SA510501	5.51	55.11	62.48	Duplicated test
SA510600	5.51	54.70	96.16	Duplicated test, E1
SA510601	5.52	55.34	96.79	Duplicated test
SA510800	5.51	54.81	134.97	E1
SA510900	5.52	54.70	35.33	Duplicated test, E1
SA510901	5.51	55.05	35.02	Duplicated test
SA512500	5.54	65.48	64.36	–
SA512600	5.51	64.97	99.60	–
SA512800	5.50	65.52	133.75	–
SA512900	5.52	65.12	40.30	–
SA516500	5.51	44.85	55.98	E1
SA516600	5.52	45.03	91.83	–
SA516800	5.50	45.28	132.07	–
SA516900	5.52	45.13	35.66	–
SA603500	7.18	10.07	51.85	–
SA603600	7.16	10.07	86.12	–
SA603700	7.17	9.98	106.75	–
SA603800	7.16	9.99	122.79	–
SA603901	7.18	10.01	25.82	–
SA605500	7.16	20.09	50.55	Duplicated test, E1
SA605502	7.17	20.07	51.44	Duplicated test
SA605600	7.17	20.19	83.57	–
SA605700	7.17	20.24	106.22	–
SA605801	7.16	20.21	127.20	–
SA605900	7.16	20.21	22.61	–
SA607500	7.13	30.02	48.35	E1
SA607600	7.15	30.23	82.55	–
SA607700	7.16	30.00	106.63	–
SA607800	7.18	30.12	126.80	–
SA607900	7.15	30.23	23.42	–
SA610503	7.17	55.20	59.39	Duplicated test, E1
SA610504	7.17	55.47	58.09	Duplicated test
SA610600	7.18	55.05	89.53	E1
SA610700	7.13	55.20	107.61	Duplicated test, E1
SA610701	7.21	54.88	113.28	Duplicated test
SA610800	7.24	55.30	137.26	E1
SA610900	7.27	55.10	37.73	Duplicated test, E1

E1: Exercise 1 case.

Table 4.3.9. Steady-state critical power measurements data – assembly type C2A (*cont.*)

Test number	Outlet pressure (MPa)	Flow rate (t/h)	Inlet sub-cooling (kJ/kg)	Experimental cases
SA610902	7.18	55.42	32.94	Duplicated test
SA611500	7.13	60.23	54.89	E1
SA611600	7.12	60.18	89.39	–
SA611700	7.23	60.10	114.29	–
SA611800	7.15	60.07	131.68	–
SA611900	7.16	60.30	33.18	–
SA612500	7.16	65.36	55.66	E1
SA612600	7.17	64.99	91.82	–
SA612700	7.17	65.19	107.82	–
SA612800	7.18	65.01	132.81	–
SA612900	7.16	65.72	32.31	–
SA616500	7.13	45.17	54.21	E1
SA616600	7.19	45.01	88.72	–
SA616700	7.23	45.13	110.60	–
SA616800	7.15	45.07	128.01	–
SA616900	7.14	45.35	30.59	–
SA805500	8.63	20.30	51.00	Duplicated test, E1
SA805501	8.64	20.30	50.28	Duplicated test
SA805600	8.62	20.26	82.58	–
SA805800	8.6	20.31	125.79	–
SA805900	8.63	20.13	27.84	–
SA810501	8.62	55.15	54.89	Duplicated test, E1
SA810502	8.64	55.16	55.12	Duplicated test
SA810600	8.56	55.00	83.85	Duplicated test, E1
SA810601	8.64	55.21	88.54	Duplicated test
SA810800	8.64	55.28	130.30	E1
SA810900	8.66	55.38	30.97	Duplicated test, E1
SA810901	8.60	55.15	27.55	Duplicated test
SA812500	8.64	65.25	58.08	E1
SA812600	8.64	64.95	91.08	–
SA812800	8.67	65.27	135.52	–
SA812900	8.65	65.22	29.55	–
SA816500	8.61	45.24	52.22	E1
SA816600	8.67	45.52	88.65	–
SA816800	8.60	45.23	128.18	–
SA816900	8.65	45.24	27.81	–

E1: Exercise 1 case.

Table 4.3.10. Steady-state critical power measurements data – assembly type C2B

Test number	Outlet pressure (MPa)	Flow rate (t/h)	Inlet sub-cooling (kJ/kg)	Experimental cases
SB603500	7.17	9.93	50.50	–
SB603602	7.15	9.96	84.59	–
SB603700	7.17	9.99	104.90	–
SB603800	7.15	10.09	128.57	–
SB603900	7.14	10.01	23.14	–
SB605500	7.15	20.03	51.66	E1
SB605600	7.14	19.93	80.09	–
SB605700	7.16	20.18	103.88	–
SB605800	7.17	20.07	126.40	–
SB605900	7.14	19.84	21.06	–
SB607500	7.13	30.05	49.90	E1
SB607600	7.17	29.95	83.37	–
SB607700	7.16	29.83	105.04	–
SB607800	7.14	29.97	126.27	–
SB607900	7.18	29.76	24.61	–
SB610500	7.20	54.84	54.28	Duplicated test, E1
SB610501	7.19	54.91	51.16	Duplicated test
SB610600	7.18	54.91	82.45	E1
SB610700	7.18	54.71	105.31	E1
SB610800	7.14	54.90	122.48	E1
SB610900	7.20	54.88	26.55	E1
SB611500	7.19	59.88	54.03	E1
SB611600	7.19	59.95	87.15	–
SB611700	7.13	59.74	101.34	–
SB611800	7.18	59.88	127.26	–
SB611900	7.13	59.83	26.83	–
SB612500	7.18	64.60	48.65	E1
SB612600	7.18	64.68	81.47	–
SB612700	7.21	64.05	106.23	–
SB612800	7.15	64.82	125.63	–
SB612900	7.16	64.85	21.18	–
SB616501	7.14	44.82	47.96	E1
SB616600	7.18	44.91	83.57	–
SB616700	7.18	44.93	107.37	–
SB616800	7.16	45.01	127.09	–
SB616900	7.18	44.82	27.54	–

E1: Exercise 1 case.

Table 4.3.11. Steady-state critical power measurements data – assembly type C3

Test number	Outlet pressure (MPa)	Flow rate (t/h)	Inlet sub-cooling (kJ/kg)	Experimental cases
SC603900	7.14	9.95	21.70	–
SC603500	7.15	9.95	50.88	–
SC603600	7.16	10.01	88.57	–
SC603700	7.17	9.93	105.55	–
SC603800	7.16	9.98	125.35	–
SC605900	7.12	19.95	22.11	–
SC605500	7.16	19.96	50.40	E1
SC605600	7.15	19.86	80.19	–
SC605700	7.13	19.93	102.45	–
SC605800	7.15	19.91	125.18	–
SC607900	7.17	29.88	23.62	–
SC607500	7.15	29.83	51.09	E1
SC607600	7.15	29.92	82.80	–
SC607701	7.15	29.91	105.59	–
SC607800	7.10	29.99	122.82	–
SC616900	7.13	44.93	22.94	–
SC616500	7.15	45.04	50.88	E1
SC616600	7.14	44.95	82.80	–
SC616701	7.12	44.91	102.89	–
SC616800	7.14	44.89	123.57	–
SC610900	7.19	54.90	31.35	E1
SC610500	7.19	54.90	50.74	Duplicated test, E1
SC610502	7.14	54.76	49.84	Duplicated test
SC610600	7.13	54.66	81.93	E1
SC610700	7.15	54.83	103.37	E1
SC610800	7.21	55.06	128.69	E1
SC611900	7.14	59.97	25.27	–
SC611500	7.19	59.72	51.05	E1
SC611600	7.13	59.91	81.73	–
SC611700	7.19	59.91	104.96	–
SC611800	7.15	59.78	124.09	–
SC612900	7.15	64.99	24.40	–
SC612500	7.17	65.02	52.32	E1
SC612600	7.17	64.87	84.39	–
SC612700	7.16	64.86	104.64	–
SC612800	7.16	64.87	125.74	–

E1: Exercise 1 case.

Table 4.3.12. Transient boiling transition measurement conditions

Assembly	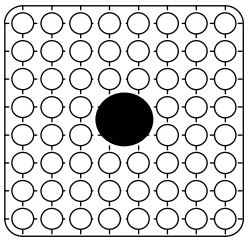 C2A	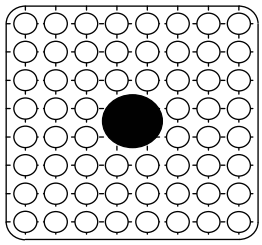 C3
Rated initial conditions	Pressure (MPa) Power (MW) Flow rate (t/h) Inlet enthalpy (kJ/kg)	7.2 6.2~8.5 45 1 217~1 227
Transients	Turbine trip without bypass Re-circulation pump trip	
Data	Time histories of cladding temperature where boiling transition occurred Timing of boiling transition, timing of rewetting, peak cladding temperature Corresponding boundary conditions during transients	
No. of cases	Data supplied cases Exercise cases	4 2

Table 4.3.13. Test matrix of transient boiling transition measurements

Assembly	**Initial conditions**				**Transients**	**Exercise cases**	**No. of cases**
	Pressure (MPa)	**Power (MW)**	**Flow rate (t/h)**	**Inlet enthalpy (kJ/kg)**			
C2A	7.2	6.2~8.5	45	1 217~1 227	Turbine trip without bypass	E2	2
					Re-circulation pump trip	E2	
C3	7.2	6.2~8.5	45	1 217~1 227	Turbine trip without bypass	–	2
					Re-circulation pump trip	–	

E2: Exercise 2 case.

Table 4.3.14. Test numbers of transient boiling transition measurements

Test no.	Assembly	Initial conditions/experimental conditions				Transients	Exercise cases
		Pressure (MPa)	Power (MW)	Flow rate (t/h)	Inlet enthalpy (kJ/kg)		
TGA10008	C2A	7.2/7.136	6.2~8.5	45/42	1 217~1 227	Turbine trip without bypass	E2
TRA10012	C2A	7.2/7.274	6.2~8.5	45/46.2	1 217~1 227	Re-circulation pump trip	E2
TGC10018	C3	7.2/7.136	6.2~8.5	45/42	1 217~1 227	Turbine trip without bypass	–
TIC10012	C3	7.2/7.274	6.2~8.5	45/46.2	1 217~1 227	Re-circulation pump trip	–

E2: Exercise 2 case.

Figure 4.3.1. Turbine trip transient experimental boundary conditions, assembly type C2A – flow rate

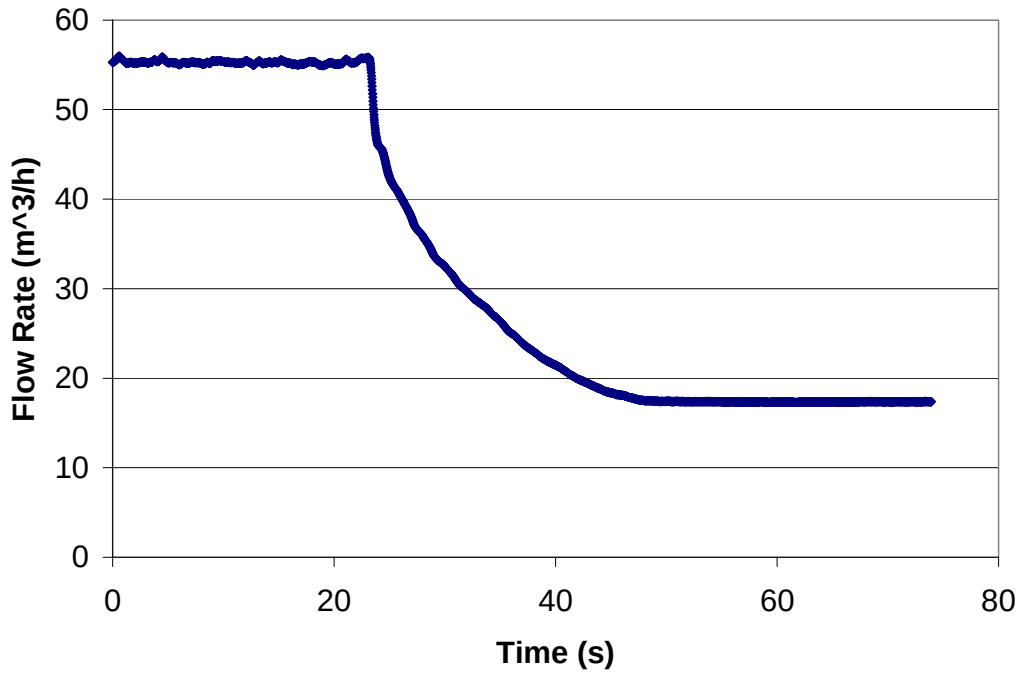

Figure 4.3.2. Turbine trip transient experimental boundary conditions, assembly type C2A – inlet pressure

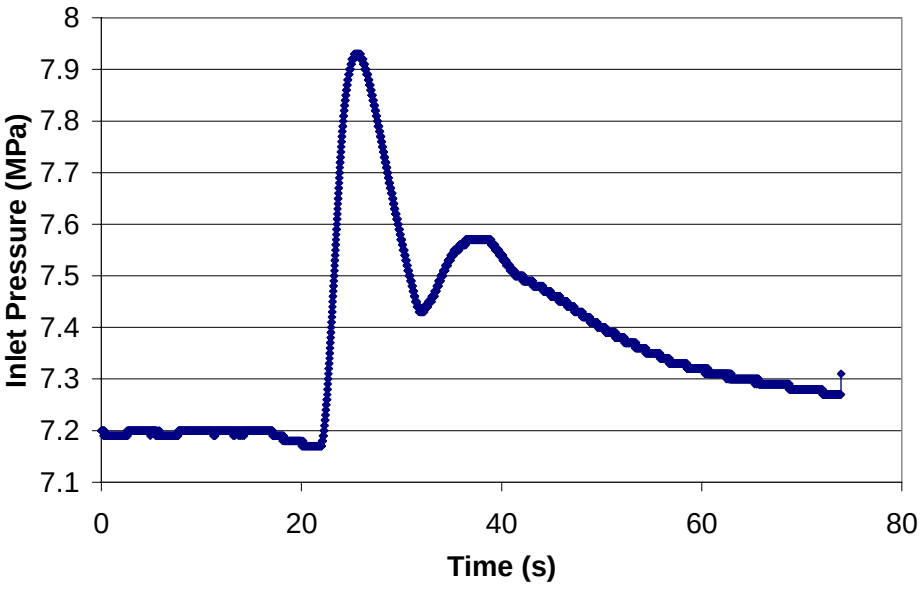

Figure 4.3.3. Turbine trip transient experimental boundary conditions, assembly type C2A – inlet temperature

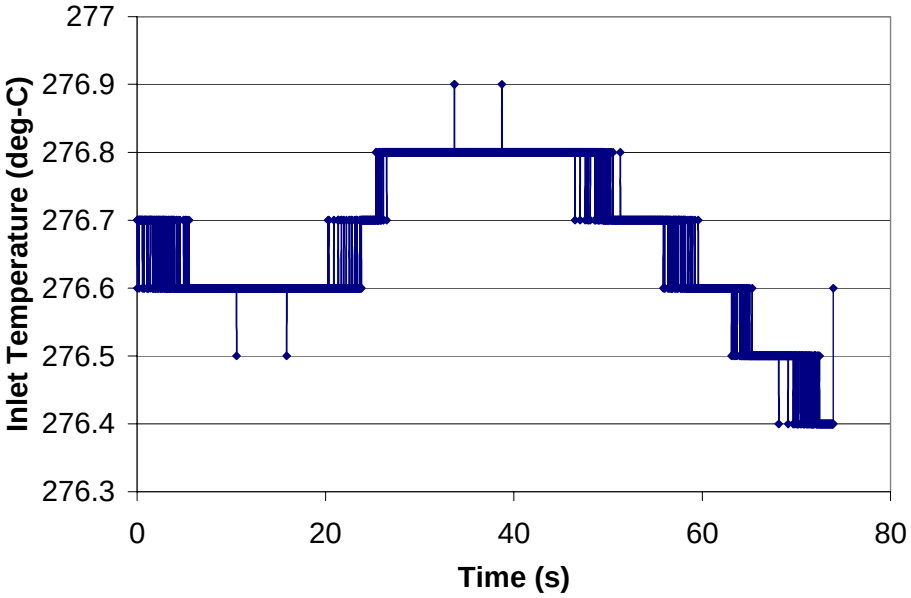

Figure 4.3.4. Pump trip transient experimental boundary conditions, assembly type C2A – flow rate

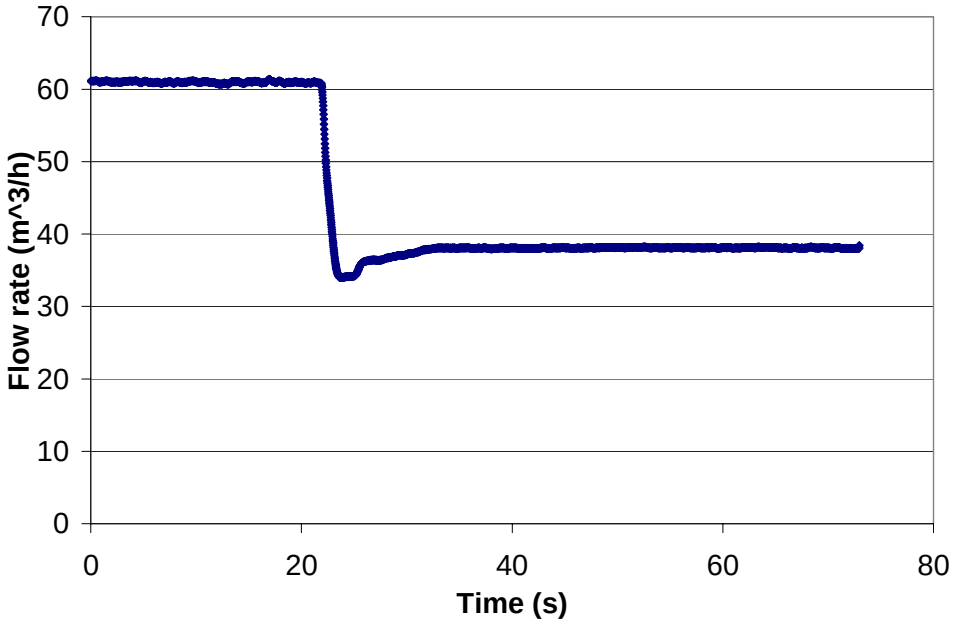

Figure 4.3.5. Pump trip transient experimental boundary conditions, assembly type C2A – inlet pressure

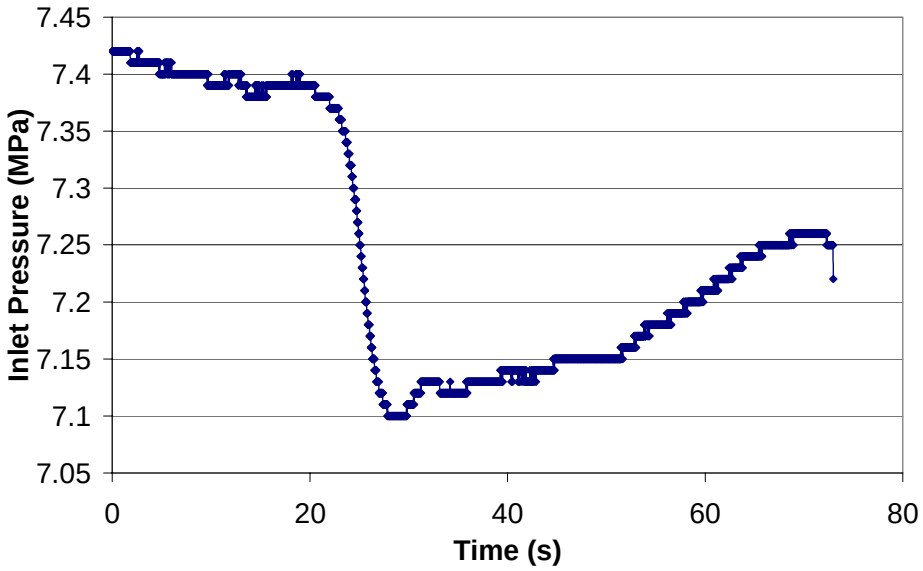

Figure 4.3.6. Pump trip transient experimental boundary conditions, assembly type C2A – inlet temperatures

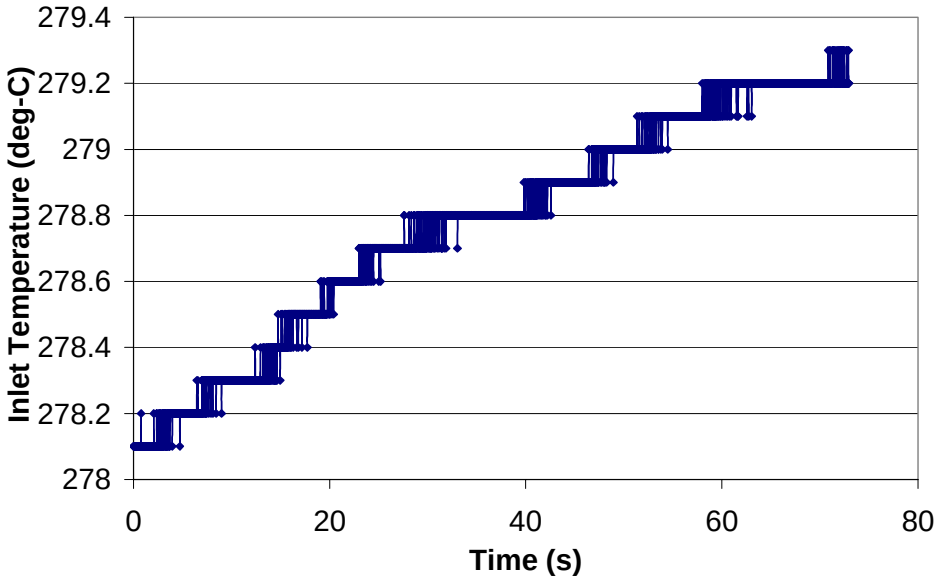

Figure 4.3.7. Turbine trip transient experimental boundary conditions, assembly type C3 – flow rate

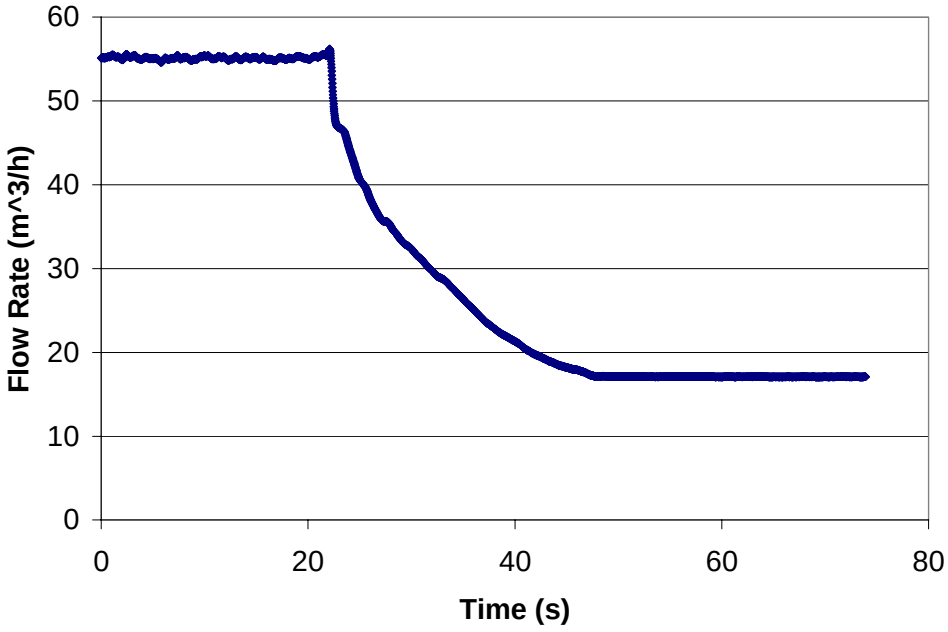

Figure 4.3.8. Turbine trip transient experimental boundary conditions, assembly type C3 – inlet pressure

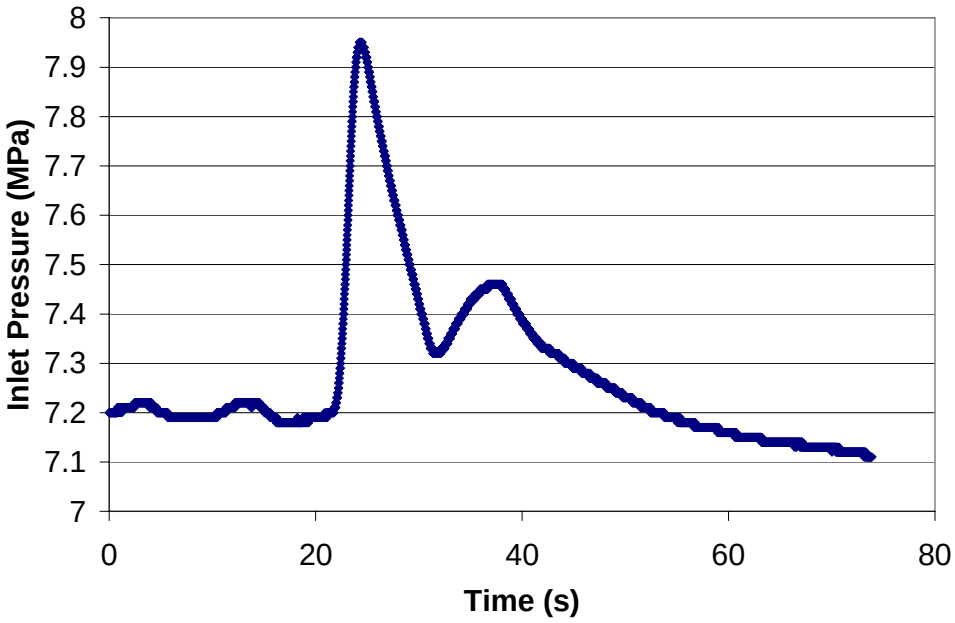

Figure 4.3.9. Turbine trip transient experimental boundary conditions, assembly type C3 – inlet temperature

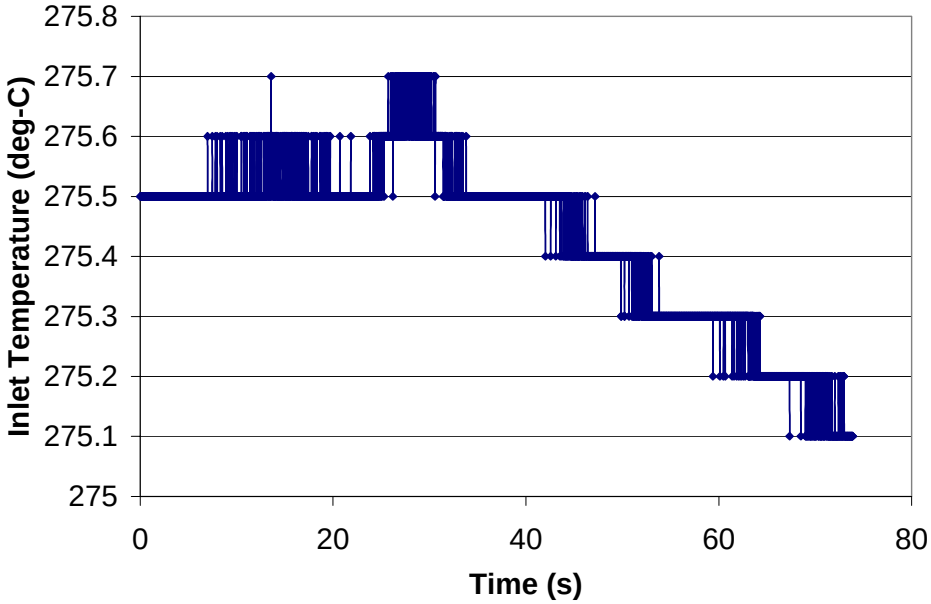

Figure 4.3.10. Pump trip transient experimental boundary conditions, assembly type C3 – flow rate

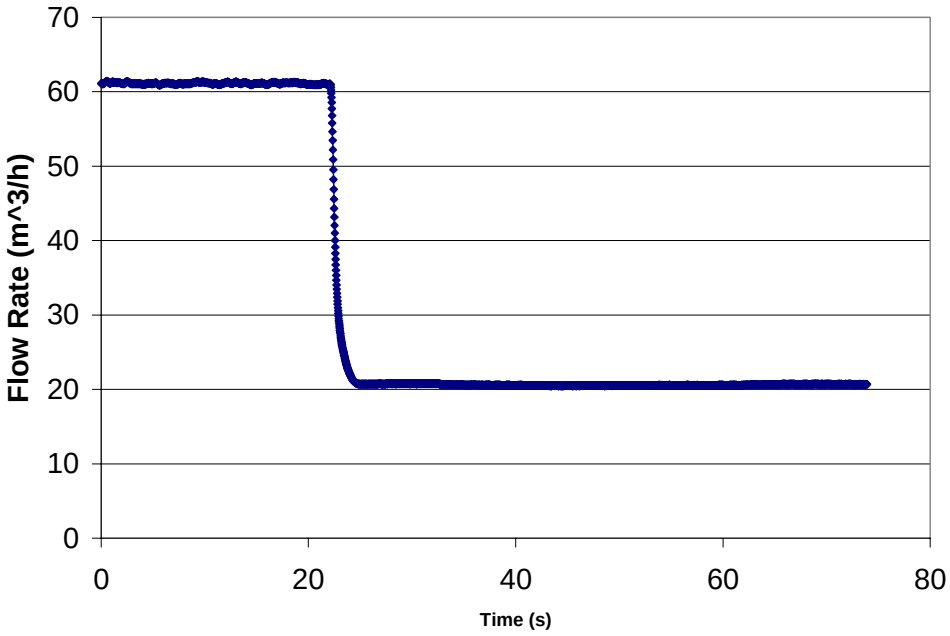

Figure 4.3.11. Pump trip transient experimental boundary conditions, assembly type C3 – inlet pressure

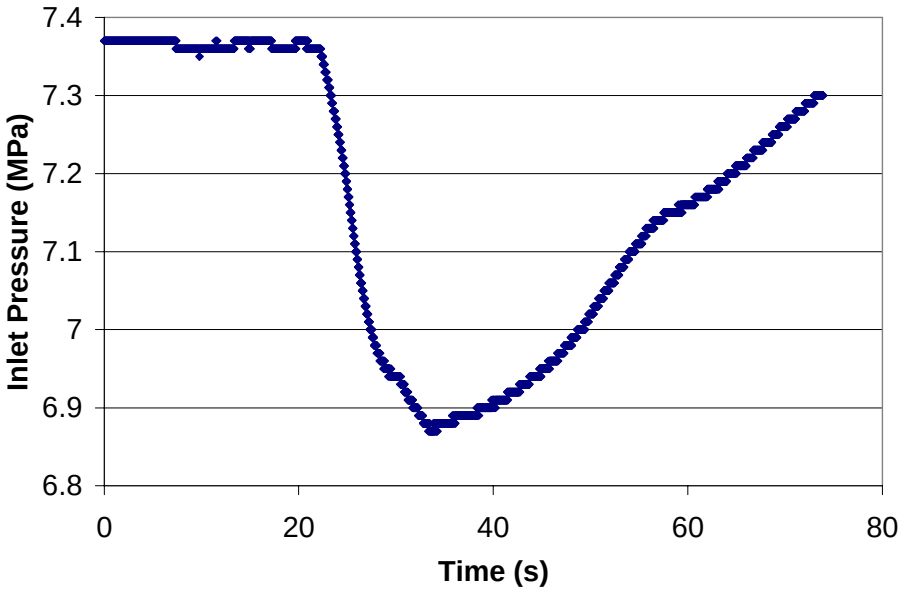

Figure 4.3.12. Pump trip transient experimental boundary conditions, assembly type C3 – inlet temperature

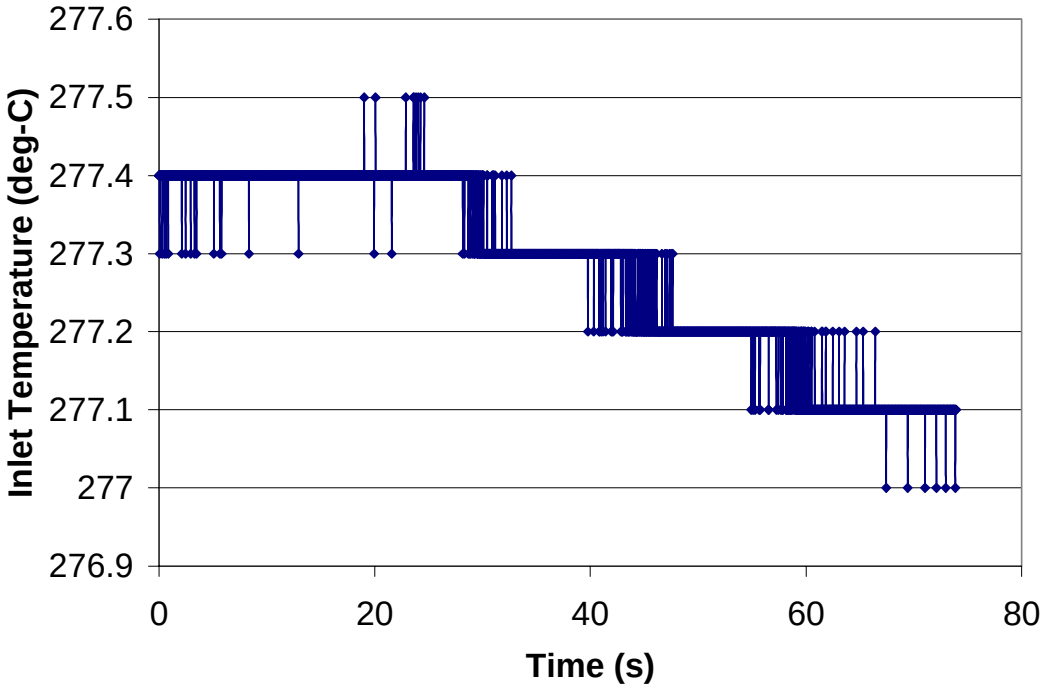

Chapter 5

BENCHMARK PHASES AND EXERCISES

5.1 Introduction

The OECD/NRC BFBT benchmark consists of two phases with each phase consisting of different exercises. The benchmark phases and exercises are described below:

- Phase I – Void distribution benchmark:
  - Exercise 1: Steady-state sub-channel grade benchmark.
  - Exercise 2: Steady-state microscopic grade benchmark.
  - Exercise 3: Transient macroscopic grade benchmark.
  - Exercise 4: Uncertainty analysis of the void distribution benchmark.
- Phase II – Critical power benchmark:
  - Exercise 0: Steady-state pressure drop benchmark.
  - Exercise 1: Steady-state critical power benchmark.
  - Exercise 2: Transient benchmark.

The sub-channel approach is categorised as the macroscopic grade approach that can resolve an element as small as a sub-channel size mesh. Time and space averaged formulations cause the loss of the heterogeneous and instantaneous void fraction information of the two-phase flow structure within the sub-channel. As a consequence, many macroscopic correlations are still indispensable for reproducing the experimental results. In recent years, newer two-phase flow numerical approaches have been developed that can be categorised into meso-, micro- or molecular dynamics approaches. Taking into account the immaturity of numerical modelling for detailed void distribution, this benchmark specification is designed to accept as many potential numerical approaches as possible.

Table 5.1.1 provides a guide to the participants as to where to find the conditions for each benchmark case within each benchmark exercise and phase. Table 5.1.2 provides a guide as to where to find the data for the involved fuel assemblies.

Table 5.1.1. Benchmark conditions

Phase	Exercises		Assembly ID	Geometrical data	Measurement conditions	Test matrix	Test numbers	Related section	Data format
Void distribution	**Steady state sub-channel**		0-1	Table 3.2.6	Table 5.2.1	Table 5.2.2	Table 5.2.3	5.2.1	Table 5.2.4
			0-2	Table 3.2.6	Table 5.2.1	Table 5.2.2	Table 5.2.3	5.2.1	Table 5.2.4
			0-3	Table 3.2.6	Table 5.2.1	Table 5.2.2	Table 5.2.3	5.2.1	Table 5.2.4
			1	Table 3.2.7	Table 5.2.1	Table 5.2.2	Table 5.2.3	5.2.1	Table 5.2.4
			2	Table 3.2.7	Table 5.2.1	Table 5.2.2	Table 5.2.3	5.2.1	Table 5.2.4
			3	Table 3.2.7	Table 5.2.1	Table 5.2.2	Table 5.2.3	5.2.1	Table 5.2.4
			4	Table 3.2.8	Table 5.2.1	Table 5.2.2	Table 5.2.3	5.2.1	Table 5.2.4
	Steady state microscopic		0-1	Table 3.2.6	Table 5.2.1	Table 5.2.2	Table 5.2.3	5.2.2	Table 5.2.6
			0-2	Table 3.2.6	Table 5.2.1	Table 5.2.2	Table 5.2.3	5.2.2	Table 5.2.6
			0-3	Table 3.2.6	Table 5.2.1	Table 5.2.2	Table 5.2.3	5.2.2	Table 5.2.6
			1	Table 3.2.7	Table 5.2.1	Table 5.2.2	Table 5.2.3	5.2.2	Table 5.2.6
			2	Table 3.2.7	Table 5.2.1	Table 5.2.2	Table 5.2.3	5.2.2	Table 5.2.6
			3	Table 3.2.7	Table 5.2.1	Table 5.2.2	Table 5.2.3	5.2.2	Table 5.2.6
			4	Table 3.2.8	Table 5.2.1	Table 5.2.2	Table 5.2.3	5.2.2	Table 5.2.6
	Transient macroscopic		4	Table 3.2.8	Table 5.2.7	Table 5.2.8	Table 5.2.9	5.2.3	Table 5.2.10, Table 5.2.12
	Uncertainty analysis		1	Table 3.2.7	Table 5.2.1	Table 5.2.15	Table 5.216	5.2.4	Table 5.2.4
Critical power	**Steady state**	*Pressure drop*	C2A – single-phase	Table 3.2.8	Table 5.3.1	Table 5.3.2	Table 5.3.7	5.3.1	Table 5.3.5
			C2A – two-phase	Table 3.2.8	Table 5.3.3	Table 5.3.4	Table 5.3.8	5.3.1	Table 5.3.6
		Critical power	C2A	Table 3.2.8	Table 5.3.9	Table 5.3.10	Table 5.3.12	5.3.2	Table 5.3.11
			C2B	Table 3.2.8	Table 5.3.9	Table 5.3.10	Table 5.3.13	5.3.2	Table 5.3.11
			C3	Table 3.2.8	Table 5.3.9	Table 5.3.10	Table 5.3.14	5.3.2	Table 5.3.11
	Transient		C2A	Table 3.2.8	Table 5.3.15	Table 5.3.16	Table 5.3.17	5.3.2	Table 5.3.18, Table 5.3.20

Table 5.1.2. Assembly specification references

Assembly ID	Radial power shape	Axial power shape	Heater rod data	Spacer type
0-1	Uniform	Uniform	Table 3.3.1	Grid
0-2	Uniform	Uniform	Table 3.3.1	Grid
0-3	Uniform	Uniform	Table 3.3.1	Grid
1	Table 3.2.2	Table 3.2.3	Table 3.3.1	Grid
2	Table 3.2.2	Table 3.2.3	Table 3.3.1	Grid
3	Table 3.2.2	Table 3.2.3	Table 3.3.1	Grid
4	Table 3.2.5	Table 3.2.3	Table 3.3.1	Ferrule
C2A	Table 3.2.5	Table 3.2.3	Table 3.3.1	Ferrule
C2B	Table 3.2.5	Table 3.2.3	Table 3.3.1	Ferrule
C3	Table 3.2.5	Table 3.2.3	Table 3.3.1	Ferrule

5.2 Phase I – Void distribution benchmark

The measured steady-state void distribution data is supplied as a time-space averaged value in a sub-channel mesh size. However, the raw image data has a resolution as small as 0.3 mm × 0.3 mm. This image data is recovered. It is transformed into the uncompressed ASCII image format and it is designed for benchmarking microscopic two-phase numerical approaches.

5.2.1 Exercise 1: Steady-state sub-channel grade benchmark

The conditions of selected cases for Exercise 1 of Phase I are summarised in Table 5.2.1. The cases are denoted with E1 in Tables 5.2.2 and 5.2.3, which provide the test matrix of these cases and their test numbers, respectively.

This exercise is designed for benchmarking sub-channel, meso- and microscopic numerical approaches. The supplied measured data includes time and space averaged void distribution matrix in sub-channel mesh size, and corresponding boundary conditions (pressure, flow, inlet sub-cooling and power shape). Table 5.2.4 shows the data format of steady-state sub-channel grade benchmark. Table 5.2.5 demonstrates an example from the database for average void fraction in a sub-channel for test 0011-55, assembly type 0-1.

5.2.2 Exercise 2: Steady-state microscopic grade benchmark

The conditions of selected cases for Exercise 2 of Phase I are summarised in Table 5.2.1 as well. The cases are denoted with E2 in Tables 5.2.2 and 5.2.3.

This exercise is designed for benchmarking meso-, microscopic and molecular dynamics numerical approaches. Table 5.2.6 demonstrates the conversion from raw image data (which has a resolution as small as 0.3 mm × 0.3 mm) into ASCII image format. The values **xx** and **aa** correspond to void fraction values measured by 512 detectors in x and y direction.

Table 5.2.1. Conditions for Exercises 1 and 2 of Phase I

Assembly	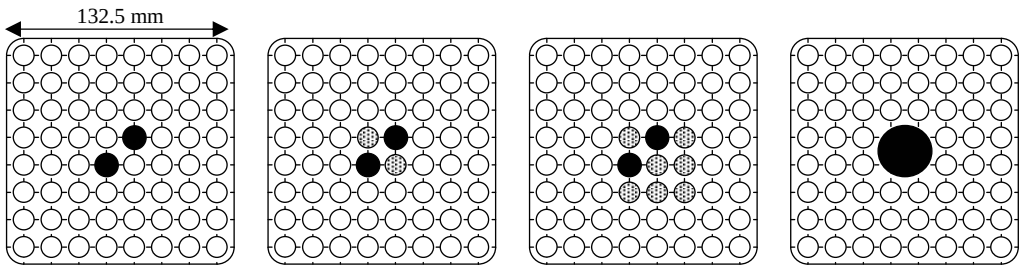 0-1, 1, 2, 3 0-2 0-3 4	
Boundary conditions	Pressure (MPa)	7.2
	Flow rate (t/h)	55
	Inlet sub-cooling (kJ/kg)	50.2
	Exit quality (%)	2 5 8 12 18 25
Data	Void distribution matrix in sub-channel mesh size Void distribution matrix in 0.3 × 0.3 mm mesh size (512 × 512 = 262K pixels) Corresponding boundary conditions	
No. of cases	Exercise cases	Sub-channel: 15 ; microscopic: 4

Exit quality: Thermal equilibrium quality.

Table 5.2.2. Test matrix of selected cases for Exercises 1 and 2 of Phase I

Assembly	Pressure (MPa)	Inlet sub-cooling (kJ/kg)	Flow rate (t/h)	Exit quality (%)					
				2	5	8	12	18	25
0-1	7.2	50.2	55		E1		E1		E1
0-2	7.2	50.2	55		E1		E1		E1
0-3	7.2	50.2	55		E1		E1		E1
1	7.2	50.2	55		E1		E1		E1
4	7.2	50.2	55	E2	E1, E2		E1, E2		E1, E2

E1: Exercise 1 case, E2: Exercise 2 case.

Table 5.2.3. Test numbers of selected cases for Exercises 1 and 2 of Phase I

Test no.	Assembly	Pressure (MPa)	Flow rate (t/h)	Inlet sub-cooling (kJ/kg)	Power (MW)	Exit quality (%)	Exercise cases	
0011-55	0-1	7.18	54.0	52.6	1.9	5.0	E1	–
0011-58	0-1	7.17	54.9	51.0	3.51	12.0	E1	–
0011-61	0-1	7.21	54.8	50.9	6.44	24.9	E1	–
0021-16	0-2	7.19	54.9	54.0	1.91	4.8	E1	–
0021-18	0-2	7.17	54.9	49.8	3.51	12.1	E1	–
0021-21	0-2	7.18	54.9	51.4	6.45	24.9	E1	–
0031-16	0-3	7.18	55.0	52.4	1.92	4.9	E1	–
0031-18	0-3	7.18	54.8	50.0	3.52	12.1	E1	–
0031-21	0-3	7.17	54.9	49.4	6.45	25.0	E1	–
1071-55	1	7.19	54.6	52.8	1.92	4.9	E1	–
1071-58	1	7.16	55.1	50.3	3.52	11.9	E1	–
1071-61	1	7.20	54.7	51.8	6.48	25.1	E1	–
4101-53	4	7.159	55	50.2	2	1.24	–	E2
4101-55	4	7.20	54.6	52.9	1.92	5.0	E1	E2
4101-58	4	7.15	54.6	50.6	3.52	12.1	E1	E2
4101-61	4	7.18	54.7	52.5	6.48	25.1	E1	E2

E1: Exercise 1 case, E2: Exercise 2 case.

Table 5.2.4. Data format of Exercise 1 of Phase I – sub-channel grade benchmark

y/x	1	2	3	4	5	6	7	8	9
1	XX	XX	XX	XX	XX	XX	XX	XX	XX
2	XX	XX	XX	XX	XX	XX	XX	XX	XX
3	XX	XX	XX	XX	XX	XX	XX	XX	XX
4	XX	XX	XX	XX	XX	XX	XX	XX	XX
5	XX	XX	XX	XX	XX	XX	XX	XX	XX
6	XX	XX	XX	XX	XX	XX	XX	XX	XX
7	XX	XX	XX	XX	XX	XX	XX	XX	XX
8	XX	XX	XX	XX	XX	XX	XX	XX	XX
9	XX	XX	XX	XX	XX	XX	XX	XX	XX

Table 5.2.5. Average void distribution for test 0011-55 for sub-channel void distribution – Exercise 1 of Phase I

y/x	1	2	3	4	5	6	7	8	9
1	39.3	38.9	36.7	27.3	32	38	38.6	44.1	37.4
2	44.4	46.8	42.5	34	41.1	37.7	50	42.4	40.7
3	38	42.9	48	44.6	49.5	45.3	48.6	41.9	34.4
4	42.4	37.6	43.7	38.2	44.3	33.1	44	35.6	35.7
5	30.9	40.7	47.7	45	41.1	42	47	45.2	30.8
6	36	35.4	40.7	30.6	38.1	38.4	44.2	38.1	38.1
7	36.3	39	45	42.8	48.7	43.7	48	44.9	41.6
8	34.8	40.4	46	38.6	39.7	37	47.4	46.8	40.7
9	29.3	45.6	41.6	40.8	28.7	34.3	36.7	47.9	32.2

Table 5.2.6. Data format of Exercise 2 of Phase I – steady-state microscopic grade benchmark

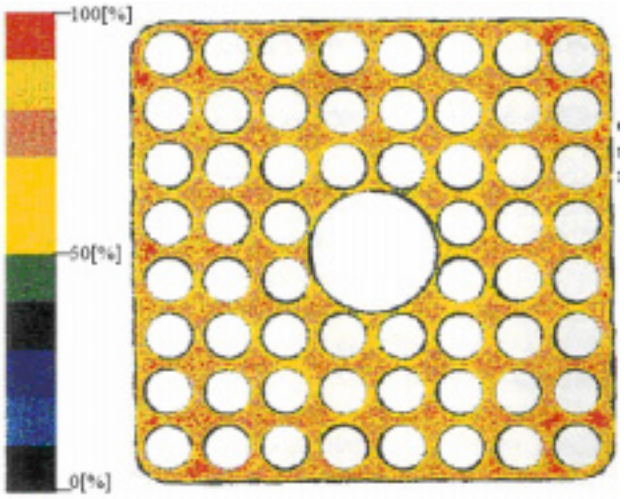

Conversion to ASCII format

	1	2	3	4	5	.	.	.	n-3	n-2	n-1	n=512
1	00	00	00	00	00	00	00	00	00	00	00	00
2	0x	xx	1x	xx	2x	xx	3x	xx	4x	xx	5x	xx
3	0a	aa	1a	aa	2a	aa	3a	aa	4a	aa	5a	aa
4	00	00	00	00	00	00	00	00	00	00	00	00
5	0x	xx	1x	xx	2x	xx	3x	xx	4x	xx	5x	xx
.	0a	aa	1a	aa	2a	aa	3a	aa	4a	aa	5a	aa
.	00	00	00	00	00	00	00	00	00	00	00	00
.	2x	xx	3x	xx	4x	xx	5x	xx	6x	xx	7x	xx
n-3	00	00	00	00	00	00	00	00	00	00	00	00
n-2	3x	xx	4x	xx	5x	xx	6x	xx	7x	xx	8x	xx
n-1	3a	aa	4a	aa	5a	aa	6a	aa	7a	aa	8a	aa
n=512	00	00	00	00	00	00	00	00	00	00	00	00

5.2.3 Exercise 3: Transient macroscopic grade benchmark

The conditions of selected cases for Exercise 3 of Phase I are summarised in Table 5.2.7. For this exercise two transient cases, turbine trip without bypass and re-circulation pump trip, are chosen. The cases are denoted with E3 in Tables 5.2.8 and 5.2.9, which provide the test matrix of these cases and their test numbers, respectively. Exercise 3 is designed for benchmarking sub-channel numerical approaches. The supplied measured data includes space-averaged instantaneous axial void profiles during the transients and the corresponding boundary conditions (pressure, flow, inlet sub-cooling and power shape). Tables 5.2.10 and 5.2.12 show the data format of the transient sub-channel grade benchmark. Tables 5.2.11 and 5.2.13 demonstrate examples of the measured data for turbine trip transient included in Exercise 3. For the pump trip transient, the data is represented in a similar way.

Table 5.2.7. Conditions for Exercise 3 of Phase I

Assembly	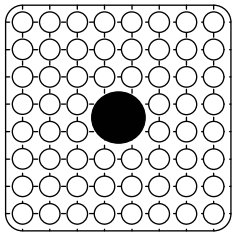 4	
Rated initial conditions	Pressure (MPa) Power (MW) Flow rate (t/h) Inlet temperature (Celsius)	7.16 4.5 55 279
Transients	Turbine trip without bypass, re-circulation pump trip	
Data	Time histories of cross-sectional averaged void fraction in each axial level during transients Corresponding boundary conditions during transients	
No. of cases	Exercise cases	2

Table 5.2.8. Test matrix of selected cases for Exercise 3 of Phase I

Assembly	**Initial conditions**				**Transients**	**Exercise cases**
	Pressure (MPa)	**Power (MW)**	**Flow rate (t/h)**	**Inlet temperature (Celsius)**		
4	7.16	4.5	55	279	Turbine trip without bypass	E3
					Re-circulation pump trip	E3

E3: Exercise 3 case.

Table 5.2.9. Test numbers of selected cases for Exercise 3 of Phase I

Test no.	Assembly	Initial conditions				Transients	Exercise cases
		Pressure (MPa)	Power (MW)	Flow rate (t/h)	Inlet temperature (Celsius)		
4102-001~009	4	7.16	4.5	55	279	Turbine trip without bypass	E3
4102-019~027	4	7.16	4.5	55	279	Re-circulation pump trip	E3

E3: Exercise 3 case.

Table 5.2.10. Data format of Exercise 3 of Phase I (boundary conditions' histories)

Histories of boundary conditions	Flow rate (t/h)	Power (MW)	Pressure at inlet (MPa)	Pressure at outlet (MPa)	Temperature at inlet (°C)
Time 1	XX	XX	XX	XX	XX
Time 2	XX	XX	XX	XX	XX
Time 3	XX	XX	XX	XX	XX
….	XX	XX	XX	XX	XX
Time M-3	XX	XX	XX	XX	XX
Time M-2	XX	XX	XX	XX	XX
Time M-1	XX	XX	XX	XX	XX
Time M	XX	XX	XX	XX	XX

Table 5.2.11. Example of data format Exercise 3 of Phase I (BCs histories)

Histories of boundary conditions	Flow rate (t/h)	Power (MW)	Pressure at inlet (MPa)	Pressure at outlet (MPa)	Temperature at inlet (°C)
0.0	54.84	4.53	7.241	7.141	280.5
0.02	54.83	4.53	7.231	7.144	280.5
0.04	54.83	4.53	7.251	7.143	280.5
0.06	54.85	4.52	7.239	7.144	280.6
…	…	…	…	…	…
57.47	20.64	4.49	7.310	7.199	281.6
57.09	20.90	4.49	7.288	7.198	281.6
57.78	20.77	4.49	7.306	7.198	281.6

Test assembly type-4.
Power shape = uniform.

Table 5.2.12. Data format of Exercise 3 of Phase I (cross-sectional averaged void fraction)

Cross-sectional averaged void fraction	X-ray densitometer 1	X-ray densitometer 2	X-ray densitometer 3
Time 1	XX	XX	XX
Time 2	XX	XX	XX
Time 3	XX	XX	XX
…	XX	XX	XX
Time M-3	XX	XX	XX
Time M-2	XX	XX	XX
Time M-1	XX	XX	XX
Time M	XX	XX	XX

Table 5.2.13. Example of data format of Exercise 3 of Phase I (cross-sectional averaged void fraction)

Cross-sectional averaged void fraction	X-ray densitometer 1	X-ray densitometer 2	X-ray densitometer 3
0.0 s	73.97	58.72	20.12
0.02 s	73.37	58.64	19.28
0.04 s	74.02	58.62	19.54
0.06 s	74.03	58.29	19.60
…	…	…	…
57.47 s	73.17	57.47	20.64
57.09 s	73.92	57.09	20.90
57.78 s	73.63	57.78	20.77

5.2.4. Exercise 4: Uncertainty analysis of void distribution

The uncertainty analysis exercise is defined as Exercise 4 of Phase I. The test cases for this exercise include some of the test cases of Exercise 1 of Phase I plus additional test cases. The BFBT benchmark provides a very good opportunity to apply techniques of uncertainty analysis, and to assess the accuracy of thermal-hydraulic models for two-phase flows in rod bundles. During the previous OECD benchmarks, participants usually carried out sensitivity analysis on their models or on the specifications (initial conditions, boundary conditions, etc.) in order to (i) identify the most sensitive models, i.e. the models which require a careful validation; (ii) improve the computed results, i.e. reduce the discrepancies with the reference data. The aim of Exercise 4 of Phase I is to develop such an approach.

The independent input parameters for the different experiments within the framework of Exercise 4 of Phase I are given as:

- pressure;
- mass flow;
- quality (or power);
- inlet sub-cooling (enthalpy).

Each of these parameters is characterised by a range of uncertainty given by the experimental measurement uncertainty as determined by the testing organisation. In addition, the uncertainties for the sub-channel void fraction are also given by the testing organisation. These uncertainties can be formulated into a probability density function (pdf). A normal distribution as a probability density function (pdf) of process parameters is suggested.

The accuracy of the measured test parameters is given in Table 2.4.3, Section 2.4 as provided by JNES. The accuracy of these void fraction measurements depends on the photon statistics of the X-ray source, the detector non-linearity and the accuracy of the known fluid condition (temperature and pressure) measurements.

Exercise 4 will be performed in two steps. The first step, described in detail in Appendix A, is a standard type of accuracy analysis of code predictions while the second step is an in-depth uncertainty analysis.

STEP 1

As mentioned earlier, there are four input independent parameters: pressure, quality, flow rate and inlet sub-cooling enthalpy. These parameters will be used for preparing measured versus predicted (M/P) plots. To see the effect of each parameter, experimental cases are selected in which the value of one of parameters is changing while the others are constant (see Table 5.2.14).

Table 5.2.14. Selected cases for Step 1 of Exercise 4 of Phase I

Analysis number	Is pressure changing?	Is flow rate changing?	Is quality changing?	Is inlet sub-cooling changing?	First selected case	Second selected case	Third selected case	Fourth selected case
1	No, constant	No, constant	No, constant	**Yes, changing**	*1071-55*	*1071-62*	–	–
2	No, constant	No, constant	**Yes, changing**	No, constant	*1071-53*	*1071-55*	*1071-58*	*1071-61*
3	No, constant	**Yes, changing**	No, constant	No, constant	*1071-34*	*1071-40*	*1071-55*	*1071-65*
4	**Yes, changing**	No, constant	No, constant	No, constant	*1071-12*	*1071-27*	*1071-55*	*1071-82*

In addition to test cases 1071-55, 1071-58 and 1071-61 of Exercise1 of Phase I, eight additional test cases will be used for accuracy analysis. These are test cases 1071-12, 1071-27, 1071-34, 1071-40, 1071-53, 1071-65, 1071-62, and 1071-82.

Tables 5.2.15 and 5.2.16 show the cases which will be used for the uncertainty analysis. The test cases included in Exercise 1 of Phase I (which are a part of Exercise 4) are also indicated in Tables 5.2.15 and 5.2.16.

Table 5.2.15. Test matrix of selected cases for Exercise 4 of Phase I

Assembly	Pressure (MPa)	Inlet sub-cooling (kJ/kg)	Flow rate (t/h)	Exit quality (%)					
				2	5	8	12	18	25
1	1.0	50.2	55	X	E4	X	X	–	–
1	3.9	50.2	55	X	E4	X	X	X	X
1	7.2	50.2	10	X	E4	X	X	X	X
1	7.2	50.2	20	X	E4	X	X	X	X
1	7.2	50.2	55	W, E4	E1, E4	W	E4	W	E1, E4
1	7.2	50.2	70	X	E4	X	X	X	–
1	7.2	126.0	55	E4	X	–	X	–	–
1	8.6	50.2	55	X	E4	X	X	W	–

X: Test case, W: Duplicated test case, E1: Exercise 1 case, E4: Exercise 4 case.

Table 5.2.16. Test numbers of selected cases for Exercise 4 of Phase I

Test no.	Assembly	Pressure (MPa)	Flow rate (t/h)	Inlet sub-cooling (kJ/kg)	Power (MW)	Exit quality (%)	Exercise cases
1071-12	1	1.016	54.92	56.2	2.32	5.0	E4
1071-27	1	3.944	54.71	50.7	2.09	5.0	E4
1071-34	1	7.164	10.22	49.5	0.36	5.0	E4
1071-40	1	7.161	20.00	63.6	0.70	5.0	E4
1071-53	1	7.185	54.58	52.2	1.23	2.0	E4
1071-55	1	7.190	54.60	52.8	1.92	4.9	E4
1071-58	1	7.160	55.10	50.3	3.52	11.9	E4
1071-61	1	7.200	54.70	51.8	6.48	25.1	E4
1071-62	1	7.147	54.85	124.6	3.07	5.0	E4
1071-65	1	7.195	69.49	53.9	2.45	5.0	E4
1071-82	1	8.633	54.69	51.7	1.85	5.0	E4

STEP 2

Step 2 of Exercise 4 is devoted to uncertainty analysis of void fraction prediction. This exercise will fulfil two main objectives: assessing the actual accuracy of thermal-hydraulic models for void fraction prediction in rod bundles, and comparison of available methods for uncertainty analysis in thermal-hydraulics. There are several steps in the uncertainty analysis:

- Definition of the *optimised* physical model; this requires an initial analysis of the physical model to be used and the relevant closure laws (here void fraction model) and an optimisation process of the model (tuning the parameters of the closure laws). This can be done by participants during Exercise 1 of Phase I.

- Analysis of experimental data and their sources of uncertainty (boundary conditions, geometry, measurement technique).

- Selection of the most sensitive parameters in the physical models and/or in the input data (*parametric identification*).

- Propagation of the selected uncertainties through the calculations; this requires a large number of calculations with *stochastic* values for all selected input parameters of the code.

- Analysis of the computation results with given criteria such as robustness, accuracy, etc.

The uncertain parameters in the experiments with their characteristics are basically of two types:

- **Input** geometry (e.g. fuel rod diameter) and boundary conditions (temperature, mass flow, pressure and power) of the test section.

- **Output** measurements of void fraction at a sub-channel level.

The uncertain input parameters with their probability density functions are indicated above. The participants are requested to propagate these uncertainties through the codes, possibly combined with uncertain parameters of the physical models, and perform the void fraction calculations associated with the uncertainty. In Step 2 of Exercise 4, in addition to the cases when one input parameter changes and the rest are constant, other cases will be analysed. In these cases all four input parameters change in order to access cross-term effects. These results will be analysed with several statistical criteria such as mean, standard deviation and maximum error, and compared to the experimental uncertainty (X-ray scanning technique).

5.3. Phase II – Critical power benchmark

Basically, two approaches can be applied in the critical power benchmark:

1) One-dimensional approach with BT correlation. Participants may develop their own BT correlations based on test points. However, this will not be a part of the objectives of this benchmark.

2) Sub-channel mechanistic approach.

5.3.1 Exercise 0: Steady-state pressure drop benchmark

The supplied data includes single- and two-phase pressure drop measurements. The test conditions are summarised in Table 5.3.1 for single-phase and Table 5.3.3 for two-phase pressure drop. The test matrices are shown in Table 5.3.2 and 5.3.4, respectively. The data format is given in Tables 5.3.5 and 5.3.6 and the data itself for the selected test cases are listed in Tables 5.3.7 and 5.3.8.

Table 5.3.1. Conditions for Exercise 0 of Phase II; single-phase pressure drop

Assembly	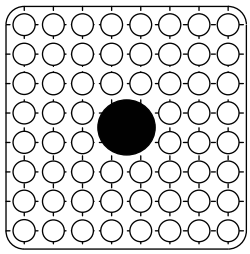 C2A	
Boundary conditions	Pressure (MPa) Flow rate (t/h)	0.2, 1, 7.2 10 15 20 25 30 35 40 45 55 60 65 70
Data	Pressure drop along with axial heated length Corresponding boundary conditions	
No. of cases	Exercise cases	10
Concerned issues	Single-phase pressure drop from bottom to top of heated length	

Table 5.3.2. Test matrix of selected cases for Exercise 0 of Phase II; single-phase pressure drop

Assembly	**Pressure (MPa)**	**Flow rate (t/h)**											**No. of data**
		10	**15**	**20**	**25**	**30**	**35**	**40**	**45**	**55**	**60**	**65**	**70**	
C2A	0.1	X	X	X	X	X	X	X	X	X	X	X	X	36
	1.0	X	X	X	X	X	X	X	X	X	X	X	X	
	7.2	X	X	E0	E0	E0	E0	E0	E0	E0	E0	E0	E0	

X: Test case, E0: Exercise 0 case.

Table 5.3.3. Conditions for Exercise 0 of Phase II; two-phase pressure drop

Assembly	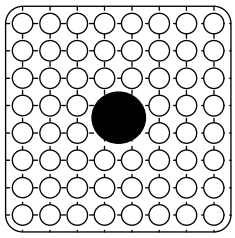 C2A	
Boundary conditions	Pressure (MPa) Flow rate (t/h) Inlet sub-cooling (kJ/kg) Exit quality (%)	7.2 8.6 20 45 55 70 50.2 7 10 15 20 25
Data	Pressure drop along with axial heated length Corresponding boundary conditions	
No. of cases	Exercise cases	22

Exit quality: Thermal equilibrium quality.

Table 5.3.4. Test matrix of selected cases for Exercise 0 of Phase II; two-phase pressure drop

Assembly	Pressure (MPa)	Flow rate (t/h)	Inlet sub-cooling (kJ/kg)	Exit quality (%)					No. of data
				7	10	15	20	25	
C2A	7.2	20	50.2	E0	X	E0	X	E0, W	21
		45		E0	X	E0	X	E0	
		55		E0	X	E0	X	E0, W	
		70		E0	X	E0	X	–	
	8.6	20	50.2	E0	–	E0	–	E0	12
		45		E0	–	E0	–	E0	
		55		E0	–	E0	–	E0, W	
		70		E0	–	E0	–	–	

X: Test case, W: Duplicated test case, E0: Exercise 0 case.

Table 5.3.5. Data format of Exercise 0 of Phase II; single-phase pressure drop

Test number	Outlet pressure (MPa)	Inlet temperature (°C)	Flow rate (t/h)	Reynolds number $\times 10^4$	dp301 (kPa)	dp302 (kPa)	…	dp309 (kPa)
XX	XX	XX	XX	XX	XX	XX	…	XX
XX	XX	XX	XX	XX	XX	XX	…	XX
XX	XX	XX	XX	XX	XX	XX	…	XX
…	…	…	…	…	…	…	…	…

Table 5.3.6. Data format of Exercise 0 of Phase II; two-phase pressure drop

Test number	Outlet pressure (MPa)	Inlet temperature (°C)	Inlet sub-cooling (kJ/kg)	Flow rate (t/h)	Power (MW)	Outlet quality (%)	dp301 (kPa)	dp302 (kPa)	…	dp309 (kPa)
XX	XX	XX	XX	XX	XX	XX	XX	XX	…	XX
XX	XX	XX	XX	XX	XX	XX	XX	XX	…	XX
XX	XX	XX	XX	XX	XX	XX	XX	XX	…	XX
…	…	…	…	…	…	…	…	…	…	…

Table 5.3.7. Test numbers of selected cases for Exercise 0 of Phase II; single-phase pressure drop

Test number	Outlet pressure (MPa)	Inlet temperature (°C)	Flow rate (t/h)	Reynolds number × 10^4	dp 301 (kPa)	dp 302 (kPa)	dp 303 (kPa)	dp 304 (kPa)	dp 305 (kPa)	dp 306 (kPa)	dp 307 (kPa)	dp 308 (kPa)	dp 309 (kPa)
P70027	7.15	284.9	20.30	8.07	0.30	0.35	0.39	0.45	0.47	0.46	1.33	0.52	3.12
P70028	7.16	285.1	24.90	9.91	0.46	0.51	0.58	0.65	0.64	0.68	1.98	0.75	4.59
P70029	7.16	285.1	29.80	11.86	0.64	0.72	0.81	0.91	0.93	0.94	2.79	1.03	6.46
P70030	7.16	285.7	34.70	13.82	0.79	0.95	1.05	1.19	1.26	1.25	3.73	1.36	8.57
P70031	7.16	285.6	39.70	15.81	1.11	1.25	1.41	1.58	1.60	1.63	4.87	1.77	11.23
P70032	7.16	285.3	44.60	17.75	1.37	1.54	1.73	1.93	1.95	1.99	5.96	2.17	13.76
P70033	7.15	284.7	55.00	21.86	2.06	2.30	2.55	2.87	2.91	2.96	8.85	3.22	20.43
P70034	7.15	284.8	59.70	23.74	2.41	2.69	2.99	3.35	3.39	3.46	10.36	3.76	23.87
P70035	7.16	284.6	64.80	25.76	2.81	3.14	3.46	3.90	3.95	4.03	12.05	4.37	27.77
P70036	7.15	284.8	69.90	27.79	3.25	3.63	3.99	4.50	4.55	4.65	13.89	5.04	32.03

Table 5.3.8. Test numbers of selected cases for Exercise 0 of Phase II; two-phase pressure drop

Test number	Outlet pressure (MPa)	Inlet temperature (°C)	Inlet sub-cooling (kJ/kg)	Flow rate (t/h)	Power (MW)	Outlet quality (%)	dp301 (kPa)	dp302 (kPa)	dp303 (kPa)	dp304 (kPa)	dp305 (kPa)	dp306 (kPa)	dp307 (kPa)	dp308 (kPa)	dp309 (kPa)
P60001	7.16	277.3	53.3	20.2	0.863	6.7	1.15	1.96	2.53	3.48	3.66	3.93	12.27	5.50	27.40
P60003	7.16	277.8	50.8	20.1	1.521	14.8	1.54	2.22	2.81	3.61	3.63	3.69	11.72	5.50	27.22
P60005	7.16	277.7	51.1	20.0	2.357	24.9	2.10	2.81	3.43	4.26	4.11	3.97	11.84	5.47	29.16
P60007	7.17	277.8	51.1	55.0	2.375	7.0	5.59	6.70	8.11	9.55	9.06	8.40	22.84	8.25	57.89
P60009	7.17	277.8	51.1	55.0	4.197	15.0	9.24	10.91	12.39	14.26	13.54	11.83	29.30	8.48	78.59
P60011	7.17	278.0	50.6	54.9	6.478	25.1	13.56	16.05	17.81	20.04	19.39	16.73	39.14	8.93	106.72
P60013	7.16	278.4	47.2	69.9	3.022	7.3	8.92	10.24	12.15	13.58	12.98	11.65	30.31	10.07	79.71
P60015	7.17	278.2	49.5	70.0	5.340	15.1	14.93	17.00	19.33	20.96	20.33	17.40	41.22	10.48	113.97
P60017	7.16	277.8	51.0	45.1	1.919	6.8	3.93	4.91	6.08	7.23	7.03	6.73	18.92	7.24	46.54
P60019	7.17	278.2	49.4	45.0	3.437	15.1	6.43	7.73	8.94	10.54	9.98	8.90	22.97	7.44	60.11
P60021	7.16	277.8	50.8	45.1	5.312	25.0	9.30	11.24	12.51	14.42	13.98	12.17	29.32	7.72	78.76
P60022	8.64	291.3	50.7	20.2	0.837	7.0	1.11	1.94	2.49	3.44	3.48	3.88	11.99	5.36	26.83
P60023	8.63	291.0	52.3	20.2	1.464	14.8	1.39	2.08	2.62	3.44	3.49	3.63	11.54	5.36	26.38
P60024	8.63	290.9	52.9	20.2	2.252	24.9	1.82	2.49	3.03	3.88	3.55	3.75	11.47	5.33	27.55
P60025	8.64	291.3	51.3	55.0	2.271	6.9	4.96	6.08	7.29	8.74	8.15	7.96	22.05	8.17	54.66
P60026	8.64	291.0	53.0	55.1	3.975	14.7	7.75	9.23	10.47	12.61	11.43	10.50	26.89	8.36	70.06
P60027	8.64	291.2	51.5	55.1	6.137	24.9	11.18	13.30	14.69	17.40	16.10	14.40	34.79	8.79	92.41
P60029	8.64	291.3	51.5	70.1	2.888	6.9	7.60	8.96	10.54	12.32	11.43	10.70	28.79	10.08	73.55
P60030	8.64	291.2	51.4	70.2	5.076	14.9	12.39	14.28	16.19	18.14	17.16	15.33	37.62	10.40	100.77
P60031	8.64	290.9	53.0	45.1	1.869	6.9	3.49	4.50	5.50	6.78	6.36	6.42	18.29	7.09	44.32
P60032	8.63	291.2	51.3	45.2	3.262	14.9	5.42	6.62	7.63	9.34	8.47	8.02	21.35	7.28	54.32
P60033	8.63	291.2	51.6	45.1	5.021	24.9	7.61	9.31	10.28	12.62	11.50	10.49	26.21	7.54	68.44

5.3.2 Exercise 1: Steady-state benchmark

The supplied measured data includes: critical power, axial location of boiling transition and corresponding boundary conditions (pressure, flow, inlet sub-cooling and power shape). The test conditions are summarised in Table 5.3.9. The test matrix is shown in Table 5.3.10. The data format is given in Table 5.3.11 and the data itself for the selected test cases are shown in Tables 5.3.12 through 5.3.14 for each assembly type and particular exercise case. The measured power is the bundle power at which dry-out was detected.

Table 5.3.9. Conditions for Exercise 1 of Phase II

Assembly	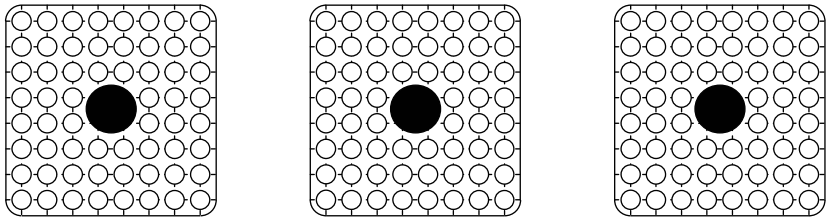 C2A C2B C3	
Boundary conditions	Pressure (MPa) Flow rate (t/h) Inlet sub-cooling (kJ/kg)	5.5 7.2 8.6 10 20 30 45 55 60 65 25 50 84 104 126
Data	Critical power, location of boiling transition Corresponding boundary conditions	
No. of cases	Exercise cases	44

Table 5.3.10. Test matrix of selected cases for Exercise 1 of Phase II

Assembly	Pressure (MPa)	Flow rate (t/h)	Inlet sub-cooling (kJ/kg)				
			25	50	84	104	126
C2A	5.5	20		E1			
		45		E1			
		55	E1	E1	E1		E1
		65		E1			
	7.2	20		E1			
		30		E1			
		45		E1			
		55	E1	E1	E1	E1	E1
		60		E1			
		65		E1			
	8.6	20		E1			
		45		E1			
		55	E1	E1	E1		E1
		65		E1			
C2B	7.2	20		E1			
		30		E1			
		45		E1			
		55	E1	E1	E1	E1	E1
		60		E1			
		65		E1			

E1: Exercise 1 case.

Table 5.3.10. Test matrix of selected cases for Exercise 1 of Phase II (*cont.*)

Assembly	Pressure (MPa)	Flow rate (t/h)	Inlet sub-cooling (kJ/kg)				
			25	50	84	104	126
C3	7.2	20		E1			
		30		E1			
		45		E1			
		55	E1	E1	E1	E1	E1
		60		E1			
		65		E1			

E1: Exercise 1 case.

Table 5.3.11. Data format of Exercise 1 of Phase II

Test no.	Assembly	Pressure (MPa)	Flow rate (t/h)	Inlet sub-cooling (kJ/kg)	Critical power (MW)	Thermocouple location
1	XX	XX	XX	XX	XX	XX
2	XX	XX	XX	XX	XX	XX
3	XX	XX	XX	XX	XX	XX
…	XX	XX	XX	XX	XX	XX

Test assembly type – C2A, C2B, C3.
Power shape = cosine, cosine and inlet peak respectively.

Table 5.3.12. Test numbers of selected cases for Exercise 1 of Phase II; assembly type C2A

Test number	Outlet pressure (MPa)	Flow rate (t/h)	Inlet sub-cooling (kJ/kg)	Experimental cases
SA505500	5.49	20.16	50.95	E1
SA510500	5.48	55.06	56.41	E1
SA510600	5.51	54.70	96.16	E1
SA510800	5.51	54.81	134.97	E1
SA510900	5.52	54.70	35.33	E1
SA612500	7.16	65.36	55.66	E1
SA516500	5.51	44.85	55.98	E1
SA605500	7.16	20.09	50.55	E1
SA607500	7.13	30.02	48.35	E1
SA610503	7.17	55.20	59.39	E1
SA610600	7.18	55.05	89.53	E1
SA610700	7.13	55.20	107.61	E1
SA610800	7.24	55.30	137.26	E1
SA610900	7.27	55.10	37.73	E1
SA611500	7.13	60.23	54.89	E1
SA612500	7.16	65.36	55.66	E1
SA616500	7.13	45.17	54.21	E1
SA805500	8.63	20.30	51.00	E1
SA810501	8.62	55.15	54.89	E1
SA810600	8.56	55.00	83.85	E1
SA810800	8.64	55.28	130.3	E1
SA810900	8.66	55.38	30.97	E1
SA812500	8.64	65.25	58.08	E1
SA816500	8.61	45.24	52.22	E1

E1: Exercise 1 case.

Table 5.3.13. Test numbers of selected cases for Exercise 1 of Phase II; assembly type C2B

Test no.	Assembly	Pressure (MPa)	Flow rate (t/h)	Inlet sub-cooling (kJ/kg)	Exercise cases
SB605500	C2B	7.15	20.03	51.66	E1
SB607500	C2B	7.13	30.05	49.90	E1
SB610500	C2B	7.20	54.84	54.28	E1
SB610600	C2B	7.18	54.91	82.45	E1
SB610700	C2B	7.18	54.71	105.31	E1
SB610800	C2B	7.14	54.90	122.48	E1
SB610900	C2B	7.20	54.88	26.55	E1
SB611500	C2B	7.19	59.88	54.03	E1
SB612500	C2B	7.18	64.60	48.65	E1
SB616501	C2B	7.14	44.82	47.96	E1

E1: Exercise 1 case.

Table 5.3.14. Test numbers of selected cases for Exercise 1 of Phase II; assembly type C3

Test no.	Assembly	Pressure (MPa)	Flow rate (t/h)	Inlet sub-cooling (kJ/kg)	Exercise cases
SC605500	C3	7.16	19.96	50.40	E1
SC607500	C3	7.15	29.83	51.09	E1
SC616500	C3	7.15	45.04	50.88	E1
SC610900	C3	7.19	54.90	31.35	E1
SC610500	C3	7.19	54.90	50.74	E1
SC610600	C3	7.13	54.66	81.93	E1
SC610700	C3	7.15	54.83	103.37	E1
SC610800	C3	7.21	55.06	128.69	E1
SC611500	C3	7.19	59.72	51.05	E1
SC612500	C3	7.17	65.02	52.32	E1

E1: Exercise 1 case.

5.3.3 Exercise 2: Transient benchmark

Exercise 2 of Phase II is designed for benchmarking a one-dimensional approach with boiling transition correlation and/or a sub-channel mechanistic approach. The supplied measured data includes: timing of boiling transition, timing of rewetting, maximum rod surface temperature, location of boiling transition, histories of thermocouples and corresponding boundary conditions (pressure, flow, inlet sub-cooling and power shape). Tables 5.3.15 and 5.3.16 represent the measurement conditions and the test matrix, respectively. Test numbers are given in Table 5.3.17. The selected cases for Exercise 2 of Phase II are denoted with E2. The data format is provided in Tables 5.3.18 (for histories of boundary conditions) and 5.3.20 (for histories of thermocouples). Tables 5.3.19 and 5.3.21 provide examples of the data format for the particular transient type.

Table 5.3.15. Conditions for Exercise 2 of Phase II

Assembly	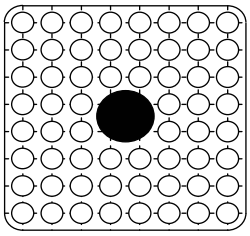 C2A	
Rated initial conditions	Pressure (MPa) Power (MW) Flow rate (t/h) Inlet enthalpy (kJ/kg)	7.2 6.2~8.5 45 1 217~1 227
Transients	Turbine trip without bypass Re-circulation pump trip	
Data	Time histories of cladding temperature where boiling transition occurred Timing of boiling transition, timing of rewetting, peak cladding temperature Corresponding boundary conditions during transients	
No. of cases	Exercise cases	2

Table 5.3.16. Test matrix of selected cases for Exercise 2 of Phase II

Assembly	**Initial conditions**				**Transients**	**Exercise cases**	**No. of cases**
	Pressure (MPa)	**Power (MW)**	**Flow rate (t/h)**	**Inlet enthalpy (kJ/kg)**			
C2A	7.2	6.2~8.5	45	1 217~1 227	Turbine trip without bypass	E2	2
					Re-circulation pump trip	E2	

E2: Exercise 2 case.

Table 5.3.17. Test numbers of selected cases for Exercise 2 of Phase II

Test no.	**Assembly**	**Initial conditions**				**Transients**	**Exercise cases**
		Pressure (MPa)	**Power (MW)**	**Flow rate (t/h)**	**Inlet enthalpy (kJ/kg)**		
TGA10008	C2	7.2	6.2~8.5	45	1 217~1 227	Turbine trip without bypass	E2
TRA10012	C2	7.2	6.2~8.5	45	1 217~1 227	Re-circulation pump trip	E2

E2: Exercise 2 case.

Table 5.3.18. Data format of Exercise 2 of Phase II (boundary conditions' histories)

Histories of boundary conditions	Power (MW)	Flow rate (t/h)	Inlet pressure (MPa)	Outlet pressure (MPa)	Inlet temperature (°C)	Outlet temperature (°C)
Time 1	XX	XX	XX	XX	XX	XX
Time 2	XX	XX	XX	XX	XX	XX
Time 3	XX	XX	XX	XX	XX	XX
Time 4	XX	XX	XX	XX	XX	XX
Time 5	XX	XX	XX	XX	XX	XX
…	XX	XX	XX	XX	XX	XX
Time N-3	XX	XX	XX	XX	XX	XX
Time N-2	XX	XX	XX	XX	XX	XX
Time N-1	XX	XX	XX	XX	XX	XX
Time N	XX	XX	XX	XX	XX	XX

Table 5.3.19. Example of data format of Exercise 2 of Phase II (BCs histories)

Histories of boundary conditions	Power (MW)	Flow rate (t/h)	Inlet pressure (MPa)	Outlet pressure (MPa)	Inlet temperature (°C)	Outlet temperature (°C)
0.00 s	7.036	55.27	7.20	7.11	276.7	286.6
0.02 s	7.036	55.29	7.20	7.11	276.6	286.6
0.04 s	7.038	55.30	7.20	7.11	276.7	286.6
0.06 s	7.041	55.31	7.20	7.11	276.7	286.6
0.08 s	7.036	55.31	7.20	7.11	276.7	286.6
…	…	…	…	…	…	…
73.86 s	0.380	17.35	7.27	7.26	276.4	288.2
73.88 s	0.381	17.35	7.27	7.26	276.4	288.2
73.9 s	0.383	17.35	7.27	7.26	276.4	288.2
73.92 s	0.372	17.42	7.31	7.30	276.6	288.5

Table 5.3.20. Data format of Exercise 2 of Phase II (thermocouples' histories)

History of thermocouples	Thermocouple-1	Thermocouple-2	…	Thermocouple-N-1	Thermocouple-N
Time 1	XX	XX	…	XX	XX
Time 2	XX	XX	…	XX	XX
Time 3	XX	XX	…	XX	XX
…	XX	XX	…	XX	XX
Time M-3	XX	XX	…	XX	XX
Time M-2	XX	XX	…	XX	XX
Time M-1	XX	XX	…	XX	XX
Time M	XX	XX	…	XX	XX

Table 5.3.21. Example of data format of Exercise 2 of Phase II (thermocouples' histories)

History of thermocouples	04-B135	04-B240	25-B240	25-B330	45-B240	59-B45
0.00 s	303.7	302.2	309.1	307.7	307.5	308.0
0.02 s	303.7	302.2	309.1	307.7	307.5	307.9
0.04 s	303.7	302.2	309.1	307.7	307.5	308.0
0.06 s	303.7	302.2	309.1	307.7	307.5	308.0
0.08 s	303.7	302.2	309.1	307.7	307.5	308.0
…	…	…	…	…	…	…
73.86 s	290.6	290.7	294.0	294.5	295.1	295.1
73.88 s	290.5	290.8	294.0	294.6	295.1	295.1
73.90 s	290.5	290.7	294.0	294.5	295.1	295.1
73.92 s	290.8	291.00	294.2	294.8	295.3	295.3

Chapter 6

OUTPUT REQUESTED

6.1 Introduction

The requested output information from the participants includes:

- Results should be presented in electronic format (CD-ROM).
- All output should be in SI units.
- For time histories, output should be at 0.02 second intervals.

Templates of requested output data for each exercise will be provided by the benchmark team.

The Pennsylvania State University will have the obligation to:

- provide code-to-data comparisons for different submittals;
- provide code-to-code comparisons for different submittals;
- provide overall conclusions on current code capabilities to represent the key phenomena.

6.2 Void distribution benchmark

Exercise 1: Steady-state sub-channel grade benchmark

The calculated results, or output data, for a given exercise case should be submitted as a 9×9 matrix of space-averaged void fraction in a sub-channel mesh size. An example of the output format of the steady-state sub-channel grade void distribution benchmark is given in Table 6.2.1.

Exercise 2: Steady-state microscopic grade benchmark

Output data should be a 512×512 matrix of void fraction in a 0.3 mm $\times$ 0.3 mm mesh size. The data format of the steady-state microscopic grade void distribution benchmark is given in Table 6.2.2.

Values should be provided at bundle exit, at CT scanner location.

Table 6.2.1. Output format of steady-state sub-channel grade void distribution benchmark

Exercise 1, Phase I
Test no.
Average void fraction, X.X%

y/x	1	2	3	4	5	6	7	8	9
1	XX	XX	XX	XX	XX	XX	XX	XX	XX
2	XX	XX	XX	XX	XX	XX	XX	XX	XX
3	XX	XX	XX	XX	XX	XX	XX	XX	XX
4	XX	XX	XX	XX	XX	XX	XX	XX	XX
5	XX	XX	XX	XX	XX	XX	XX	XX	XX
6	XX	XX	XX	XX	XX	XX	XX	XX	XX
7	XX	XX	XX	XX	XX	XX	XX	XX	XX
8	XX	XX	XX	XX	XX	XX	XX	XX	XX
9	XX	XX	XX	XX	XX	XX	XX	XX	XX

Cross-sectional averaged: %

Table 6.2.2. Output format of steady-state microscopic grade void distribution benchmark

Exercise 2, Phase I
Test no.
Void fraction, xx aa %

	1	2	3	4	5	.	.	.	n-3	n-2	n-1	n=512
1	00	00	00	00	00	00	00	00	00	00	00	00
2	0x	xx	1x	xx	2x	xx	3x	xx	4x	xx	5x	xx
3	0a	aa	1a	aa	2a	aa	3a	aa	4a	aa	5a	aa
4	00	00	00	00	00	00	00	00	00	00	00	00
5	0x	xx	1x	xx	2x	xx	3x	xx	4x	xx	5x	xx
.	0a	aa	1a	aa	2a	aa	3a	aa	4a	aa	5a	aa
.	00	00	00	00	00	00	00	00	00	00	00	00
.	2x	xx	3x	xx	4x	xx	5x	xx	6x	xx	7x	xx
n-3	00	00	00	00	00	00	00	00	00	00	00	00
n-2	3x	xx	4x	xx	5x	xx	6x	xx	7x	xx	8x	xx
n-1	3a	aa	4a	aa	5a	aa	6a	aa	7a	aa	8a	aa
n=512	00	00	00	00	00	00	00	00	00	00	00	00

Cross-sectional averaged: %

Exercise 3: Transient macroscopic grade benchmark

Output data should be space averaged instantaneous axial void profiles at the specified times during the transient. This data should be for the turbine trip without bypass and the re-circulation pump trip transients.

Output format for this exercise is summarised in Table 6.2.3.

Table 6.2.3. Output format of transient macroscopic grade void distribution benchmark

Exercise 3, Phase I
Test no.
Void fraction, X.X%

Cross-sectional averaged void fraction	X-ray densitometer 1	X-ray densitometer 2	X Ray densitometer 3
Time 1	XX	XX	XX
Time 2	XX	XX	XX
Time 3	XX	XX	XX
…	XX	XX	XX
Time M-3	XX	XX	XX
Time M-2	XX	XX	XX
Time M-1	XX	XX	XX
Time M	XX	XX	XX

Exercise 4: Uncertainty analysis of void distribution benchmark

This section specifies the requested output for Exercise 4. Several statistical criteria are necessary to qualify and quantify the uncertainty of the computations – see Appendix A.

The M/P plots for the different experiments against the four independent experimental parameters of pressure, flow rate, exit quality and inlet sub-cooling are requested. M/P figures can be drawn with using one of the four parameters. These figures are:

- M/P exit void fraction and pressure;
- M/P exit void fraction and flow rate;
- M/P exit void fraction and exit quality;
- M/P exit void fraction and inlet sub-cooling enthalpy.

The tabulated M/P ratios are requested electronically for each experiment that is compared such that it could be plotted and assessed.

The histogramme plots on a sub-channel basis are requested to assess the computer code's ability to represent the geometrical difference in the different sub-channels.

A file of the measured and predicted void fraction for each sub-channel as well as a plot similar to the one shown in Figure A.1 (Appendix A) for all sub-channels (81) of each test case is requested. A composite plot from all test cases of the measured and predicted sub-channel void fraction similar to Figure A.1 is also requested.

6.3 Critical power benchmark

Exercise 0: Steady-state pressure drop benchmark

The requested output is the pressure drop profile along the heated length at critical power. It includes:

- Pressure drop measurements – single phase:
  - pressure drop across the spacer grids (dPT1) (see Figure 2.5.1);
  - overall bundle pressure drop (dPT9).
- Pressure drop measurements – two phase:
  - pressure drop across the spacer grids and rods (dPT1, dPT2, dPT6, and dPT8);
  - average void/quality over the ΔP range; (axial profile of void/quality over the ΔP range;
  - overall bundle pressure drop (dPT9).

Exercise 1: Steady-state critical power benchmark

The requested output is the critical power location of boiling transition and critical power value. The output for the steady-state benchmark includes:

- critical power, value and location (axial and chordal);
- quality/void profile at critical power;
- rod surface temperature profile at critical power;
- sub-channel normalised flow at critical power.

For the three-field sub-channel codes, the additional requested output is:

- detailed radial location of boiling transition;
- liquid film thickness profile at critical power;
- droplet entrainment fraction profile at critical power.

The data format for this exercise is summarised in Table 6.3.1.

Table 6.3.1. Output format of steady-state critical power benchmark

Test no.	Assembly	Pressure (MPa)	Flow rate (t/h)	Inlet sub-cooling (kJ/kg)	Critical power (MW)	Thermocouple location
1	XX	XX	XX	XX	XX	XX
2	XX	XX	XX	XX	XX	XX
3	XX	XX	XX	XX	XX	XX
…	XX	XX	XX	XX	XX	XX
151	XX	XX	XX	XX	XX	XX

Exercise 2: Transient critical power benchmark

The requested output data is the timing of boiling transition, the timing of rewetting, the maximum rod surface temperature, the location of boiling transition and the histories of six specified thermocouples. The data format for this exercise is summarised in Tables 6.3.2 and 6.3.3.

Table 6.3.2. Output format of transient critical power benchmark

Test no.	Location of BT	Maximum rod temp.	Timing of rewet.	Timing of BT
TRA10012	XX	XX	XX	XX
TGA10008	XX	XX	XX	XX
TIC10012	XX	XX	XX	XX
TGC10018	XX	XX	XX	XX

Table 6.3.3. Output format of transient critical power benchmark

History of thermocouple	TC1 (°C)	TC2 (°C)		TC6 (°C)
Time 1	XX	XX		XX
Time 2	XX	XX		XX
Time 3	XX	XX		XX
…	XX	XX		XX
Time M-3	XX	XX		XX
Time M-2	XX	XX		XX
Time M-1	XX	XX		XX
Time M	XX	XX		XX

The methods envisioned for analysis of submitted benchmark results are presented in Appendix A.

Chapter 7

CONCLUSIONS

The objective of the BFBT benchmark specification is to provide the participants with information on the benchmark database. Although it contains detailed information on the test cases and measurements for the complete NUPEC BWR database, specific exercises were selected for the OECD/NRC BFBT benchmark to reduce the amount of work; to make the analysis more precise; and to avoid confusion among the comparison of the participants' results.

7.1 Phase I – Void distribution benchmark

Exercise 1: Steady-state sub-channel grade benchmark

The goal of this exercise is to benchmark the sub-channel, meso- and microscopic numerical approaches. The supplied measured data includes time- and space-averaged void distribution matrix in sub-channel mesh size. The test cases are selected at BWR rated conditions. Different types of assemblies are used to investigate the effect of geometry and/or power distribution on phenomenon of concern.

Exercise 2: Steady-state microscopic grade benchmark

This exercise is designed for benchmarking meso-, microscopic and molecular dynamics numerical approaches. The measurement resolution is as fine as 0.3×0.3 mm. The test cases for this exercise are chosen at BWR rated conditions and deviations of quality from the rated conditions.

Exercise 3: Transient macroscopic grade benchmark

The NUPEC BFBT database includes a simulation of two representative transients of BWRs, turbine trip without bypass and re-circulation pump trip. Both transients are selected as benchmark cases. Exercise 3 of Phase II is designed for benchmarking sub-channel numerical approaches.

Exercise 4: Uncertainty analysis of the void distribution benchmark

The BFBT benchmark provides an opportunity to apply techniques of uncertainty analysis and to assess the accuracy of two-phase flow models. The steady-state void fraction predictions can be used to analyse these uncertainties and their propagation in the thermal-hydraulic models. The test cases for this exercise include some of the test cases of Exercise 1 of Phase I plus additional test cases.

7.2 Phase II – Critical power benchmark

Exercise 0: Steady-state pressure drop benchmark

The goal of Exercise 0 of Phase II is to asses the thermal-hydraulic codes' capability of correct prediction of pressure drop along rod bundles. This exercise provides the possibility for validation of different rod friction models/correlations for single- and two-phase flows. The test cases are selected on the basis of BWR rated conditions.

Exercise 1: Steady-state critical power benchmark

Exercise 1 of Phase II was designed to enhance the currently underway development of truly mechanistic models for critical power prediction. Since these models must account for void distributions, droplet deposition, liquid film entrainment and spacer grid behaviour, the BFBT benchmark provides an excellent envelope/database by covering a wide range of flow rate, inlet sub-cooling and pressure conditions for different assembly types (C2A, C2B and C3).

Exercise 2: Transient critical power benchmark

Exercise 2 of Phase II is an extension of Exercise 1 of Phase II, but under BWR power and flow transient conditions. Turbine trip without bypass and re-circulation pump trip events are included in this exercise. All the provided data is based on assembly type C2A.

REFERENCES

[1] Lahey, R.T. and F.J. Moody, "The Thermal Hydraulics of Boiling Water Nuclear Reactor", American Nuclear Society (ANS) (1977).

[2] Lahey, R.T., *et al*., *Two-phase Flow and Heat Transfer in Multi-rod Geometries: Sub-channel and Pressure Drop Measurements in Nine-rod Bundle for Diabatic and Adiabatic Conditions*, AEC Research and Development Report, GEAP-13049, March 1970.

[3] Herkenrath, H., *et al*., *Experimental Investigation of the Enthalpy and Mass Flow Distribution in 16-Rod Cluster with BWR, PWR – Geometries and Conditions*, Joint Research Center, Ispra, Italy, Final Report EUR 7575 EN (1981).

[4] *Summary of the 4th OECD/NRC BWR TT Workshop*, Seoul, Korea, 4 October 2002, NEA/NSC/DOC (2002).

[5] Inoue, A., T. Kurosu, T. Aoki and M. Yagi, "Void Fraction Distribution in BWR Fuel Assembly and Evaluation of Sub-channel Code", *Journal of Nuclear Science and Technology*, July 1995.

[6] Utsuno, H., N. Ishida, Y. Masuhara and F. Kasahara, "Assessment of Boiling Transition Analysis Code Against Data from NUPEC BWR Full-size Fine-mesh Bundle Tests", *Proceedings of the NUTHOS-6 Conference*, Nara, Japan, 5-8 October 2004.

[7] Sartori, E., L. Hochreiter, K. Ivanov and H. Utsuno, "The OECD/NRC BWR Full-size Fine-mesh Bundle Tests Benchmark (BFBT) – General Description", *Proceedings of the NUTHOS-6 Conference*, Nara, Japan, 5-8 October 2004.

[8] *TRAC-PF1/MOD2 Theory Manual, Appendix B, Material Properties*, NUREG/CR-5673 (1993).

[9] Gaudier, F. and M. Dumas, "Uncertainties Analysis by Genetic Algorithms", *Proceedings of NURETH 11*, Avignon, 2-6 October 2005.

Appendix A

METHODS FOR ANALYSIS OF BENCHMARK RESULTS

Definition of "accuracy" and "comparative analysis"

"Accuracy" is the degree of conformity of a measured or calculated quantity to its actual, nominal or some other reference value. Precision characterises the degree of mutual agreement among a series of individual measurements, values or results.

The parameter given as an example is the sub-channel void fraction. Comparisons will be performed between the sub-channel computer code predictions of the void fraction to the measured void fraction values given in the experimental data.

To examine the degree of agreement between the calculated sub-channel void fractions X_{iC} and the measured sub-channel void fractions X_{iE} for each participant, an approach, similar to the uncertainty analysis of the CHF (DNB) [Duke Power Company Thermal-Hydraulic Statistical Core Design Methodology, BWU-Z CHF Correlation, April 1996] data is proposed. The parameter to be compared is the ratio of the measured (M) void X_{iE} to the predicted (P) void X_{iC} on a sub-channel basis. This gives an M/P ratio that can be used to assess the uncertainty and degree of agreement of the analysis model and data over the range of the independent variables of pressure, mass flow, quality and inlet sub-cooling. Examples of this approach application to the CHF (DNB) data are shown in the figures below. Figure A.1 shows measured CHF versus predicted CHF. In addition to the comparisons of the measured to predicted void fractions, there will also be comparisons of the absolute values of the predicted and measured void fractions in the same fashion as Figure A.1 for the measured and predicted CHF data.

Several meaningful comparisons can be obtained by comparing the measured void fraction to the predicted void fraction, on a sub-channel basis and plotting the M/P ratios. As seen in Figure A.2, a histogramme can be developed for each experiment using the M/P ratio. In addition, M/P histogramme plots can be developed for different sub-channel types using all the experiments. For example, all corner sub-channels could be grouped together and plotted as a histogramme plot. A similar approach could be used for each geometrically different sub-channel in the bundle. These plots would indicate a potential bias in the computer code's ability to model the different sub-channel types.

The other plots of interest are the M/P plots as a function of the test independent variables of pressure, mass flow, quality and inlet sub-cooling. Examples of these are shown in Figures A.3 to A.5 using CHF data as an example. These plots will indicate a possible bias with the independent variables of the experiments and will indicate potential deficiencies of the different computer code models.

The accuracy of these void fraction measurements depends on the photon statistics of the X-ray source, the detector non-linearity and the accuracy of the known fluid condition (temperature and pressure) measurements.

Figure A.1. Example of measured CHF versus predicted CHF

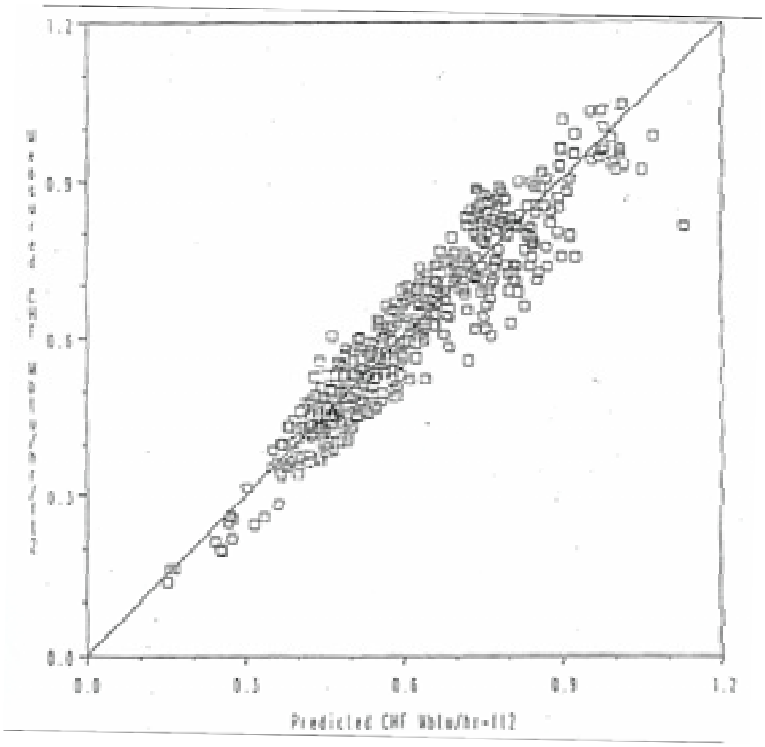

Figure A.2. Example of the distribution of CHF ratios

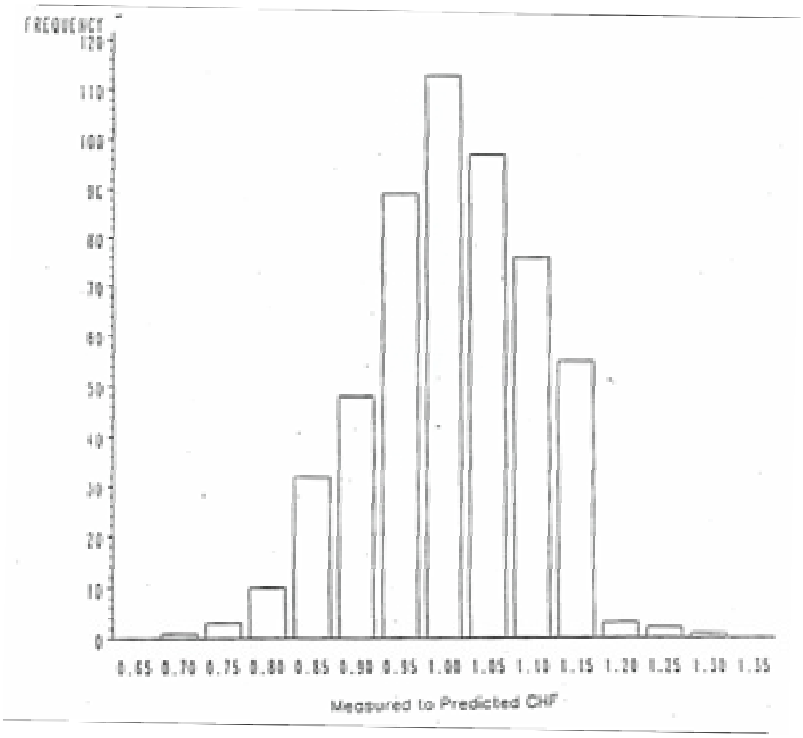

Figure A.3. Example of measured to predicted CHF versus mass velocity

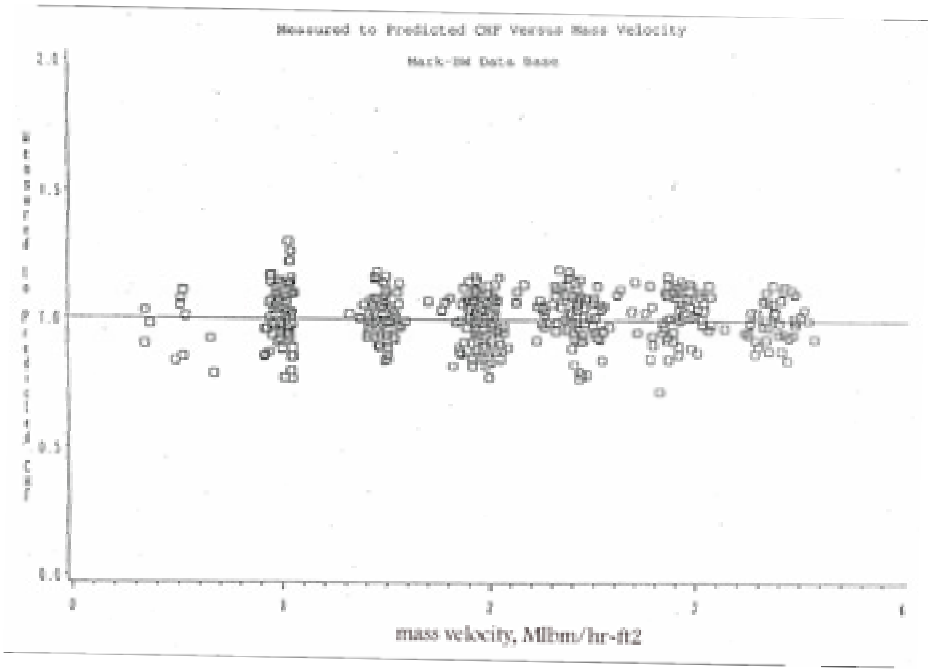

Figure A.4. Example of measured to predicted CHF versus quality

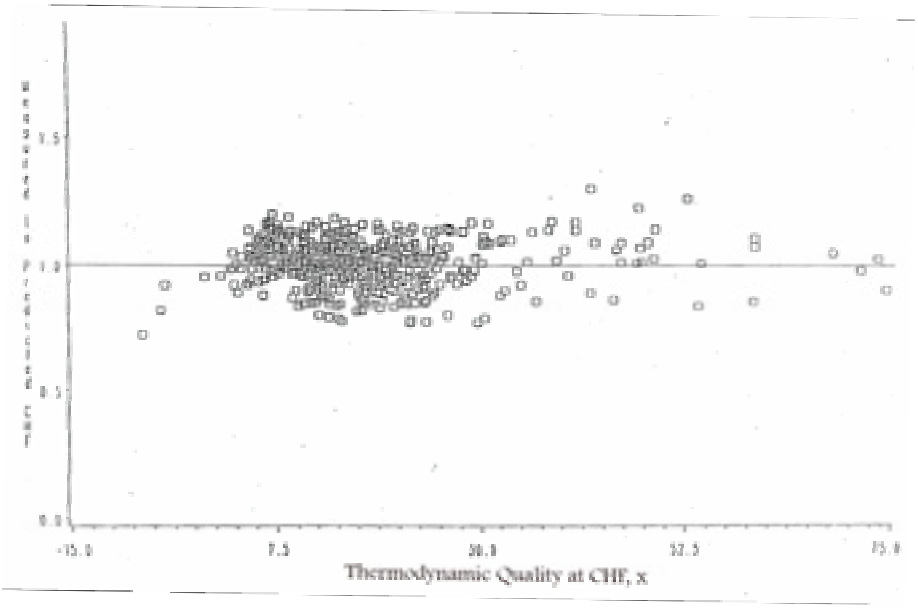

Figure A.5. Example of measured to predicted CHF versus pressure as an independent variable

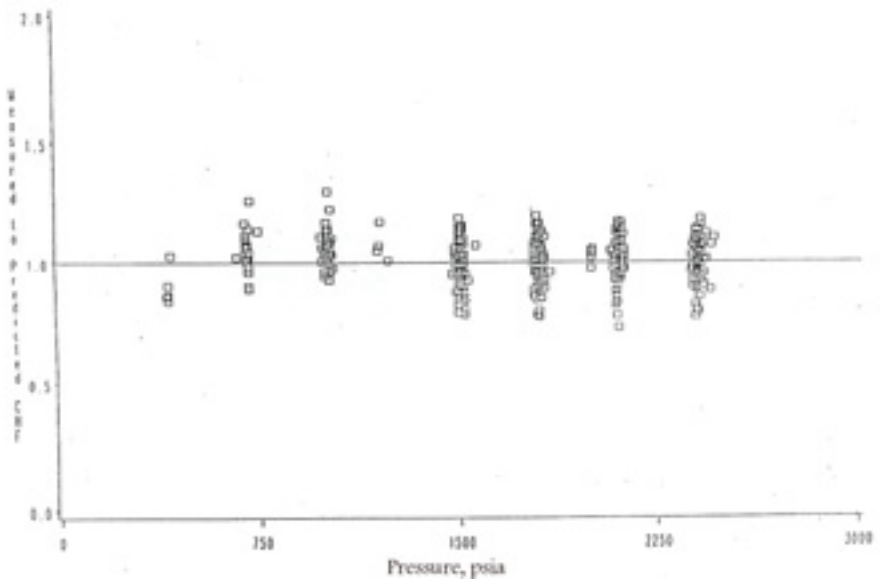

Methods for analysis of benchmark results

Standard statistical techniques will be used to assess the accuracy in the calculated void distribution as compared to the measured values where the computer code prediction is the estimated value of the void fraction and the actual value is the measured value of the void fraction. The statistical parameters to be calculated are:

Root Mean Square (RMS)
$$\mathrm{RMS} = \frac{1}{N}\sum_{i}^{N}\left(X_{iC} - X_{iE}\right)^2$$

Standard Variance (SV)
$$\mathrm{SV} = \frac{1}{N-1}\sum_{i}^{N}\left(X_{iC} - X_{iE}\right)^2$$

Standard Deviation (SD)
$$\mathrm{SD} = \sqrt{\frac{1}{N-1}\sum_{i}^{N}\left(X_{iC} - X_{iE}\right)^2}$$

where X_{iC} is the computer code estimated value, X_{iE} is the experimental measured actual value and N is the number of data.

Void fraction uncertainty analysis can only be performed at the CT scanner's elevation level. In this formula, X_{iC} is the calculated void fraction for a given sub-channel, and X_{iE} is the experimental void fraction in database for the same sub-channel. The calculated void fractions will be taken from the participant's code results.

An example of the calculated void fractions are given below for the test case 0011-55:

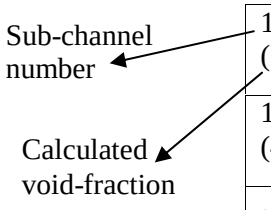

1 (39.8)	2 (38.7)	…	9 (37.0)
10 (45.7)	11 (47.8)	…	18 (41.4)
…	…	…	…
73 (30.0)	74 (46.7)	…	81 (33.5)

Calculated void fraction table – X_{iC} values.

The experimental sub-channel void fractions for the same test case are given below:

1 (39.3)	2 (38.9)	…	9 (38.0)
10 (44.4)	11 (46.8)	…	18 (37.7)
…	…	…	…
73 (29.3)	74 (45.6)	…	81 (34.3)

The standard deviation formula can be applied to these data as shown below:

N=81

$$SD_{whole\_assembly} = \sqrt{\frac{1}{(81-1)}\sum_{i}^{81}(X_{iC} - X_{iE})^2}$$

If the X_{iE} and X_{iC} values are inserted in this formula the standard deviation of whole assembly will be determined.

Methods for comparison of benchmark results

In the graph shown below, the error bars can only be used for the measured void fraction values. As shown in Table 2.4.3, the accuracy of the cross-sectional void fraction is 2%. Therefore, 2% accuracy for measured values is shown in this graph.

Figure A.6. Example of predicted versus measured void fraction with uncertainties

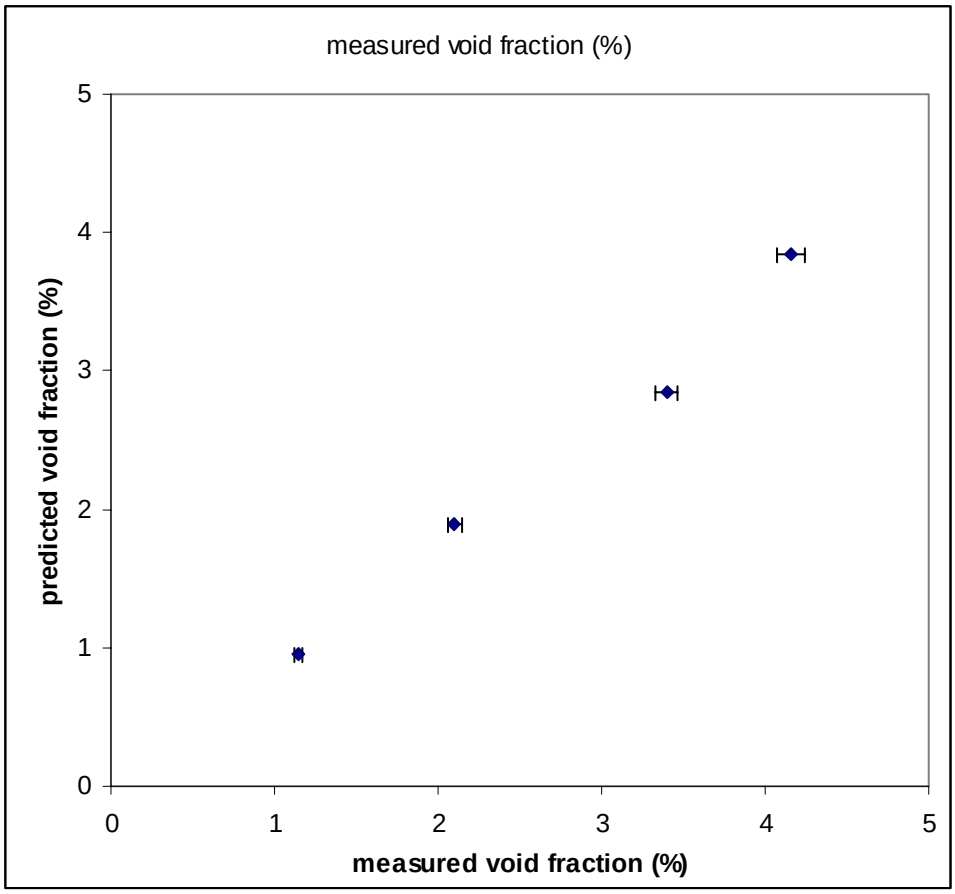

OECD PUBLICATIONS, 2 rue André-Pascal, 75775 PARIS CEDEX 16
Printed in France.